Unclassified

M.I.T. Lincoln Laboratory
ARCHIVES
COPY
Please Return to
A-082
pif-2203 U3150555A

Quarterly Progress Report

Division 5

15 September 1959

Information Processing

AFCRC-TN-59-1014

Lincoln Laboratory

MASSACHUSETTS INSTITUTE OF TECHNOLOGY

DISTRIBUTION STATEMENT A. Approved for public release. Distribution is unlimited.

This material is based upon work supported by the United States Air Force under Air Force Contract No. AF19-(604)-5200. Any opinions, findings, conclusions or recommendations expressed in this material are those of the author(s) and do not necessarily reflect the views of the United States Air Force.

ARCHIVE COPY

Unclassified

Unclassified

PLEASE DO NOT RETURN

Permission is given to destroy this document when it is no longer needed.

The work reported in this document was performed by Lincoln Laboratory, a center for research operated by Massachusetts Institute of Technology with the joint support of the U. S. Army, Navy, and Air Force under Air Force Contract AF 19(604)-5200.

Unclassified

584

Quarterly Progress Report

Division 5

Information Processing

15 September 1959

Issued 4 December 1959

231 801

AFCRC-TN-59-1014

Lincoln Laboratory

MASSACHUSETTS INSTITUTE OF TECHNOLOGY

Lexington, Massachusetts

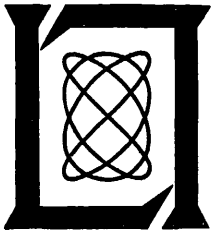

Unclassified

DISTRIBUTION STATEMENT A. Approved for public release. Distribution is unlimited.

INTRODUCTION

Division 5 is continuing to work on materials and components, computer development, digital data transmission, organization of information processes and man-machine integration.

Materials and components work is progressing with emphasis given to the basic understanding of the properties of thin magnetic films. Of major importance is theoretical and experimental work related to the problem of making thin magnetic films uniform.

Within the computer development area, the past quarter was highlighted by the successful installation and operation of the magnetic film memory for word-configuration control. This first film memory to go into operation in a computer has a maximum speed of 0.4 μsec for a read-write cycle, and runs with an 0.8-μsec cycle in the computer proper.

Digital data transmission work is proceeding with the near completion of ECCO (Error Checking and Correcting Coder). This machine, when complete will encode a 64-bit word into a 128-bit transmitted message at an input bit rate of up to 1000 bits/second with sufficient redundancies so that a maximum of seven errors in 128 transmitted bits can be corrected.

The Morse Automatic Decoder (MAUDE) is now complete and on field test with the sponsoring government agency. In addition, the "Pandemonium" approach is showing promise of success with the hand-printed character recognition problem.

Effective means for men to communicate with machines continues to be a major goal of the Division. Projects dealing with speech segmentation, visual and auditory perception, judgment, learning and memory are in process. In addition, work on computer interpretation of English language inputs has been started.

W.B. Davenport, Jr.
Head, Division 5

F.C. Frick
Associate Head, Division 5

24 September 1959

TABLE OF CONTENTS

Introduction iii
Published Reports of Authors From Division 5 vii

DIGITAL COMPUTERS
GROUP 51

I. SUMMARY 3

II. COMPUTER DEVELOPMENT 3

A. TX-2 3
B. Fabrication Techniques 5
C. Advanced Circuits 7

III. MAGNETIC-FILM ENGINEERING 11

A. TX-2 Configuration Memory 11
B. Film Fabrication 13
C. Testing and Instrumentation 13
D. Circuits 13
E. Fixed Storage Using Films 15

IV. INFORMATION PROCESSES 15

DATA PROCESSING
GROUP 52

I. MEMORY DEVELOPMENT 19

A. Magnetics Research 19
B. High-Speed Memory 19
C. Circuit Research 20

II. DIGITAL DATA TRANSMISSION 24

A. Probability of Error in Group Codes 24
B. Error Correcting Coder Circuits 24

III. COMPUTER COMPONENTS 26

A. High-Speed Computer Circuits 26
B. Computer Readout 30

COMPUTER COMPONENTS
GROUP 53

I. SUMMARY 33

A. Magnetic Materials 33
B. Magnetic Films 33
C. Semiconducting Components 35

II. MAGNETIC MATERIALS 35

A. Chemistry and Crystallography 35
B. The Magnetic Properties of Hausmannite 38
C. Theory 41

III. MAGNETIC FILMS 43

A. The Physical Origin of H_k and H_w 43
B. Growth of the Magnetic Moment of Films During Deposition 47
C. Flux Reversal by Noncoherent Rotation 47
D. Evaporated Wiring for High-Density Magnetic Film Memories 48

IV. SEMICONDUCTING COMPONENTS 48

A. High-Temperature Storage Tests on Microalloy Transistors 48
B. TX-0 Transistor Retest Program 48
C. Transistor Switching Theory 49
D. Diode Characteristics at Microwave Frequencies 53

PATTERN RECOGNITION
GROUP 54

I. INTRODUCTION 59

II. MAUDE 59

A. MAUDE Tests 59
B. Degarble 59

III. LEARNING 61

A. Pandemonium Studies 61
B. Dynamic Programming and Adaptive Processes 62
C. Hill-Climbing 63

IV. MISCELLANEOUS 63

V. RECOGNITION AND LEARNING IN MAN 63

A. Hierarchies in Human Pattern Recognition 63
B. Process and Procedure in Induction 66
C. Human Recognition of Hand-Printed Characters 66

ANALYSIS
GROUP 55

I. INTRODUCTION 69

II. HAUSDORFF DIMENSION AND INDEPENDENT FUNCTIONS 69

III. A TRANSIENT DISCRETE TIME QUEUE 70

IV. ON A SYSTEM OF INTEGRODIFFERENTIAL EQUATIONS OCCURRING IN REACTOR DYNAMICS 70

V. COMMUNICATIONS THROUGH UNSPECIFIED ADDITIVE NOISE 71

VI. REED-MULLER CODES 72

VII. DECODING LINEAR ERROR-CORRECTING CODES 72

PSYCHOLOGY
GROUP 58

I. INTRODUCTION 77

II. MAN-MACHINE COMMUNICATION 77

A. Automatic Speech Recognition 77
B. Syllable Segmentation 78
C. Speech Synthesis 78
D. Information Processing Language (IPL-V) 79
E. Information Retrieval and Analysis – "Baseball" 79

III. HUMAN INFORMATION PROCESSING 79

A. Auditory Encoding of Text 79
B. Visual Psychophysics 80
C. Prediction of Complex Judgments 80
D. Remembering the Present States of a Number of Variables 81
E. Rote Verbal Learning 83

IV. METHODOLOGY 84

A. Queuing Studies 84
B. The Stochastic Design of Psychophysical Experiments 84

PUBLISHED REPORTS OF AUTHORS FROM DIVISION 5

15 June through 14 September 1959

Journal Articles

JA No.			
1089	The Morse Distribution	M. Freimer B. Gold A.L. Tritter	Trans. I.R.E., PGIT IT-5, 25 (1959)
1123	Machine Recognition of Hand-Sent Morse Code	B. Gold	Trans. I.R.E., PGIT IT-5, 17 (1959)
1164	Operating Characteristics of a Thin Film Memory	J.I. Raffel	J. Appl. Phys. 30, 60S (1959)
1284	Noncomputational Uses of Digital Computers	B.F. Green, Jr.	Behavioral Sciences 4, 164 (1959)
1288	Thin Magnetic Films for Digital Computer Memories	D.O. Smith	Electronics 32, 44 (1959)

* * * * *

UNPUBLISHED REPORTS

Journal Articles

JA No.			
1372	A Review of Panel Type Display Devices	J.J. Josephs	Submitted to Proc. I.R.E.
1373	Classical Spin-Configuration Stability in the Presence of Competing Exchange Forces	T.A. Kaplan	Submitted to Phys. Rev. Letters
1374	Remembering the Present States of a Number of Variables	D.B. Yntema G.E. Mueser	Submitted to J. Exptl. Psychol.
1378	IPL-V: The Newell-Shaw-Simon Programming Language	B.F. Green, Jr.	Submitted to Computers in Behavioral Science
1381	On a System of Integrodifferential Equations Occurring in Reactor Dynamics	J.J. Levin J.A. Nohel†	Submitted to J. Math. Mech. (Math. Research Center Report)
1382	Transistor-Capacitor Shift Register	R.W. Hofheimer	Submitted to Semiconductor Products Mag.
1399	Studies in the Kinetic Depth Effect	B.W. White G.E. Mueser	Submitted to J. Exptl. Psychol.
1407	A Hausdorff Dimension Property of a Peano Square Filling Curve	W.A. Beyer	Submitted to Pac. J. Math.
1408	Hausdorff Dimension of Level Sets of Non-Absolutely Convergent Rademacher Series	W.A. Beyer	Submitted to Pac. J. Math.
1415	Note on the Distribution of Locally Maximal Elements in a Random Sample	B. Gold M. Freimer	Submitted to Ann. Math. Stat.

† Mathematics Research Center, U.S. Army.

Journal Articles (Continued)

JA No.			
1419	Hausdorff Dimension of Level Sets of Rademacher Series Whose Coefficients Form a Geometric Progression	W.A. Beyer	Submitted to Pac. J. Math.
1443	The TX-2 Light.Pen	B.M. Gurley C.E. Woodward	Submitted to Electronics
1450	Microwave Properties of Thin Magnetic Films	R.F. Soohoo	Submitted to Microwave J.

Meeting Papers

Titles of Meeting Papers are listed here for information only. No copies are available for distribution.

JA No.			
1386	Some Structure-Sensitive Magnetic Properties of Permalloy Films	D.O. Smith	International Conference on Structures and Properties of Thin Films, Lake George, 9-11 September 1959
1387	A First Passage Time Distribution	J.R. Kinney	American Math. Society Meeting, Salt Lake City, 2-4 September 1959
1403	High Efficiency Flux Concentrating Magnet	B. Howland S. Foner	Second Symposium on Magnet Design, Princeton, 1-2 October 1959
1421	Initial Susceptibility Spectra of Permalloy Films	R.F. Soohoo	Conference on Magnetism and Magnetic Materials, Detroit, 16-19 November 1959
1424	On the Direct Cation-Cation Interactions in Primarily Ionic Solids	J.B. Goodenough	Conference on Magnetism and Magnetic Materials, Detroit, 16-19 November 1959
1425	An Interpretation of the Magnetic and Crystallographic Properties of Several Iron, Nickel, and Iron-Nickel Nitrides	J.B. Goodenough A. Wold R. Arnott	Conference on Magnetism and Magnetic Materials, Detroit, 16-19 November 1959
1426	On the Classical Theory of Spin Configurations in the Cubic Spinel	T.A. Kaplan	Conference on Magnetism and Magnetic Materials, Detroit, 16-19 November 1959
1432	Electron Diffraction and Microscopy of Permalloy Films	M.S. Cohen	Conference on Magnetism and Magnetic Materials, Detroit, 16-19 November 1959
1433	Flux Reversal by Noncoherent Rotation in Thin Films	K.J. Harte	Conference on Magnetism and Magnetic Materials, Detroit, 16-19 November 1959
1434	Inverted Films	E.E. Huber, Jr. D.O. Smith	Conference on Magnetism and Magnetic Materials, Detroit, 16-19 November 1959
1435	Techniques for Uniformity in Magnetic Film Production	T.S. Crowther G.P. Weiss	Conference on Magnetism and Magnetic Materials, Detroit, 16-19 November 1959
1444	On Stochastic and Adaptive Dynamic Programming Processes	M. Freimer	American Standards Association, New York University, 16-17 October 1959
1446	Research on Speech Recognition at Lincoln Laboratory	F.C. Frick	Air Force Seminar on Speech Compression and Processing, Bedford, 28-30 September 1959

DIGITAL COMPUTERS
GROUP 51

PAPIAN, W. N., *Leader*

CLARK, W. A., *Associate Leader*

ANDERSON, A. H.
BLATT, H.
CASE, A. W.
CROWTHER, T. S.
FARLEY, B. G.
FERGUS, P. A.
FORGIE, J. W.
FRANKOVICH, J. M.
GILMORE, J. T., Jr.
GOULD, R. H.
GUDITZ, E. A.
HERNDON, T. O.
HURWITZ, C. E.*
KLEINROCK, L.†
KONKLE, K. H.
LAYNOR, J. E.
LIN, C. S.
MITCHELL, J. L.
MOLNAR, C. E.†
NEUMANN, L.
NORMAN, C. A.
PETERSON, H. P., Jr.
RAFFEL, J.
ROBERTS, L.*
SANDEL, T. T.
SAVELL, R. E.
STOCKEBRAND, T. C.
STRASSBERG, D. D.
VANDERBURGH, A.
WOODWARD, C. E.

---

* Temporary.
† Staff Associate.

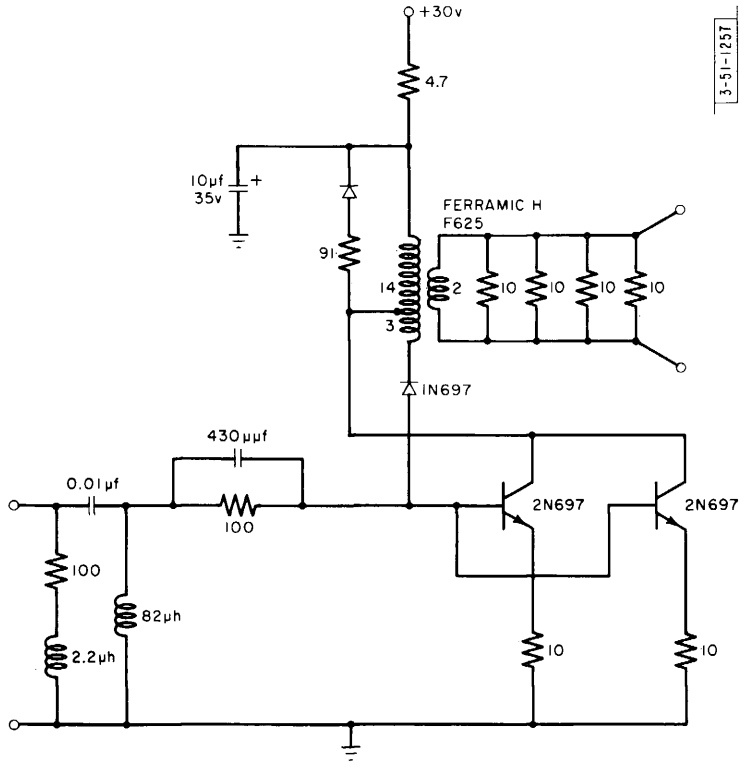

Fig. 51-1. The basic amplifier circuit.

DIGITAL COMPUTERS
GROUP 51

I. SUMMARY

Operation of the TX-2 computer continues as outlined in the Division 5 Quarterly Progress Report for 15 June 1959; an increasing amount of time is devoted to applications, while checking and changes and additions continue apace. The highlight of the quarter was the successful installation and operation of the magnetic-film memory for word-configuration control; this first film memory to go into operation in a computer has a maximum speed of 0.4 μsec for a full cycle, and runs with an 0.8-μsec cycle in the computer proper.

Work has commenced on logic circuits to operate at speeds that are reasonably compatible with those of magnetic-film memories. Several transistor types show promise of fitting into circuits designed for clock rates of 50 megapulses per second; a computer designed around such a combination would have an operating speed ten times greater than TX-2.

Early results from neural-network simulation on TX-2 include some interesting displays of the propagation of activity in a net with periodic external excitation.

W. A. Clark
W. N. Papian

II. COMPUTER DEVELOPMENT

A. TX-2

1. Central Machine

Increasing the reliability and usefulness of the TX-2 system continues to be a major activity. The simplification of the operation modes of the input-output devices and the modification of the "transfer data" instructions, indicated in the Division 5 Quarterly Progress Report, 15 June 1959, have been completed; operation of the system has improved noticeably. The new power supplies for the major voltages have been ordered, and requirements for the remainder of the machine are being analyzed.

A pulse amplifier to be used in a transistorized replacement for the present vacuum-tube clock-pulse generator for the TX-2 has been designed and is in the final stages of testing. The circuit (Fig. 51-1) is a nonsaturating type using a diode and autotransformer circuit to divert base current and thus keep the transistor out of saturation. Some negative feedback by means of emitter resistors is used to help shape the pulse and to minimize the effect of variation in transistor current gain β. The transistors are 2N697 silicon mesa type, and two are paralleled in each amplifier to hold the collector dissipation well within limits. The final stage drives a 2.5-ohm load with a 3.3-volt pulse, 90 mμsec wide, at a prf of 2.5 Mcps when driven from 9-volt 100-mμsec pulses. The two stages previous to the final stage are identical except for the pulse transformers that supply 9-volt pulses and are capable of driving six paralleled amplifiers.

C. E. Hurwitz
K. H. Konkle
J. L. Mitchell
L. Neumann
C. A. Norman

2. Memories

The magnetic-film memory for configuration control has been installed in the computer and is operating satisfactorily. It is covered in more detail under magnetic films in a following section.

The 4096-word transistor-driven magnetic-core memory has been assembled and is being debugged and tested using a tester that writes and checks several different patterns in memory. The memory will be tied into TX-2 early in the next quarter.

T. O. Herndon
J. L. Mitchell

3. Input-Output

The prototype Lincoln Writer is complete and is now available to programmers. Five other units are under construction and should be completed during the fall quarter. Installation of the random-number generator in TX-2 has been completed. Initial tests indicate some bias in the generator output; its cause is being investigated. An 180-line/sec Soreban paper-tape punch and a tape handler have been installed as shown in the photograph of Fig. 51-2.

During this quarter the drafting for the Mk II photoelectric tape reader (PETR) progressed to the point where construction could be started. Presently, a cabinet to house two active units and their controls, with a readily interchangeable spare unit, is being built, as are the three housings for the individual units. These contain the necessary motors, clutches, brakes and switches, as well as the local controls required for remote operation, and provide mounting for the reading assemblies. The latter are still in the drafting stage, although some of their component subassemblies have been built. The Mk II PETR was designed primarily for operation in its cabinet, as shown in Fig. 51-3. However, the separate units can be used as table-top readers at locations remote from the cabinet. When operated in this manner, they are

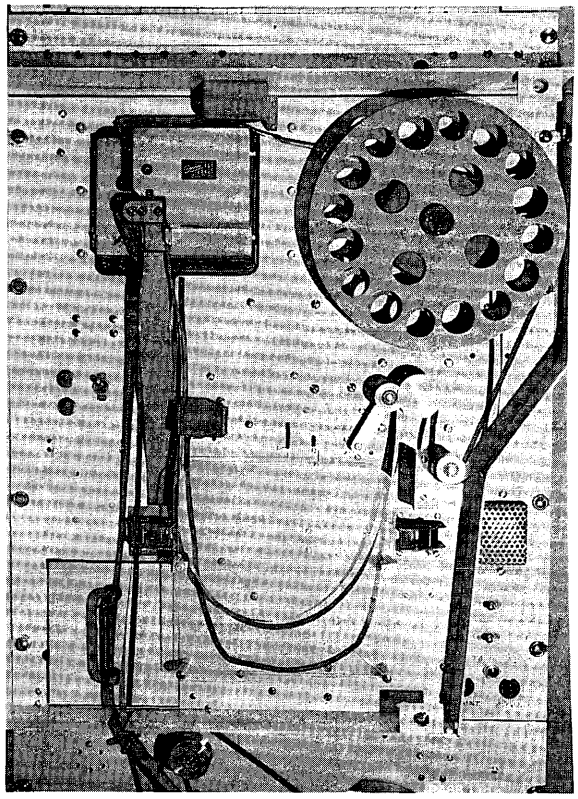

Fig. 51-2. High-speed paper tape punch and tape handling mechanism.

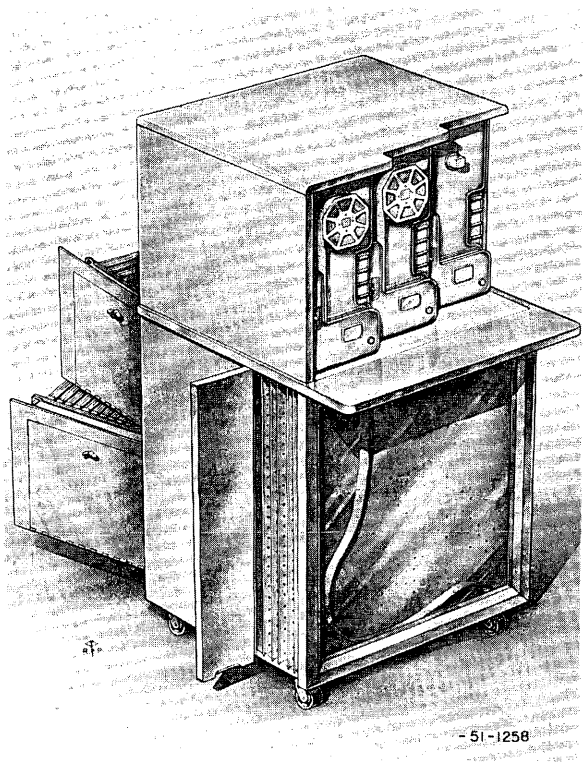

Fig. 51-3. Mk II PETR.

used without a bin and are placed on their sides. In this position they do not require a fixed mounting. Horizontal mounting is also possible in a standard 19-inch rack and in this case a built-in bin can be used.

Checkout of the magnetic tape system control and information handling equipment is complete and debugging of the read and write amplifiers will be completed within a month. Initial operation of the tape system with the computer will get under way early during the next period. Several changes have been made in the system's characteristics since it was first described at the 1957 Western Joint Computer Conference. The reel diameter has been increased from $10\frac{1}{2}$ to 14 inches allowing 80,000,000 bits to be stored on each reel at a recording density of 300 bits/inch. There are four read speeds, 30, 50, 100 and 300 inches/sec and a search speed of up to 900 inches/sec, depending on the amount of tape on the reel, and one write speed, 50 inches/sec. More writing speeds will probably be incorporated after the system is operational.

A.W. Case R.E. Savell
J.E. Laynor T.C. Stockebrand
C.S. Lin

B. Fabrication Techniques

1. Plated Interconnections

The encapsulated high-speed flip-flop with plated wiring and connections has accumulated 1425 hours of successful operation in the TX-2 computer.

Three TX-2 type P-5 inverter units (Fig. 51-4) were made and tested. All worked perfectly. Each has 21 components interconnected by these plating techniques.

The demonstration counter, utilizing a 3-layer plated piece of "back panel" and 5 encapsulated and plate-wired plug-in units, has been in successful bench operation since 11 July 1959. The combined units contain 219 components and 654 plated connections.

An alternate approach to the problem of connections between layers of multilayer plated wiring utilizes plated-through holes instead of pin extensions. A 64-hole 2-layer test sample is shown in Fig. 51-5. After the first layer of wiring and plated connections is finished, the unit is reinserted into a wider mold and a layer of plastic is cast over the wiring on each

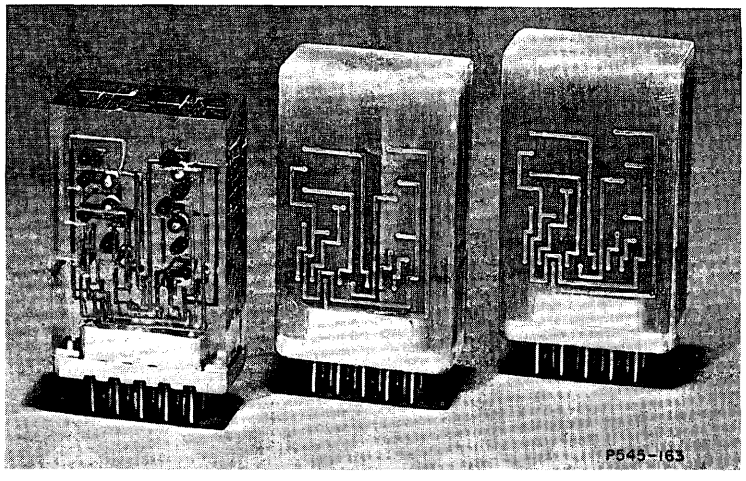

Fig. 51-4. Three electrically identical TX-2 computer type P-5 inverter units that have encapsulated components, deposited wiring and plated connections.

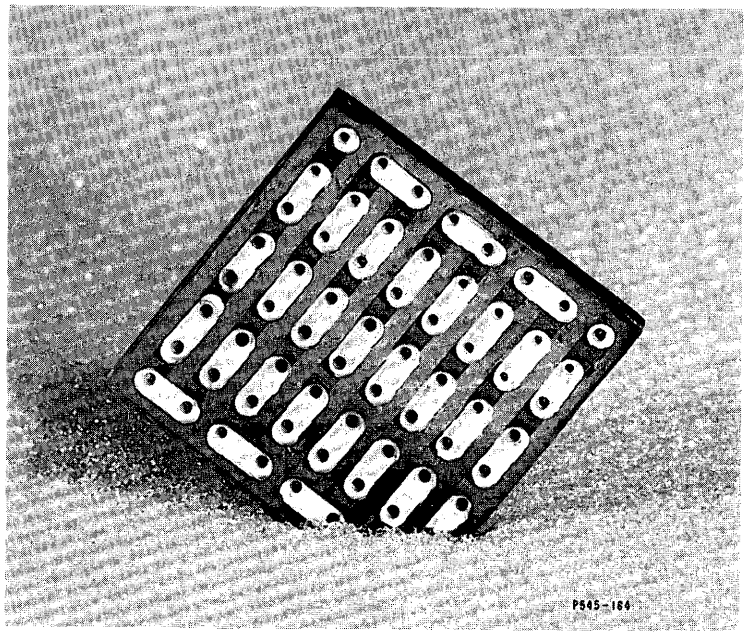

Fig. 51-5. Two encapsulated layers of deposited jumper wires are interconnected at 64 points by means of drilled and plated-through holes.

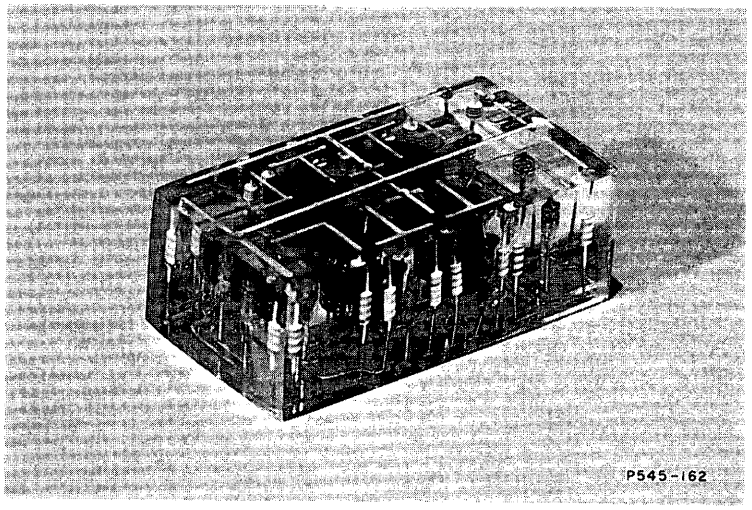

Fig. 51-6. Encapsulated dual flip-flop unit has two separate layers of deposited wiring on each of two sides. Layers are interconnected at appropriate points by drilled and plated-through holes.

face. Tapered holes (30° included angle) are drilled at positions where layer interconnections must be made. Copper is deposited on both faces and into the holes, making contact to the underneath layer of wiring. After more copper is added by electroplating, conventional photoetching produces the outer layer of wiring on each face. If desired, the wiring can be engraved as in the flip-flop shown in Fig. 51-6. In this case, the engraving is done prior to copper deposition and plating. To avoid problems associated with copper deposition and plating inside blind holes, it is recommended that the hole be tapered and have a top diameter at least equal to hole depth.

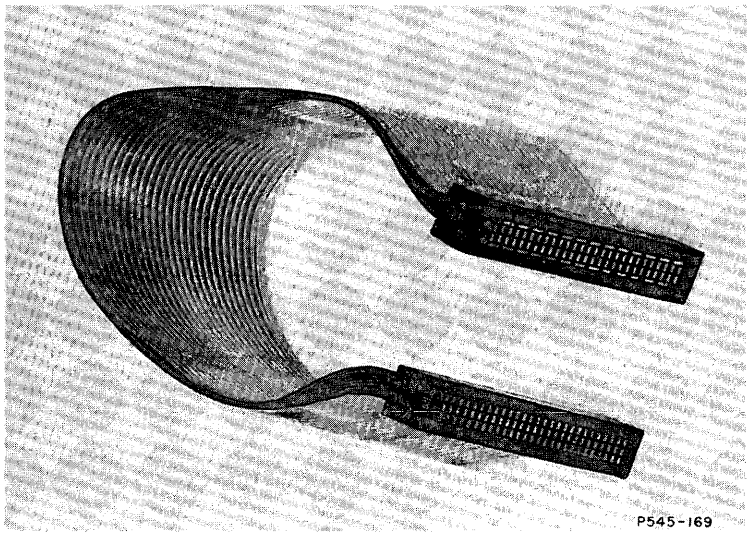

Fig. 51-7. Six layers of tape cable have conductors connected in series by means of plated connections on encapsulated and faced-off ends.

A proposed use for plated connections is illustrated in Fig. 51-7. The conductors in six layers of tape cable are connected in series by means of plated connections formed on embedded and faced-off ends of the cable. Again the conductor pattern can be photoetched or engraved and filled. The technique should be especially useful in coordinate-driven devices employing large numbers of narrow conductors at high densities.

E. A. Guditz

C. Advanced Circuits

1. Fifty Megapulse Logic

Work has started on transistor logic circuits to operate at an effective clock rate in the region of 50 megapulses per second. This is in the speed range that is reasonably compatible with the magnetic-film memories now under development.

An example of a nonsaturating circuit that has been investigated is shown in Fig. 51-8. It makes use of high-frequency mesa transistors in an arrangement that operates the transistor between two points in the active region, thereby maintaining a high-frequency response at all times. This flip-flop responds nicely to 1-volt 5-mμsec pulses separated by 20 mμsec and has a transition time under 10 mμsec.

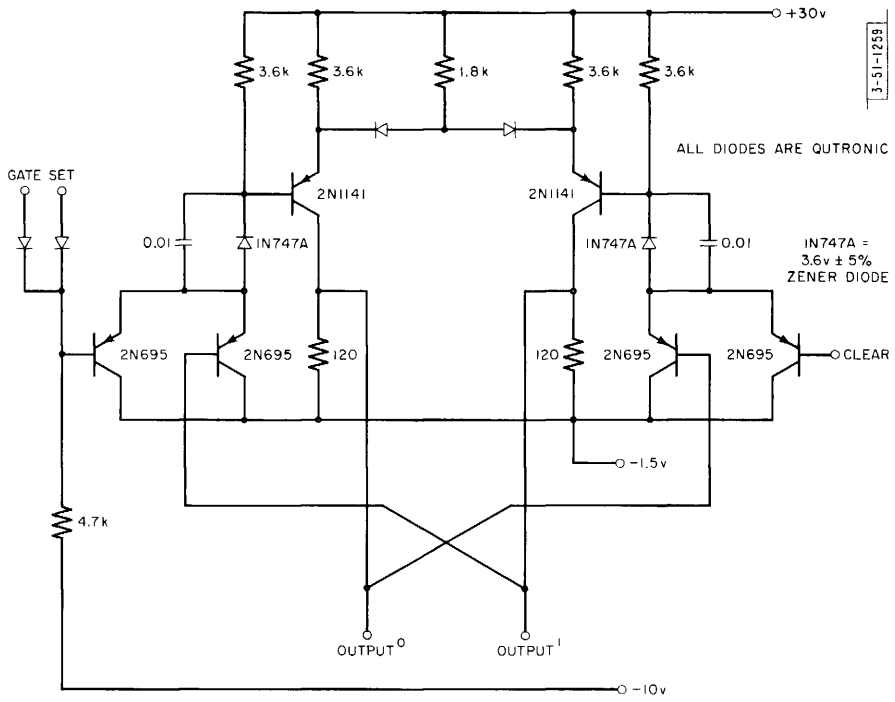

Fig. 51-8. Nonsaturating circuit.

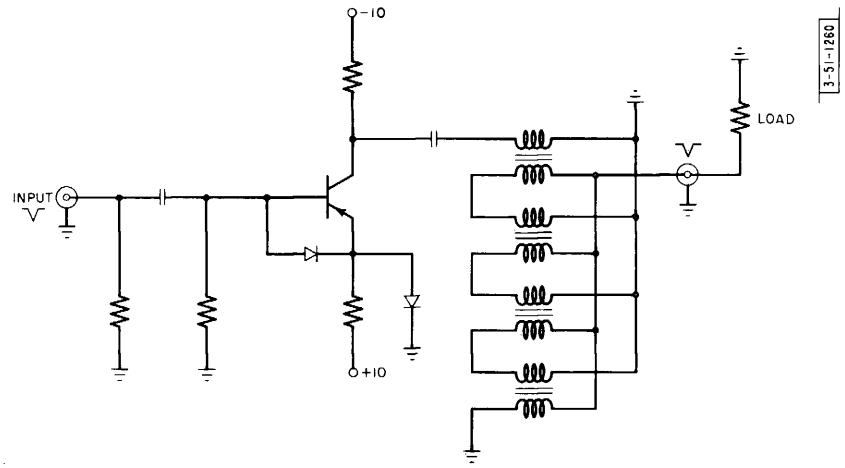

Fig. 51-9. Simple pulse amplifier using 4:1 distributed transformer.

Further work will include saturated DC logic circuits and pulse amplifier logic circuits.

K. H. Konkle

2. Pulse Amplifier

A transistor pulse amplifier for computer logic is simply and efficiently made using an inverting stepdown pulse transformer; fast rise-time pulse transformers suitable for use in a 5-mμsec pulse amplifier are being investigated.

Two important parameters which tend to limit the rise time of an inverting transformer are interwinding capacitance and leakage inductance. One solution is to design the transformer to include the distributed interwinding capacitance and leakage inductance in the transmission line configuration having the same transformation ratio as the transformer.*† A time-delay effect is thus substituted for the less desirable rise-time degeneration. The net result (if the high- and low-frequency ratios are made equal) is a high-frequency response determined by the transmission line characteristics, and a low-frequency response determined by the magnetizing inductance of the transformer operating in the conventional mode. A pulse amplifier with a 4:1 stepdown inverting transformer configuration using four separate, twisted-pair bifilar-wound cores is shown in Fig. 51-9. A rise time of 1.5 mμsec was obtained using a 2N501 transistor in this configuration. The switching time of the transistor was the limiting factor.

L. Neumann

3. Switching Response of a Parametron

Experiments have been performed to verify the calculations by C. T. Kirk‡ of the switching response of a charge-pumped parametron. The calculations were modified slightly to match a practical experimental circuit more closely.

The parametron consists of a circuit parallel-resonant at a frequency ω with one element a variable-capacitance diode. The diode is "pumped" by a charge source varying at a frequency 2ω. Regeneration occurs at a frequency ω. A small current of frequency ω is fed to the parametron to set the oscillation phase before the pump is applied.

A variable-capacitance diode has an incremental capacitance

$$C = \frac{K}{(v + \psi_c)1/n} \tag{1}$$

where v is the applied reverse bias, ψ_c is the diode contact potential, K is numerically equal to the capacitance at $v = \psi_c = 1$ volt and n is a constant depending on junction grading, $2 \leqslant n$. If the pump charge is

$$q = Q_o(1 + \beta \sin 2\omega t) \quad , \quad 0 \leqslant \beta \leqslant 1 \quad , \tag{2}$$

where Q_o is the total diode stored charge at bias voltage V_B and β is the pumping ratio or fraction of possible pump charge, the parametron signal-frequency voltage or current should vary as

$$v_\omega \quad \text{or} \quad i_\omega \propto e^{\alpha t} \sin(\omega t + \varphi) \quad , \tag{3}$$

---

*H. G. Rudenberg, "The Distributed Transformer," Research Division Raytheon Manufacturing Company, 1952.

†C. Winningstad, "Nanosecond Pulse Transformer," IRE Transformer Nuclear Science, Vol. NS6, No. 1 (March 1959).

‡ Division 5 Quarterly Progress Report, Lincoln Laboratory, M.I.T. (15 March 1959), pp. 68-71.

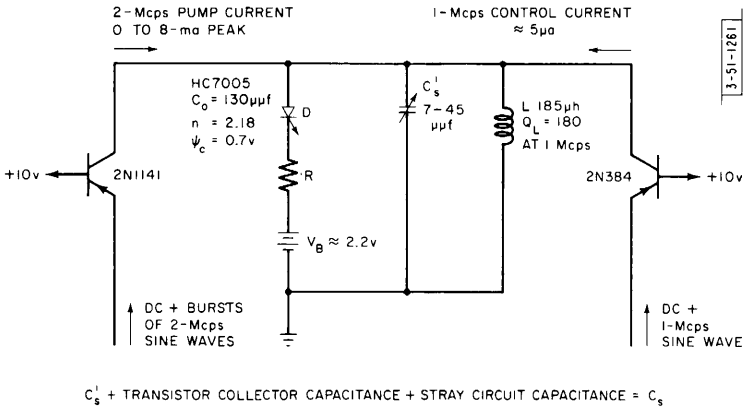

Fig. 51-10. One-Mcps experimental parametron.

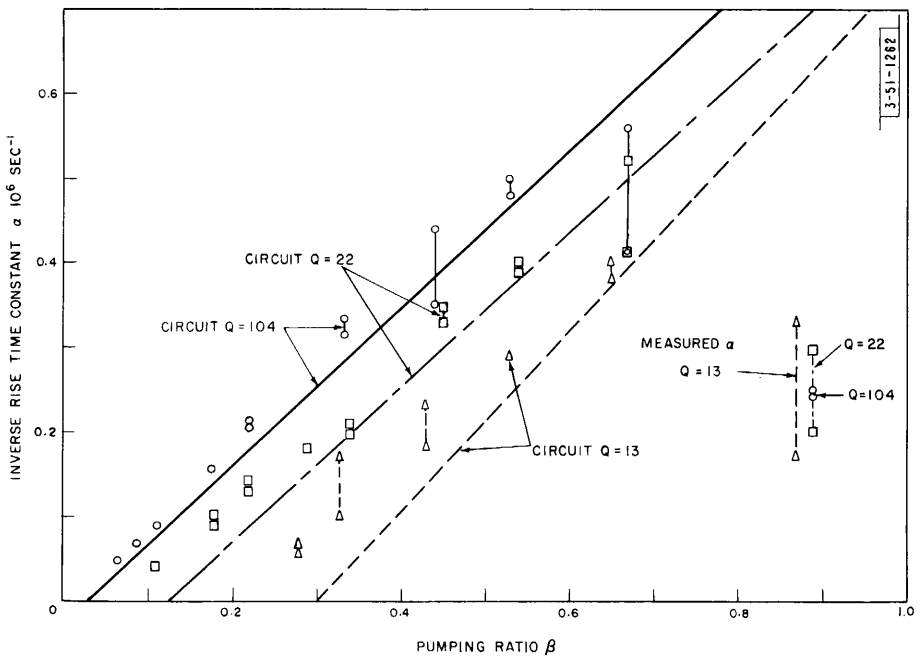

Fig. 51-11. Charge-pumped parametron rise speed. (Lines represent computed speed. Points represent measured speed. Vertical lines show range of measured results.)

where α is the inverse rise-time constant. The inverse rise-time constant is dependent on the phase angle φ. The maximum α is

$$\alpha = \frac{\omega}{2(1 + C_s/C_o)} \left[\frac{\beta}{2(n-1)} - \omega C_o R \right] , \quad (4)$$

or

$$\alpha = \frac{\omega}{2} \left[\frac{\beta}{2(n-1)(1 + C_s/C_o)} - \frac{1}{Q} \right] , \quad (5)$$

where C_o is the diode capacitance at bias voltage V_B, C_s is the circuit capacitance shunting the diode, R is the diode series resistance and Q is the total circuit Q at the signal frequency ω.

The experimental circuit is shown in Fig. 51-10. Low frequencies (2-Mcps pump and 1-Mcps signal) were used for ease of instrumentation. Capacitance C_s was adjusted to be in parallel resonance with inductor L at 2 Mcps so that the 2-Mcps pump current flowed only in the variable-capacitance diode. Diode bias was adjusted so that the entire circuit resonated at 1 Mcps. Bursts of 2-Mcps sine-wave currents were applied as pump. The envelope of the 1-Mcps parametron tank voltage was observed for inverse-rise-time-constant measurements. Measured α's for three different circuit Q's are compared with calculated α's [from Eq. (4)] in Fig. 51-11.

The measured α drops to a low value for $\beta > 0.7$ because the diode is driven far into conduction during part of the cycle. Conduction effects are neglected in the theory, so the calculated α continues to increase with increasing β.

For lower values of the pumping ratio β the measured α is consistently higher than the computed α. This is possibly caused by the presence in the "stray" capacitance C_s of a small additional nonlinear capacitance in the form of the collector capacitances of the pump and control-current-source transistors.

C. E. Woodward

III. MAGNETIC-FILM ENGINEERING

A. TX-2 Configuration Memory

During the middle of July, the magnetic-film configuration memory was installed in TX-2 (Figs. 51-12 and 51-13). The memory-to-computer connections were made pluggable to permit rapid exchange with the fixed configuration memory.

Initial testing produced rather poor results which were traced to the disturbing of "zero's" by write currents on adjacent lines. Reducing the write current to a level that did not disturb a "zero" into a "one" state, made it impossible to write in some films. New films having lower outputs but higher wall coercive force (H_c) were tried. This cleared up the write disturbing, and readjustment of read currents took care of minor read disturbing which had been observed. The sense amplifiers had sufficient gain to accommodate the lower film outputs which were on the order of 0.5 – 0.7 mv.

A program was written to check spot-by-spot read-write disturb levels comprehensively and automatically. The memory is examined bit-wise by surrounding the check-bit holding a "zero" with all "one's". The "one's" are read and rewritten for the number of times specified in toggle-switch storage. At the end of this cycle, the "zero" check-bit is read and checked to see if it has been disturbed into a "one" state. The opposite check can be made for read-disturbing. Margin checking of all plug-in units has been provided, and the margins are quite good throughout.

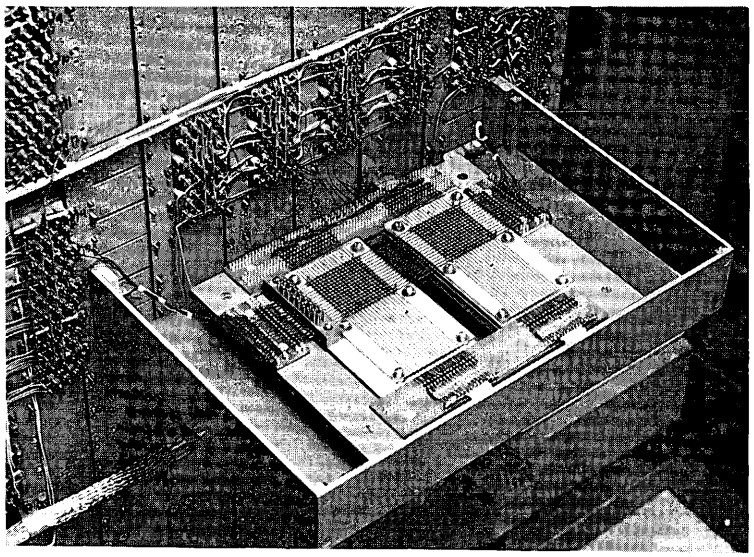

Fig. 51-12. Magnetic-film memory operating in TX-2 computer. The cover is removed, showing 32 word-lines (in two halves) running parallel to the short dimension of the rectangular case, and the 16 orthogonal bit-lines, the best ten of which are in use.

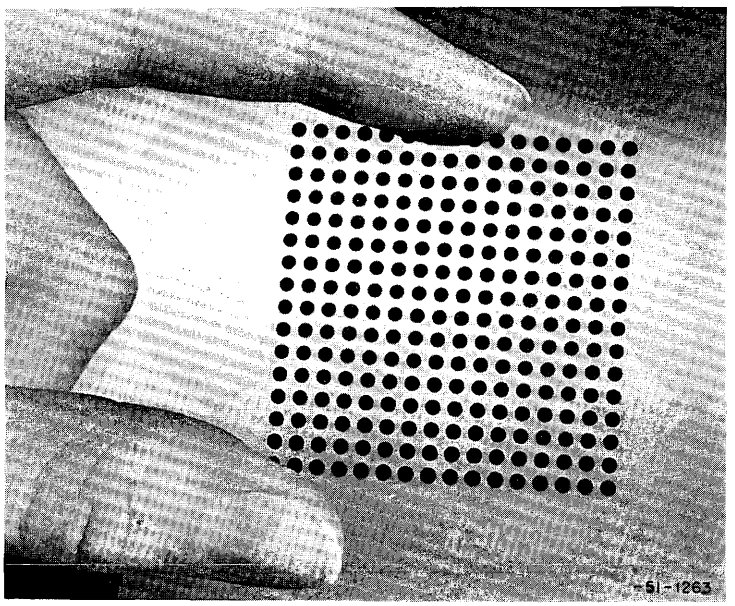

Fig. 51-13. One plate of 16 × 16 permalloy spots is sandwiched in each half of the wiring of Fig. 51-12. Each spot is 1/16 inch in diameter and about 600 Å thick. The best ten rows of spots of each plate are used; the remaining rows remain as spares.

The memory has been in use for approximately one month. During this period, two instances of information loss have been recorded.

T. O. Herndon

B. Film Fabrication

1. Ionic Bombardment Cleaning

Ionic bombardment cleaning of glass substrates is being investigated. Argon is introduced at a rate that maintains 50 to 100 microns pressure. The substrate is held at a negative potential of about 500 volts resulting in a current density of approximately 2 ma/inch^2. This requires that the exposed substrate holder be of a material having a low sputtering rate such as tantalum. The glass substrate is then removed from the bell jar, and observed by a breath test. Excellent cleaning is observed after a bombardment as short as six seconds. Under subsequent high vacuum, visible recontamination begins to occur within 30 minutes following cleaning. Preliminary tests on films deposited on ionically cleaned glass indicate better uniformity and closure of the loop in the hard direction.

T. S. Crowther

2. Electrodeposition

The subcontract at General Electric has been producing arrays of $\frac{1}{16}$-inch^2 spots. We have tested some of them in both looper and pulse tester and find uniformity to be encouraging. At present, it is necessary to make the permalloy about 400 Å thick (slightly thinner than in vapor deposited films) in order to obtain the desired ratio of H_c/H_k and both H_c and H_k are about 1.5 times as high as in vapor-deposited films.

A new unit, which will permit annealing as well as sputtering, has been installed in one of the vacuum systems; recorders to monitor current and voltage during sputtering have also been added. Equipment is nearing completion to make possible the application of a rotating magnetic field during plating.

D. D. Strassberg

C. Testing and Instrumentation

The second hysteresis looper is in operation and its performance is satisfactory. It can be operated at higher gain than the old, probably because of slight differences in winding the pickup coils. We are attempting to increase the sensitivity of the first looper by replacing its coils.

Techniques for looping arrays of $\frac{1}{16}$-inch-diameter permalloy spots one spot at a time are under study. Because of the geometry of the fringing fields, a pancake configuration is indicated for the pickup coil to eliminate adjacent spot pickup. This requires the use of a transformer to step up the coil output to the point where it is above the noise level of the preamplifier. With this technique we have been able to loop 16 spots at once, but more gain is required before measurements on a single spot are practical.

D. D. Strassberg
J. Raffel

D. Circuits

A second pilot model of the 128-position diode matrix switch has been constructed and evaluated. In this model a ground plane is used as an electrostatic shield to reduce capacitive coupling between the matrix conductors. As a result, switch transients have been reduced considerably and clean signals are obtained at the output.

H. Blatt

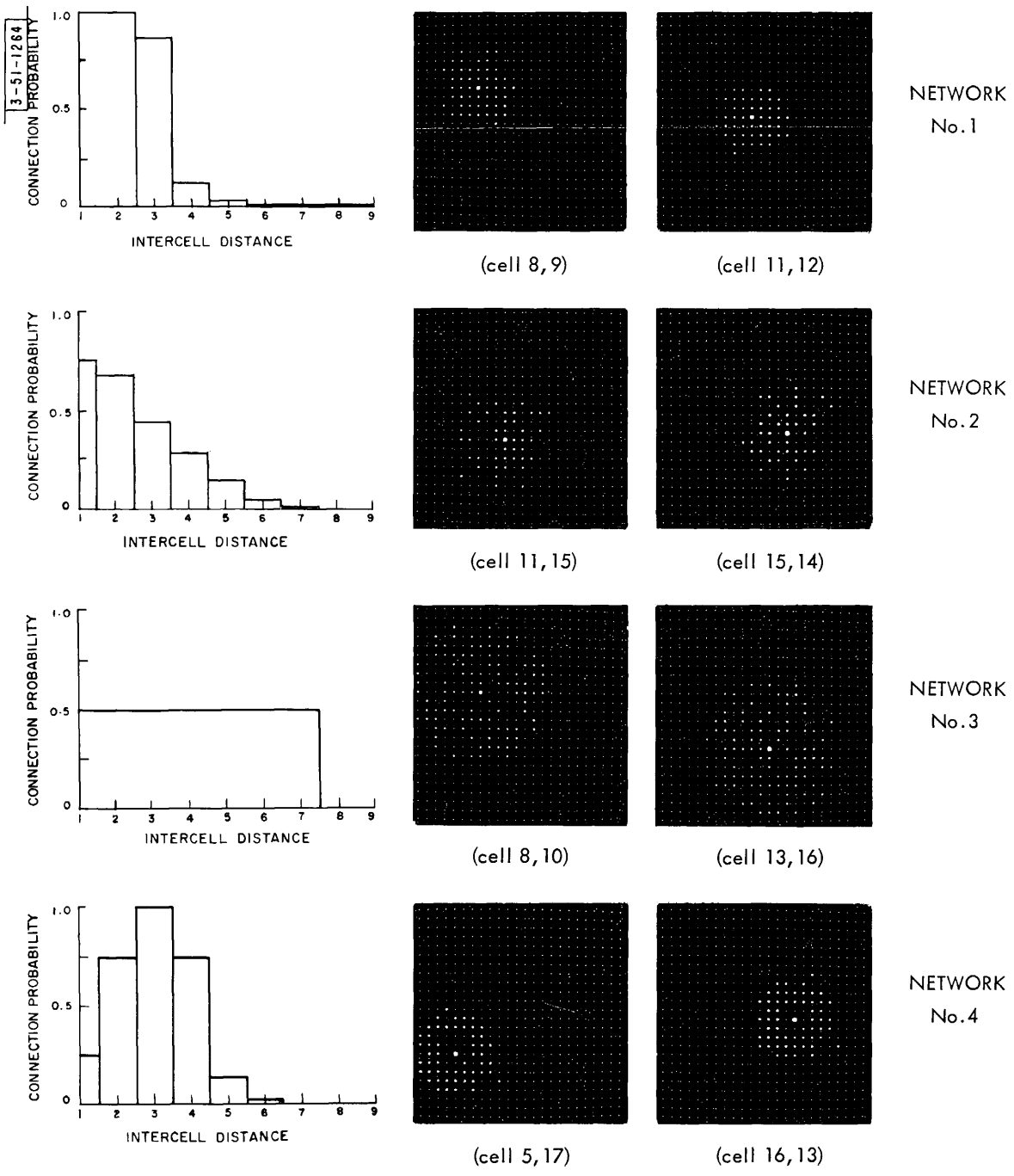

Fig. 51-14. Input connections to representative elements in four different isotropic neuronlike networks. 24×24 element networks formed in accordance with the indicated connection probability functions. Representative cells are shown as heavy dots, surrounding cells which connect to, and hence are capable of exciting, these designated cells are shown as dots of medium size. All other cells in each net are shown as light dots.

E. Fixed Storage Using Films

A storage sense-line similar to the paper mockup shown in the last quarterly progress report, but with a capacity of 256 words, has been assembled and is ready for test. "One"-to-"zero" signal ratios of 10:1 have been measured with a sense-line containing one word. However, with a word density of 100 words/inch^2 adjacent-word pickup degrades this ratio to about 3:1.

A. H. Anderson

IV. INFORMATION PROCESSES

We are continuing the study of networks of interconnected nonlinear elements described in earlier reports.* Abstract networks of the kind studied are suggestive of physiological neuron networks but the resemblance is, of course, a superficial one. The present work is directed toward gaining a better understanding of the properties of a particular class of such networks, namely, the class of two-dimensional isotropically connected arrays (i.e., arrays in which the probability of connection between any two elements is a function only of geometrical distance between those elements). The elements themselves are somewhat simpler than those of the earlier work. They are excited by activity introduced into the network from external sources and by activity received from other elements within the net. An element "fires" whenever the level of excitation presented to it exceeds its threshold. When an element fires, its threshold rises to a relatively large value from which, after a short delay, it decays exponentially to its quiescent value. Furthermore, at some short time after firing, an element transmits one unit of excitation to each element to which it is connected. Excitation received at each element is additive, and the sum decays exponentially toward zero with time. The quiescent threshold value is the same for all elements in the net.

A simulation program for the TX-2 which can accommodate networks of 1296 elements has been written and operated on a limited basis. This program constructs a net by forming a connection matrix based on a specified probability function of the distance between network elements.

Two representative cells in each of four different 24 × 24 nets constructed by the program are shown as heavy dots in photographs of the TX-2 display (Fig. 51-14). Surrounding cells which connect to, and hence are capable of exciting, these designated cells are shown as dots of medium size. All other cells in each net are shown as faint dots. Connections in each case are formed in accordance with the indicated connection probability function.

After a network is thus formed and stored in the TX-2 memory, activity is introduced at a designated set of elements and the processes of excitation, firing and transmission are simulated. After each time step of the calculation, the resulting activity present in the net is displayed and stored for future redisplay and analysis. Figure 51-15 illustrates the kind of behavior encountered in a particular network with periodic external stimulation. Several different modes of activity apparently can be set up and have yet to be explained fully. No quantitative data have been obtained as yet. Experiments to determine the conditions under which coherent patterns of activity are sustained and to measure rates of propagation and number of active elements are planned.

W. A. Clark L. Roberts
B. G. Farley A. Vanderburgh

---

* B. G. Farley and W. A. Clark, Group Report 51-3, Lincoln Laboratory, M.I.T. (31 March 1959) (not generally available).

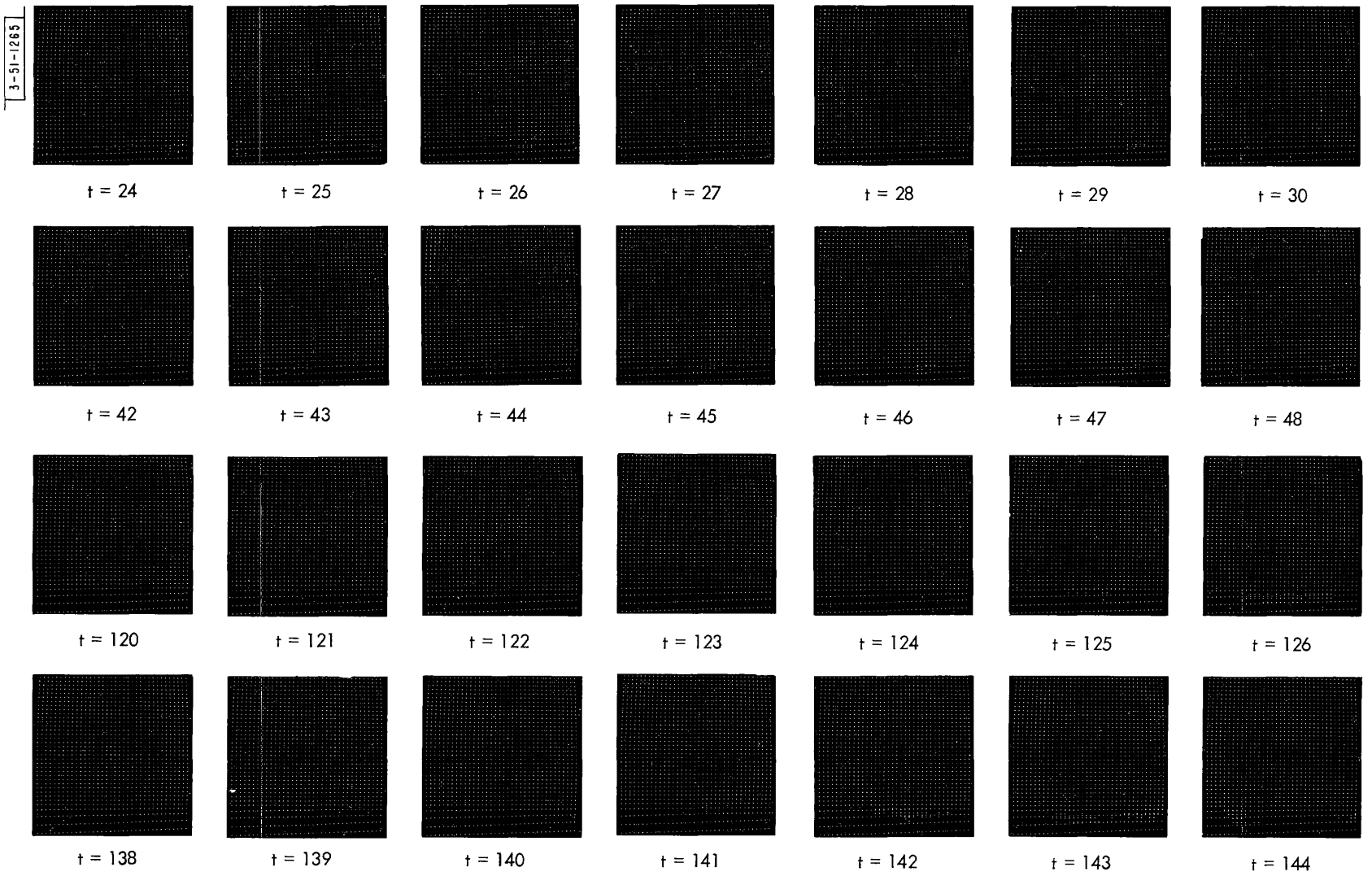

Fig. 51-15. Activity patterns in a periodically stimulated 36 × 36 element network (connection probability = 0.25 for intercell distance ⩽ 4 units). A small group of central cells are externally stimulated at six time-unit intervals. Active cells at each time step are shown as heavy dots; other cells are shown as light dots in the 36 × 36 element array (irregularity of spacing is caused by malfunctioning of the film transport mechanism).

DATA PROCESSING
GROUP 52

BIVANS, E. W., *Leader*
DINNEEN, G. P., *Assistant Leader*
WOOD, R. V., Jr., *Assistant Leader*

AHO, E. J.
BINSACK, J. H.
CHATTERTON, E. J.
DUMANIAN, J. A.
ESHLEMAN, D. B.
HARRIS, J. N.
HOFHEIMER, R. W.
HOROWITZ, R. M.
KOLB, J. M.
LEBOW, I. L.
LONG, W. H.
LYON, E. F.
NAGY, F., Jr.
PARKER, A. C.
PERRY, K. E.
POPP, F. G.
REINECKE, H.
SFERRINO, V. J.
TANCRELL, R. H.

DATA PROCESSING .
GROUP 52

I. MEMORY DEVELOPMENT

A. Magnetics Research

Mathematical models have been proposed to describe the partial switching process in ferrite cores, as reported in the Division 5 Quarterly Progress Report for 15 June 1959. Programs have been written for the CG 24 computer to solve these equations, and solutions have been obtained for special cases of core size and drive current. With this program it is possible to find the switching waveform for different regions of a core as well as the switching waveform for the whole core. The percentage of flux switched in different regions of a core under partial switching conditions can also be obtained. Comparison between the calculated and experimental results shows agreement to within 10 per cent for a core of 0.215 inch o.d. with four small sense holes drilled into the body of the core for sensing the flux change of the different regions.

Experimental equipment has been set up for observing the AC output of a partially switched ferrite core in the frequency range of 10 Mcps. Cores of several different materials have been examined. Work is now in progress to study the core response to very narrow drive pulses of less than 0.1 μsec in width.

R. H. Tancrell

B. High-Speed Memory

Assembly of the high-speed memory system continues. A new system of sequential address clocks was developed in order to reduce the duty cycle of the clock drivers. A set of four clocks, shifted in time, is derived from a matrix arrangement which is shown in the system block diagram (Fig. 52-1). A p clock and an s clock are generated by the p and s matrices, respectively. The p clock turns on the first read-write driver of a subset composed of 260 drivers.

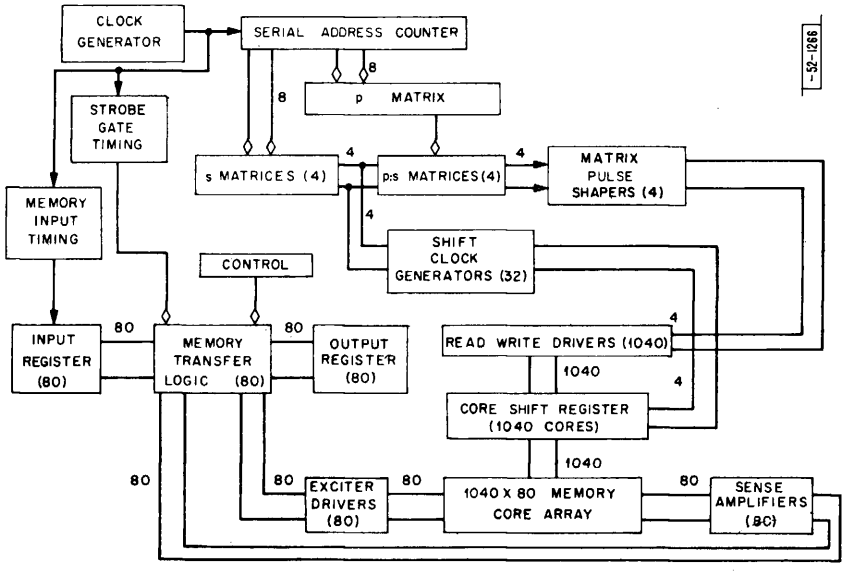

Fig. 52-1. Block diagram of high-speed memory.

This sets up the switch core in that word line whereupon the sequential address is advanced by the application of the corresponding s clock to the switch core shift register line. There are four sets of p and s combinations arranged as follows: p_1s_4, p_2s_3, p_3s_2, p_4s_1. The shift clock driver was modified in order to use the 2N504 in place of the 2N501 because the availability of the latter transistor is presently rather poor. Figure 52-2 is a diagram of the modified shift clock driver.

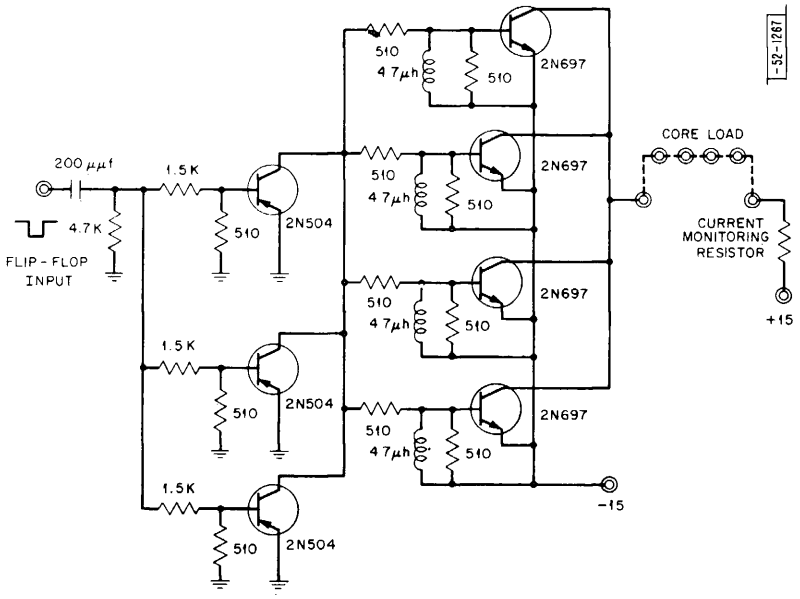

Fig. 52-2. Shift clock driver.

About 260 words have been operated in the memory and the addition of words is proceeding smoothly. Some work of establishing an optimum impedance value for shunting the sense and exciter windings was necessitated by the complex nature of the impedance of these windings. If the lines are improperly terminated occasional ringing is encountered. The optimum impedance is chosen to damp the ringing and not contribute any recovery problems. A total of eight bit channels has been set up with sense amplifiers and exciter drivers. The performance of these channels is being evaluated to establish the operating margins under various memory modes. Because of the length of the sense windings for the complete array of 10 core assemblies, the input clip level on the sense amplifiers was lowered by the addition of two bias resistors at the base of the input transistors.

A paper* describing the memory system has been written and was presented at the Western Electronics Conference on 18 August 1959.

V. J. Sferrino

C. Circuit Research

Since p-n-p-n 4-layer diodes have been utilized as core driving elements in a memory system, it has become more important to be able to predict the applicability of these devices to other circuits. An investigation was initiated to look into the characteristics of the Shockley

* V. J. Sferrino, "Transistor Circuit Techniques for a Core Memory with 500 Millimicrosecond Cycle Time," 1959 WESCON Convention Record.

4-layer diode in order to understand their operation better. The immediate goal of this investigation might be the design of a high-speed random-access driver using p-n-p-n devices. The static voltage-current characteristics of a typical Shockley diode is shown in Fig. 52-3.

The characteristics of interest in the p-n-p-n devices which are being investigated include the breakdown voltage V_b, the sustaining current I_s, the static resistance R, the turn-on time, the storage time and turn-off time. From one of these, or from a combination of more than one, it is hoped that further insight will be gained into the basic operation of the Shockley diodes.

To facilitate matters, several Shockley diodes known to have unsuitable characteristics for the high-speed memory are used in these tests. The breakdown voltage and the sustaining current for a number of Shockley diodes were noted. The breakdown voltage varied from 39 to 57 volts (with a peak in the distribution near 52 volts) and the sustaining current varied from 4.6 to 22 ma. However, no conclusive results could be obtained to correlate them with other memory operation.

In order to determine whether or not the turn-on time of the Shockley diodes had an important effect on their operation in a memory, the test circuit in Fig. 52-4 was used. Normally the

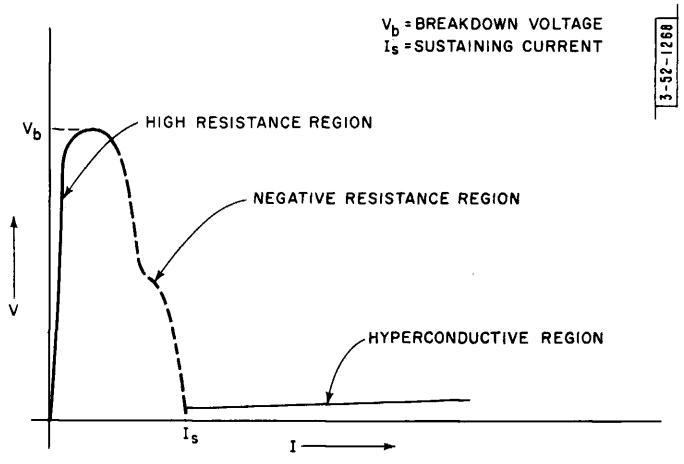

Fig. 52-3. Static voltage-current characteristic of Shockley diode.

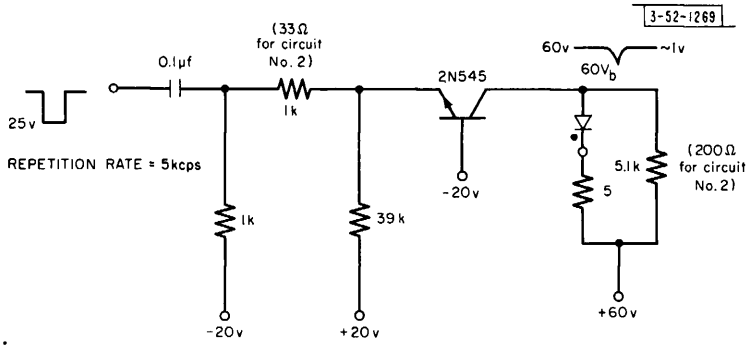

Fig. 52-4. Test circuit No. 1.

transistor is biased off with the emitter sitting approximately at −18 volts. When an input pulse occurs, the transistor starts to conduct and current flows into the collector through the load R, thereby dropping the collector voltage. When this collector voltage drops sufficiently, the voltage across the Shockley diode is sufficient to break it down. Accordingly, the turn-on time of the diode is seen, and also the current that the diode delivers by inserting a 5-ohm monitoring resistor in the circuit. This circuit operates at a low current level. There was no discernible correlation between performance of the Shockley diodes in the memory and the waveforms obtained. It will be noticed that the test circuit is operated at low current level. To raise the current level, the input resistor (1 k) and the load resistor (5.1 k) were lowered (as illustrated). In this way more current was supplied to the diodes and the apparent turn-on times decreased. This is apparently due to the increase in the rate of rise of the current source at the higher current level.

A useful tool in the analysis of the p-n-p-n device is a time vs impedance plot. This can then be correlated with the (DC) steady state characteristics and might give a clue as to why the device cannot be characterized, with respect to memory performance, from only the DC test. To do this, it was necessary to make a good pulse voltage source. Figure 52-5 is the circuit that gives the desired results.

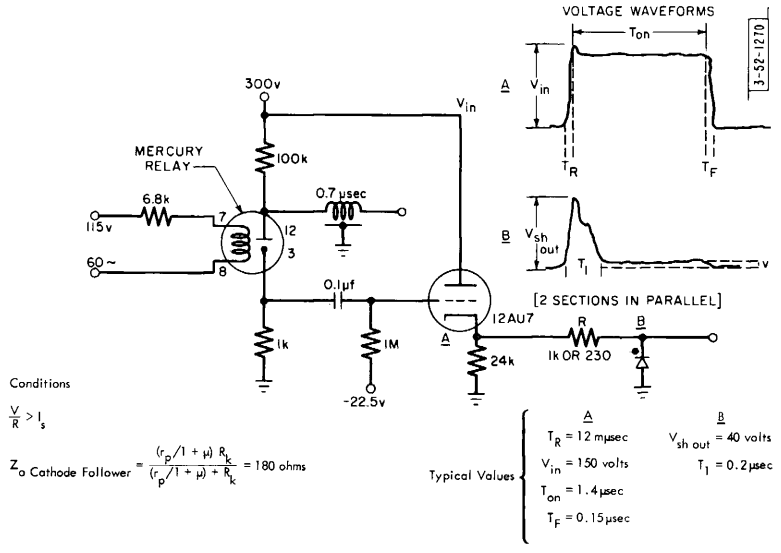

Fig. 52-5. Test circuit for impedance vs time plot.

The open ended delay line (0.7 μsec) gives us a 1.4-μsec pulse due to the reflection back down the line. The 1 k is the characteristic impedance of the delay line. The cathode follower is used for impedance matching. Essentially then, we have a voltage source driving the Shockley diode. The limiting resistor R is such a value as to keep $150/R > I_s$. Thus we see the voltage output of the Shockley diode with respect to time. The impedance vs time plots are obtained in the following manner:

at any instant

$$\frac{V_{in} - V_{sh}}{R} = I_{sh} \qquad \frac{V_{sh}}{I_{sh}} = R_{shockley}$$

In the above manner we are able to plot a curve of the static resistance of the device vs time, and hence consider the p-n-p-n diodes in a static mode. Diodes with different memory characteristics are being plotted in an attempt to ascertain whether the static resistance (static in the sense that we concern ourselves with only one point in time) has an important effect on the behavior of the diodes. Noticeable differences appear in the voltage output. The slots of impedance vs time illustrate this, but no conclusions have been drawn. Work continues on this approach. Figures 52-6 and 52-7 are impedance vs time plots for two Shockley diodes. For each diode, there are two curves representing the two values of R used.

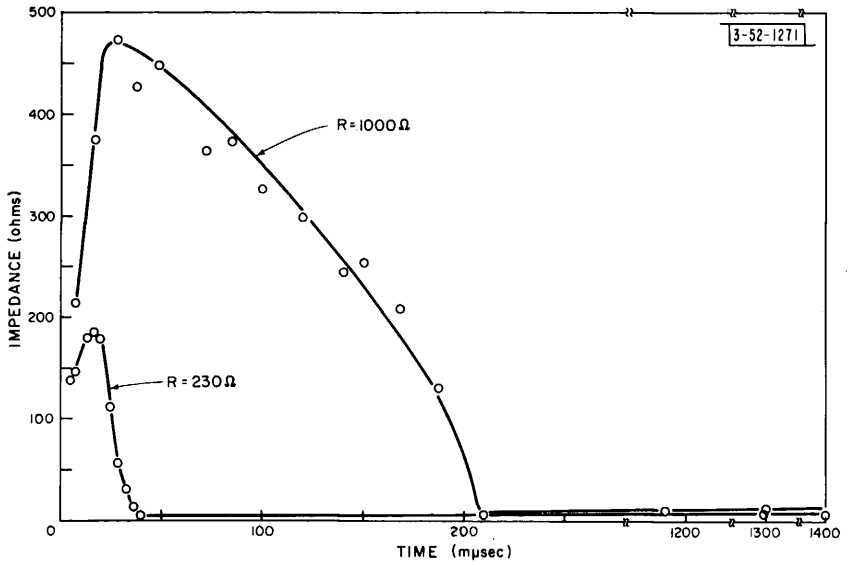

Fig. 52-6. Impedance vs time plot – Shockley diode No. 17.

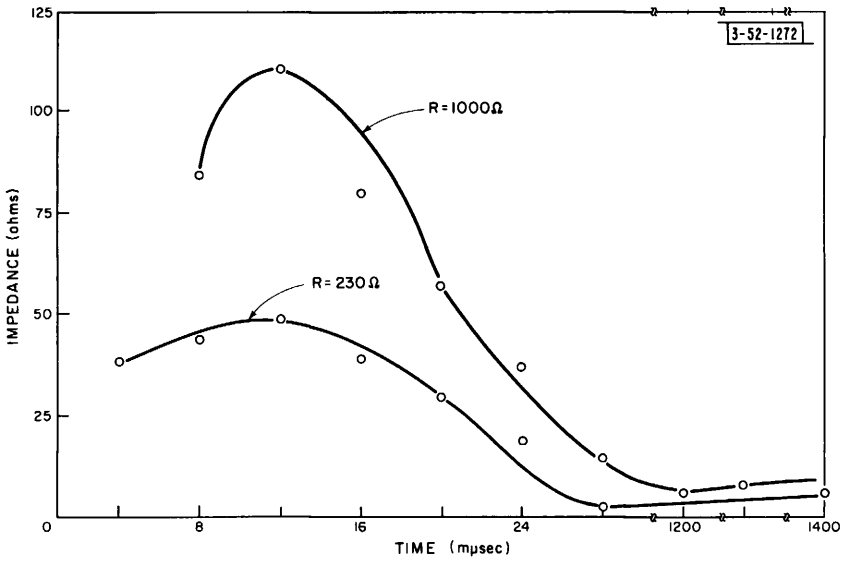

Fig. 52-7. Impedance vs time plot – Shockley diode No. 34.

Work is being conducted with the Shockley 4-layer diode to understand more completely their operation. Investigation of various characteristics such as breakdown voltage (V_b), sustaining current (I_s) and turn-on-time, have not resulted in any correlation between the units under test and memory operation. Static resistance tests (Z vs time plots) are currently being run. Work will be continued on turn-off time and storage time phases.

R. M. Horowitz

II. DIGITAL DATA TRANSMISSION

In the digital data transmission area, work has continued on ECCO (error checking and correcting coder). This machine, which encodes a 64-bit word into a 128-bit transmitted message with sufficient redundancies so that up to seven transmission bit errors can be corrected, is nearly complete. Some of the theoretical work that supports this project, as well as some further details on circuit design, are reported below.

G. P. Dinneen

A. Probability of Error in Group Codes

Two programs for CG 24 were written: the first computes various binomial coefficients for use in Hamming and Gilbert bound determinations; the second computes the standard deviations for all numbers in the range $1 \leqslant n \leqslant 256$ and for probabilities $p = 0.01 - 0.50$ in 0.01 steps. If A_n^k is a group code with k message bits and n-k check bits, and if e_1 and e_2 represent the maximum and minimum number of errors, respectively, which the best code A_n^k can correct, then the Hamming bound is

$$2^{(n-k)} \geqslant \sum_{r=0}^{e_1} \binom{n}{i} ,$$

and the Gilbert bound is

$$2^{(n-k)} \geqslant \sum_{i=0}^{2e_2} \binom{n}{i} .$$

An application of the above to the Reed code Φ_3^7 yields $e_1 = 15$, $e_2 = 7$.

An analysis of the error correcting probabilities for the Reed codes and several simpler types of codes, for example, codes that consist of repeating the message three times, was performed showing the Reed codes to be superior when the channel transition probability is less than 0.1.

Work is in progress on a program for CG 24, which simulates the Reed encoding and decoding procedures for the code space Φ_3^7. The results are to be applied to a determination of the partial error correcting properties of the code space Φ_3^7. That is, we seek to find the probabilities that errors of order 9 and greater are corrected.

S. Shatz

B. Error Correcting Coder Circuits

Accessory circuits involved in the operation of the ECCO system have been designed and are being constructed. These include circuitry for counting the errors in the channel, and a servo system for timing synchronization.

The basic timing is provided by a tuning fork oscillator at the encoder. The use of a local timing standard at the decoder provides continuity of timing in case of short-term drop-outs or errors in the received timing. If the received timing itself were used to clock the decoder, the loss of a cycle could throw the decoder out of synchronization with the incoming words, causing incorrect decoding of the Reed code.

The two tuning forks are matched in frequency to 0.01 per cent. A servo system, shown in Fig. 52-8, is used to compensate for small frequency differences. The incoming timing signal and the local signal are fed to the two windings of a 2-phase servo motor. When the two inputs are in phase, no rotating field is produced, and there is no motion. If one signal lags the other, the motor rotates, driving a resolver through a 1000:1 reduction gear. The resolver shifts the phase of the local signal to eliminate the phase difference.

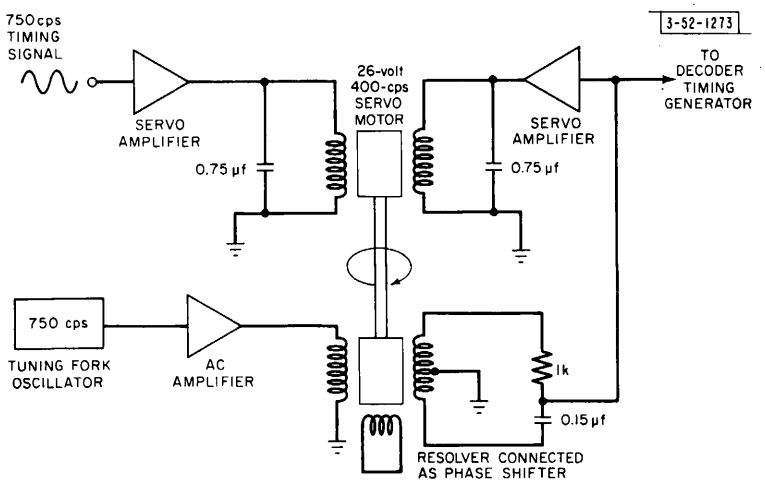

Fig. 52-8. Servo system for timing synchronization.

Thus a frequency difference between oscillators will cause a continuous rotation of the resolver, at a rate sufficient to equalize the frequencies. If the incoming signal drops out, the inertia of the motor will tend to maintain the same correction. When the signal returns, the local timing source will lock in correctly, provided that less than 90° phase difference has accumulated.

The method of phase comparison in the motor itself has a number of advantages over the more conventional method using a phase detector with a DC output. No DC amplifiers are needed. It is not necessary to chop a DC error signal to recover an AC signal to operate the servo motor.

Some disadvantages are also apparent. The error signal is not available electrically, making damping and rate control difficult. The servo amplifiers must have equal phase shift, to avoid error. Changes in the operating frequency are limited by the characteristics of the servo motor. For a specialized application, however, the present system is simple and effective.

D. B. Eshleman

III. COMPUTER COMPONENTS

A. High-Speed Computer Circuits

For several months we have worked on pulse-no-pulse logic circuits using capacitor storage. During this past quarter other approaches to the high-speed circuit problem were investigated, resulting in the development of an "impulse logic" circuit which seems well suited for use as a high-speed computer module.

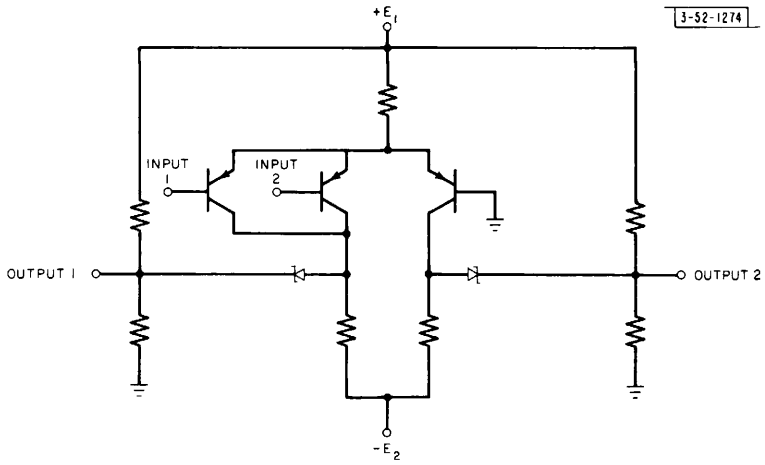

Fig. 52-9. Current switching logic module.

The first approach considered was described in a paper on current switching circuits.* The essence of this paper is the "nor" DC logic module shown in Fig. 52-9. Two interesting techniques are incorporated in this circuit:

(1) The technique of switching a current of controlled amplitude by means of small signal voltages applied to the bases of the transistors.

(2) The technique of level shifting by using a Zener diode in which the value of the breakdown voltage is not critical.

Without going into the details of operation of this circuit, we shall mention some of the advantages and disadvantages.

Advantages

(1) Transistors are not operated in or near saturation.

(2) Signal voltage swings are small.

(3) Voltage and current amplitudes can be closely controlled.

(4) Circuits are direct coupled, and can therefore be operated at any speed below their maximum. Circuit design can be on a DC basis.

Disadvantages

(1) The circuit dissipates a relatively large amount of power in: (a) the resistors used in the constant current generators, (b) the transistor, since it is operated out of saturation, and (c) the Zener diode.

(2) The relatively high base-to-emitter capacitance of high-speed switching transistors imposes a relatively heavy load on signal or clock sources.

(3) Items 1(b) and 2 place severe limitations on the number of logic units which can be driven in parallel.

(4) A flip-flop that includes means for gating the clock requires eight transistors.

* H.S. Yourke, "Millimicrosecond Transistor Current Switching Circuits," IRE-AIEE Conference on Transistor and Solid State Circuits, University of Pennsylvania, February 1957.

Despite the advantages of the circuit of Fig. 52-9, we felt that an attempt to incorporate it into a large system would be accompanied by severe practical difficulties. A circuit was then sought in which the advantages of current switching could be combined with the advantages of pulse-no-pulse dynamic logic. We used the concept that the impulse response of a properly designed low-pass Bessel filter has a shape that is well suited for gating another impulse. This technique was first used in a logic system called "di-pulse logic."*

Figure 52-10 shows a functional diagram of a typical impulse logic module, and an abbreviated symbol; Fig. 52-11 shows the corresponding schematic diagram. The symbol T denotes the time between two successive clock pulses. Figure 52-12 shows the signal waveforms corresponding to a typical serial logic sequence. Such a sequence might occur at any of the input (A_t, B_t, C_t) or output (R_{t+T}, $\overline{R}_{t+T}$) terminals of the logic module.

In Fig. 52-11, the operation of the circuit is as follows: A sine wave voltage applied at the clock terminal switches transistor T_1 on and off. While transistor T_1 is off, capacitor C_1 charges via the 1.5 K resistor. If logic signals A_t and B_t are both "high" (+1 volt) when transistor T_1 turns on, an impulse of current will flow through transistor T_4, and a redistribution of charge will take place between capacitors C_1 and C_3. For the other three possible configurations of the logic signals A_t and B_t, the charge redistribution takes place between capacitors C_1 and C_2. The two low-pass filters are Bessel filters. They provide both delay and pulse shaping. The responses (R_{t+T} and $\overline{R}_{r+T}$) of these filters to various input impulse patterns are typified by the logic signal waveform shown in Fig. 52-12. These responses are the logic signals transmitted between logic circuit modules.

For the following reasons the Bessel filter impulse response curve is almost ideal for a logic signal:

(1) It starts to rise gradually, and it starts to fall gradually. This avoids the "race" problem which arises in conventional DC logic.

(2) Since the response is delayed, the filter can store information.

(3) The peak of the response curve is broad, permitting timing tolerances between the impulse and the signal gating it.

(4) The response curve is smooth, and should have relatively low harmonic content. This makes it useful at high repetition rates.

(5) The "tail" of the pulse dies away quickly with no ringing. Hence it does not interfere with the next succeeding pulse.

One of the design parameters of the Bessel filter as used in impulse logic is the clock pulse repetition rate. An impulse logic module must be operated at the clock rate for which its filters were designed. The module shown in Fig. 52-11 was designed for a clock rate of 20 megapulses per second. In all tests made so far, this module has operated with satisfactory margins.

It is interesting to note that, although impulse logic is dynamic, it can use DC circuits to advantage. For example, the circuit of Fig. 52-11 is essentially direct coupled. Furthermore, the input and output logic signals of the circuit of Fig. 52-11 are compatible with those of the circuit of Fig. 52-9. Thus in applications requiring the generation of logic functions, but no storage, circuits of the type shown in Fig. 52-9 can be used. Output signals from these circuits can be transmitted directly to impulse logic modules for further processing.

In addition to the work on logic modules, work was also done on pulse generators with high repetition rates. Circuits were sought which would generate pulses of 1- or 2-volt amplitude

---

*K.E. Perry, Group Report 52-7, Lincoln Laboratory, M.I.T., 25 June 1959.

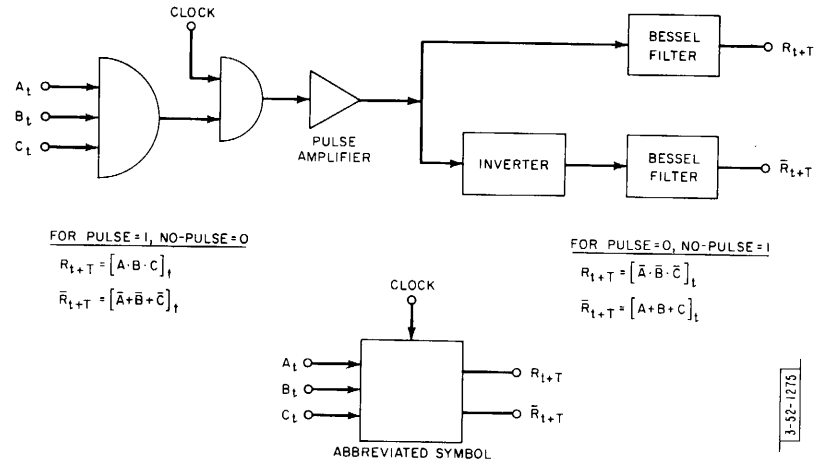

Fig. 52-10. Functional diagram of impulse logic module.

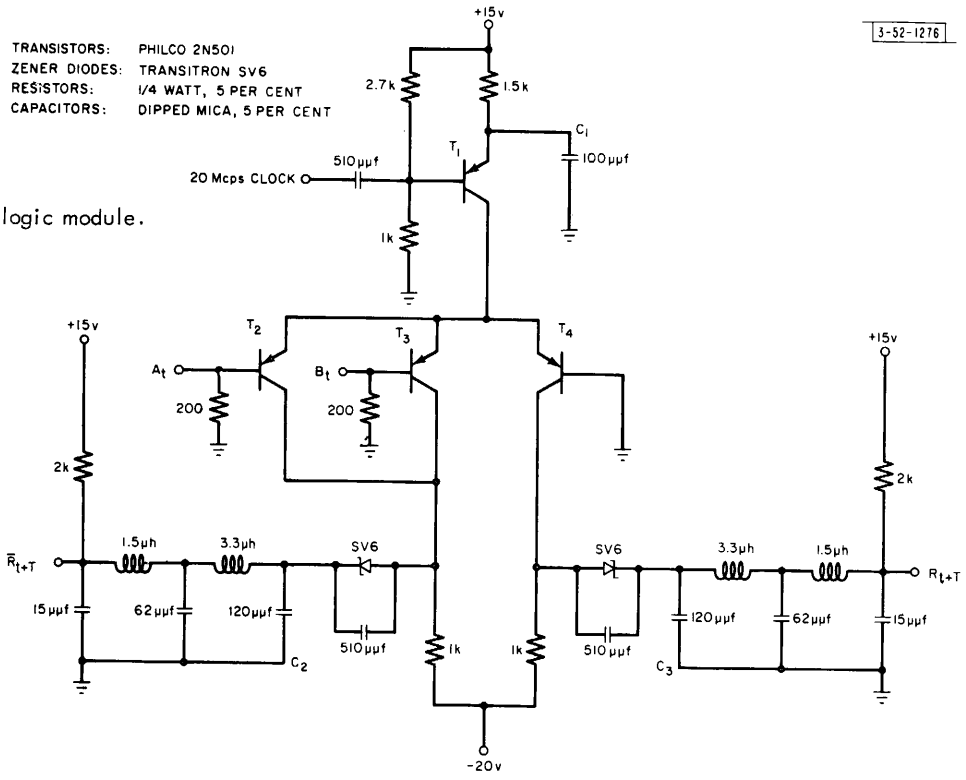

Fig. 52-11. Impulse logic module.

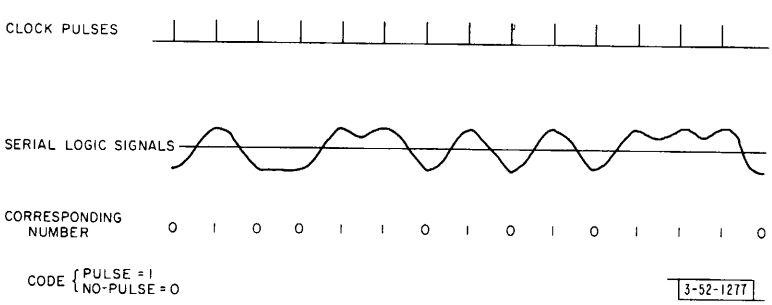

Fig. 52-12. Typical logic signal waveform.

across relatively low impedances. Three approaches were investigated. In all the approaches, the circuits are essentially sine-to-pulse converters. All produce suitable pulses.

In the first approach the circuit of Fig. 52-9 is used as an overdriven amplifier to produce a square wave. Two such square waves having a suitable phase relationship are overlapped to produce the desired pulses. This technique is similar to that described in the Division 5 Quarterly Progress Report for 15 March 1959, pp. 37-39. The main disadvantage of the circuit is the large number of components required.

The second approach makes use of the clock pulse generator portion of Fig. 52-11. Only transistor T_1 and its associated circuitry is required. The collector of T_1 would return to a negative voltage via a load resistor. The output pulse would be developed across this resistor. For generating pulses of constant width and repetition rate, this appears to be a good method.

The third approach is an overlap technique. However, sine waves are overlapped, instead of square waves. A circuit that operates in this way is shown in Fig. 52-13. Figure 52-14 is a photograph showing the packaging of the circuit of Fig. 52-13. Figure 52-15 shows a typical output waveform. The advantages of the circuit of Fig. 52-13 are circuit simplicity, and ease of changing pulsewidth, amplitude and repetition rate.

J. H. Binsack
R. W. Hofheimer
K. E. Perry

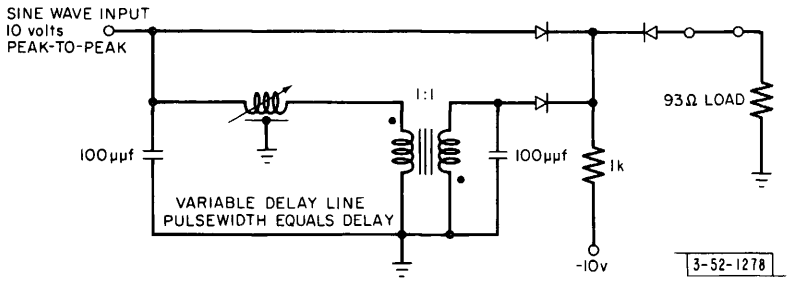

Fig. 52-13. Pulse generator using overlapping sine waves.

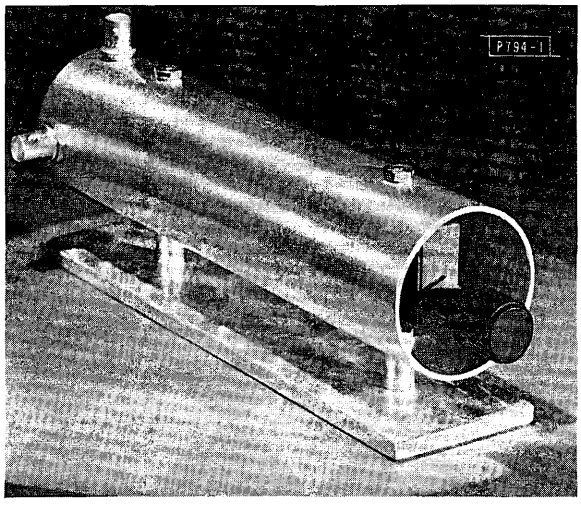

Fig. 52-14. Photograph of pulse generator.

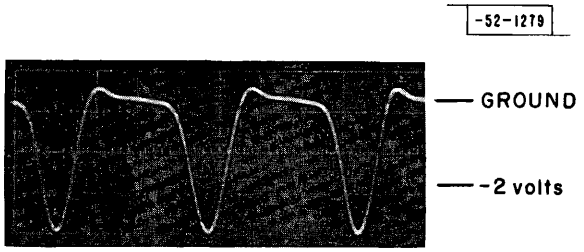

SWEEP SPEED:
20 mμsec/large division

Fig. 52-15. Typical pulse generated by the circuit of Fig. 52-5.

B. Computer Readout

Possible practical applications for the transistorized digital display described in the Division 5 Quarterly Progress Report for 15 March 1959 (p.19) are quite numerous. Outstanding among these is a method of fast computer readout. One method by which this could be accomplished is by photographing the display with some fast-developing film such as Polaroid. Unfortunately, the largest film Polaroid has on the market today is 4 × 5 inches and the developmental cost of the desired $8\frac{1}{2} \times 11$-inch size is prohibitive. The standard $3\frac{1}{4} \times 4\frac{1}{4}$-inch Polaroid transparencies that can be projected for enlarged viewing seem to be a promising area of experimentation. The 4 × 5-inch positive paper print with possibly less information per frame could be a handy second method easily altered to handle the $3\frac{1}{4} \times 4\frac{1}{4}$-inch transparencies if so desired.

We are presently modifying and developing the digital display for Group 314. The new machine will have two high-resolution (2000-line) cathode-ray tubes, one 17-inch rectangular for viewing and the other 5 inches for photographing. A Speed-Graphic camera, which is adaptable to both $3\frac{1}{4} \times 4\frac{1}{4}$ inches and 4 × 5-inch films will be used. The width and height of the machine will be dictated very closely by the size of the back door, which will be the standard CG 24-type rear door (about 6 ft high × 30 inches wide). The depth will be approximately 40 inches. The camera and tube will be mounted to one side of the machine, adding about one foot to the over-all width. The 17-inch viewing tube will be about 4 feet off the floor, set at a convenient angle. In order to make this machine compatible with other computers such as, for example, the IBM 709, a space has been allowed for a ±6.5-volt and ±30-volt power supply. When used with CG 24 these voltages will, of course, be supplied by the computer. There is also plenty of space for logic modification in the eight subracks located in the rear door.

A summary of the liaison between CG 24 and the digital display is as follows:

There will be two orders from CG 24; (d.p.) indicating positional display and (d.c.) indicating display character. CG 24 will also send 12 bits of "X", 12 bits of "Y" and 6 bits of symbol information.

I. (d.p.)
   (a) (N) $\Longrightarrow$ X (A) $\Longrightarrow$ Y
   (b) H(B) $\Longrightarrow$ SSR (Symbol Storage Register)
   (c) Starts Status Register
      (1) Ring (2) Intensity (3) Add up "X" (4) Reset.

II. (d.c.)
   (a) H(B) $\Longrightarrow$ SSR
   (b) Starts Status Register
      (1) Ring (2) Intensity (3) Add up "X" (4) The preceding three are true unless SSR = C.R. then 0 $\Longrightarrow$ X and Y counts. (5) Reset.

III. If an unused code is accidentally transferred to SSR then: (1) No intensity (2) No reset (3) Warning light (4) No add up "X".

IV. If the last "Y" line is reached and a C.R. is sent then: (1) No intensity (2) No reset (3) Warning light (4) No add up "X".

E.J. Aho
K.E. Perry

COMPUTER COMPONENTS
GROUP 53

GOODENOUGH, J. B., *Leader*
SMITH, D. O., *Assistant Leader*

ARNOTT, R. J.
BARCK, P. E.
COHEN, M. S.
DWIGHT, K., Jr.
ECKL, D. J.
FERRETTI, A.
HUBER, E. E., Jr.
JOHNSTON, R. C.
KAPLAN, T. A.
KIRK, C. T.
LARSON, E. G.
MENYUK, N.
SOOHOO, R. F.
WEISS, G. P.
WICKHAM, D. G.
WOLD, A.

COMPUTER COMPONENTS
GROUP 53

I. SUMMARY

A. Magnetic Materials

There are four principal problems that are currently being pursued in our attempt to determine the underlying principles that govern the relationship between chemistry and the electrical and magnetic properties of transition-element metals, alloys and oxides: (1) the correct description of the outer-electron energy bands in metals and alloys, (2) the nature of the cation-cation interactions in oxides, (3) the stable spin configurations (magnetic ordering) in materials with atomic moments that are subject to competing exchange forces and (4) the preparation and properties of pure, stoichiometric ferrites. The approach to the band structure of transition metals and their alloys which has been discussed in previous quarterly progress reports has continued to evolve, and a series of experiments on transition-metal nitrides has been initiated to test the extension of this thinking to interstitial alloys. During this quarter the conditions favorable to direct cation-cation interactions have been formulated and the consequences of these interactions have been used to coordinate a great many isolated, previously unexplained physical phenomena that are extant in the literature. Experimentation relative to this problem has concentrated on the preparation of nd^m-cation oxides where $m \leqslant 3$. The Ti^{3+} compounds have proved difficult to prepare because of the powerful reducing action of Ti^{3+}. Experiments on the $NiMn_2O_4$-Mn_3O_4 system (originally initiated to investigate thermistor-type materials) are also found interpretable only if direct interactions are present. These direct interactions are competitive with indirect interactions; and where the magnitude of the effects is comparable, unexpected magnetic properties are frequently observed. A more general theory for the resulting spin configurations is being worked out. Experiments on natural crystals of Mn_3O_4 appear to rule out the possibility of the Yafet-Kittel angular configuration previously assumed for this tetragonal spinel, but the correct configuration has not yet been worked out. In b.c.c. chromium the probable ground state has been shown to be a spiral configuration. The preparation of nearly stoichiometric manganese, cobalt and nickel ferrites has been accomplished, and some of their properties are reported.

B. Magnetic Films

From a practical point of view, the most important problem to be solved continues to be the physical origins of H_k and H_w. Control of these parameters is of principal importance for uniformity of large arrays for the memory application. Control of the ratio H_w/H_k is also important for the disturb levels of a magnetic film memory. H_k is a measure of the uniaxial anisotropy within the plane of the film: the direction of such an easy axis may be controlled during preparation either by deposition in a DC magnetic field or by depositing the film with an incident beam that makes an angle other than 90° with the plane of the substrate. During this quarter experiments have been performed to investigate the validity of the hypothesis that texture plus magnetostrictive effects are responsible for the angle-of-incidence effect. These experiments appear to demonstrate that this hypothesis is not correct for Permalloy films. A study of the change in magnetic moment of films during deposition is in preparation to help clarify the film-formation process. Other experiments have been directed at correlating various physical parameters with

TABLE 53-I

CHEMICAL ANALYSIS AND PROPERTIES OF FERRITES PREPARED BY IGNITION OF PYRIDINATES

Compound Sought	Weight of Iron (per cent)		Weight of M^{2+} (per cent)		$\frac{\text{Mole Fe}}{\text{Mole } M^{2+}}$	Ignition Temperature (°C)	Active Oxygen equiv/mole	Lattice Constant a_o (Å)	n_B* μ_B/molecule
	Obtained	Theory	Obtained	Theory					
$MgFe_2O_4$	55.69 ± 0.03	55.84	12.41 ± 0.06	12.16	1.954 ± 0.012	1000	–	8.384 ± 0.002	1.37 ± 0.02
$MnFe_2O_4$	48.32 ± 0.02	48.43	23.68 ± 0.03	23.82	2.008 ± 0.005	1300†	0.034†	8.512 ± 0.002	4.5 ± 0.2
$CoFe_2O_4$	47.55 ± 0.01	47.60	25.24 ± 0.08	25.12	1.990 ± 0.01	1000	–	8.388 ± 0.002	3.57 ± 0.01
	47.52 ± 0.01								
	47.53 ± 0.01						0.004‡		
$NiFe_2O_4$	47.54 ± 0.03	47.65	25.03 ± 0.01	25.05	1.997 ± 0.004	1000	–	8.338 ± 0.002	2.12 ± 0.01

* Measured at 4.2°K in a field of 10,000 oersteds.

† Quenched in nitrogen.

‡ Corresponds to a formula $Fe^{3+}[Co^{2+}_{1.000}Co^{3+}_{0.004}Fe^{3+}_{0.996}]\ O_4$ and Fe/Co ratio = 1.988.

the ratio H_w/H_k. It is believed that an understanding of the mechanism responsible for a ratio $H_w/H_k > 1$ will provide an important clue to several properties of magnetic films. In the meantime, experiments on substrate cleaning by means of ion bombardment have demonstrated that an important factor for film uniformity is substrate cleanliness. Initial experiments with this technique are most encouraging. Another important problem for both theory and practice is the damping mechanism operative during flux reversal. In the engineering application, flux reversal occurs by a noncoherent rotation. A model for this process has been proposed and is being studied theoretically. The usefulness of magnetic film arrays will also be determined by the capacities (numbers of bits) that can be practically achieved. An investigation of wiring techniques for high-density magnetic film arrays was initiated this quarter. Considerable attention will have to be given to this problem in the future.

C. Semiconducting Components

A shortage of manpower forced suspension, for one quarter, of the investigations of the cryosar as a possible memory device. Recent improvements in material preparation are most encouraging, and work will be resumed next quarter. Interest in diode parameters at microwave frequencies has been prompted by the possibility of parametron computer elements operating at these frequencies. Measurement techniques are under consideration. In the meantime, test setups are being developed for measuring the parameters of VHF transistors, and transistor-switching theory has been extended in order to help improve the design of VHF transistors for computer switches. Finally, transistor life tests have been continued.

II. MAGNETIC MATERIALS

A. Chemistry and Crystallography

1. Stoichiometric Ferrites

Procedures have been described in previous Solid State Research Quarterly Progress Reports for preparing nearly stoichiometric magnesium, manganese, cobalt and nickel ferrites. A brief study of the properties of the ferrites so prepared in relation to their purity has been completed and is summarized in Table 53-I.

The chemical analyses indicate that the procedures are reasonably successful for manganese, cobalt and nickel ferrites. An attempt to refine the procedures for magnesium ferrite was abandoned when Paladino[1] discovered that a compound corresponding to the formula $MgFe_2O_4$ does not exist as a single spinel phase in air at temperatures above 1000°C.

Manganese ferrite fired in air to 1300°C and quenched in nitrogen appears to contain a small amount of excess oxygen, 0.034 oxidation equivalents per mole ($MnFe_2O_{4.017}$). A careful x-ray examination failed to reveal the presence of anything but a spinel phase.

Chemical analysis of cobalt ferrite also revealed the presence of a small amount of excess active oxygen, 0.004 equivalents per mole. Smiltens[2] and Jonker[3] have shown that a small excess of cobalt in cobalt ferrite will assume a +3 oxidation state and replace +3 iron. The formula for the cobalt ferrite listed in Table 53-I would thus be $Fe^{3+}[Co^{2+}Co^{3+}_{0.004}Fe^{3+}_{0.996}]O_4$ which gives a value for Fe/Co equal to 1.988 in agreement with that based on determination of total iron and cobalt present.

The magnetic moments n_B, with the exception of that for manganese ferrite, are in good agreement with reported values. The value of n_B is less sensitive to small deviations from

stoichiometry than it is to variations in heat treatment which influences the distribution of cations between the tetrahedral and octahedral sites of the spinel structure. The low value for $MnFe_2O_4$ reported here is probably caused by quenching the sample from 1300°C, the octahedral-site manganese probably reduces some iron to Fe^{2+} by becoming Mn^{3+}.

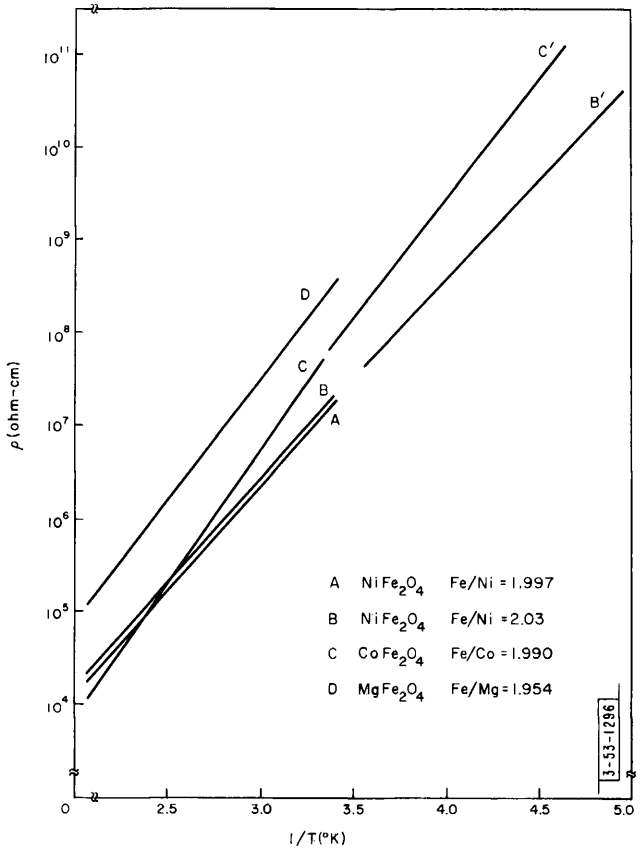

Fig. 53-1. Log ρ vs 1/T (°K) for several ferrites.

The DC resistance of the ferrites is given by $\rho = \rho_o \exp[+q/kT]$ where ρ_o and q are experimental constants and T is the absolute temperature. The activation energy q can be obtained from a plot of log ρ vs 1/T. Such graphs obtained for ceramic specimens of the magnesium, cobalt and nickel ferrites listed in Table 53-I are given in Fig. 53-1. The values of q computed from the slopes of the high-temperature portions of the curves are 0.514, 0.574, 0.454 ev, respectively.

Jonker[3] has carried out a very thorough investigation of the semiconducting properties of cobalt ferrite. The value of q which he is able to calculate for the composition $Co^{2+}[Co^{2+}Co^{3+}_{0.004}Fe^{3+}_{0.996}]O_4$ is exactly that which we have observed, 0.57 ev. The Seebeck voltage for a specimen of this same composition is found to be +347 μvolts/°C, again in agreement with the value predicted by Jonker. Physical measurements in this case confirm the formula determined by chemical analysis.

It is seen in Fig. 53-1 that two samples of nickel ferrite with different Fe/Ni ratios, 2.03 and 1.997, give identical values for q. This fact is in accord with the recent phase studies of Paladino[4] who has found that under equilibrium conditions for oxygen pressures equal to or

greater than 10^{-2} atmos, it is impossible to prepare single-phase spinels deviating from the stoichiometric formula $NiFe_2O_4$. The sample with the Fe/Ni ratio equal to 2.03 should contain a little Fe_2O_3 precipitated between the grains of $NiFe_2O_4$ and offer a slightly higher electrical resistance.[5] The fact that the observed resistance of this material is higher than that of the pure material is significant because the density is considerably greater (the pure material exhibited a pronounced reluctance to sinter as pure materials often do) and should for this reason offer a lower resistance. The Seebeck voltage measured for the pure nickel ferrite is $-219\,\mu$volts/°C.

D. G. Wickham
E. Whipple
E. G. Larson

2. Transition-Metal Nitrides

The magnetic moment of Fe_4N was measured as a function of field strength H at 4.2°K. Extrapolation of the curve of magnetization vs 1/H to infinite field strength yielded the correct value of $2.25\,\mu_B$ per iron atom. The discrepancy between this value and the value reported in the Solid State Research Quarterly Progress Report for 15 July 1959 apparently is caused by a large demagnetizing factor for Fe_4N.

It was noted that whereas stoichiometric Fe_4N was obtained, other members of the composition series $Fe_{4-x}Ni_xN$ contained excess nitrogen. Further analysis of several members of the series indicates that the excess nitrogen is necessary for stabilization of the $\gamma'(Fe_4N)$ structure when nickel is substituted for iron. An analysis of the intensities of lines in the x-ray powder diffraction patterns suggests that the first nickel atom enters the structure in an ordered position: the corner of the unit cell when the nitrogen atom is considered to lie on the body center. Further nickel atoms replace iron in a random manner.

A. Wold
R. J. Arnott

3. Spinels Containing Ti^{3+}

Attempts to prepare spinels containing Ti^{3+} are being continued and have been greatly assisted by construction of a furnace capable of attaining temperatures >1600°C while maintaining a sufficiently low partial pressure of oxygen to prevent oxidation of trivalent titanium.

Attempts to prepare $MnTi_2O_4$ by reacting MnO and Ti_2O_3 at 1450°C resulted in an apparently complete reaction, the product of which appears to be homogeneous and is jet black in color. The x-ray powder patterns indicate a phase very similar in structure to pseudobrookite. There is no evidence of spinel formation.

The preparation of $FeTi_2O_4$ was attempted by reacting iron with TiO_2. There is no evidence here for spinel formation either.

The reaction of ZnO with Ti_2O_3 resulted in the reduction of zinc to the metallic state. All other attempts to prepare this spinel have likewise resulted in reduction of zinc to free metal and it appears to be an impossible synthesis.

D. B. Rogers

4. The System $Ni_{1-x}Mn_{2+x}O_4$ ($NiMn_2O_4$-Mn_3O_4)

Values for the magnetization (at 4.2°K in a field of 10,000 oe) as a function of composition in this spinel system have been reported in the Solid State Research Quarterly Progress Report for 15 January 1959. The unusual shape of the magnetization (M) vs composition curve indicates not only that the simple Néel coupling scheme is not applicable, but also that the ion distribution is complex.

The study of the electrical conductivity and the crystal symmetry of this system led to the conclusion that a correct formulation should combine the simple formulas $Mn_x^{2+}Mn_{1-x}^{3+}[Ni_{1-x}^{2+}Mn_{1+x}^{3+}]O_4$ and $Mn^{2+}[Ni_{1-x}^{2+}Mn_{2x}^{3+}Mn_{1-x}^{4+}]O_4$ (where $x \leq 1$). Since the choice of an exact formula on the basis of present information is not possible, a simple one was chosen so that a tentative interpretation of the observed magnetic moments could be presented. This formula is

$$Mn_{\frac{1+x}{2}}^{2+}Mn_{\frac{1-x}{2}}^{3+}\left[Ni_{1-x}^{2+}Mn_{\frac{1+3x}{2}}^{3+}Mn_{\frac{1-x}{2}}^{4+}\right]O_4 \quad . \qquad (1)$$

According to formula (1) material will possess tetragonal symmetry if more than 56.5 per cent (experimental value of $x = 0.42$) of the octahedral sites are occupied by Mn^{3+} ions. This critical composition for several other systems containing Mn^{3+} has been found to be 60 to 65 per cent (Ref. 6). However, if the other B-site cation is Cr^{3+} ($3d^3$), tetragonal distortions exist with only 50 per cent of the B-site cations Mn^{3+}. Mn^{4+} ($3d^3$) is similar in size to Cr^{3+} so that the presence of B-site Mn^{4+} may also be expected to lower the critical composition for tetragonal distortion below 60 per cent.

Interpretation of the magnetic properties is based on the fact that the Mn^{4+} ($3d^3$) ion experiences relatively weak indirect A-B interactions and relatively strong B-B interactions with other B-site Mn^{3+} and Mn^{4+} ions.[7] There can be no B-B interactions with Ni^{2+} ions. Therefore, only those Mn^{4+} ions that have more than a critical number of B-site Mn neighbors can have their moments coupled parallel to the A-site moments because the B-B interactions predominate. Figure 53-2 shows the observed magnetic moments for the system and the number of Mn^{4+} moments that must be parallel to the A-site moments if spin-only atomic moments are oriented collinearly. As x increases, the concentration of Mn^{3+} ions increases more rapidly than the concentration of Mn^{4+} ions decreases, so that an increasing fraction of Mn^{4+} ions with reversed moments is compatible. In the cubic phase, both Ni^{2+} and Mn^{3+} ions have strong A-B interaction so that only Mn^{4+} ions can have reversed moments. In the tetragonal phase (and some short-range order exists in compositions with $x < 0.42$), the Mn^{3+} A-B interactions are strong in some directions, weak in others so that the magnetic ordering is undoubtedly complex. Therefore, the numbers of reversed manganese moments given for the tetragonal region in Fig. 53-2 are only effective numbers based on a collinear-moment model: such a model is certainly not correct as the composition Mn_3O_4 is approached (Sec. II-B).

E. G. Larson
D. G. Wickham

B. The Magnetic Properties of Hausmannite

The study of the magnetic properties of single-crystal hausmannite has been continued.[8] Measurement of the saturation magnetic moment of both (100)- and (001)-faced samples of hausmannite gave

$$n_B = 1.89 \pm 0.02 \text{ Bohr magnetons/molecule} \quad .$$

This result is well below the value of 3.0 Bohr magnetons/molecule predicted by the simple Néel model of ferrimagnetism.

Work by Jacobs[9] on polycrystalline Mn_3O_4 gave the value $n_B = 1.56$ Bohr magnetons/molecule, which he attributed to the existence of Yafet-Kittel[10] angles in the material. He used the notation and formulation of Lotgering[11] in his analysis, and concluded that the resultant moment due

to A-site cations was greater than that of the B-site cations. This conclusion was consistent with the results of neutron diffraction experiments carried out by Kasper.[12]

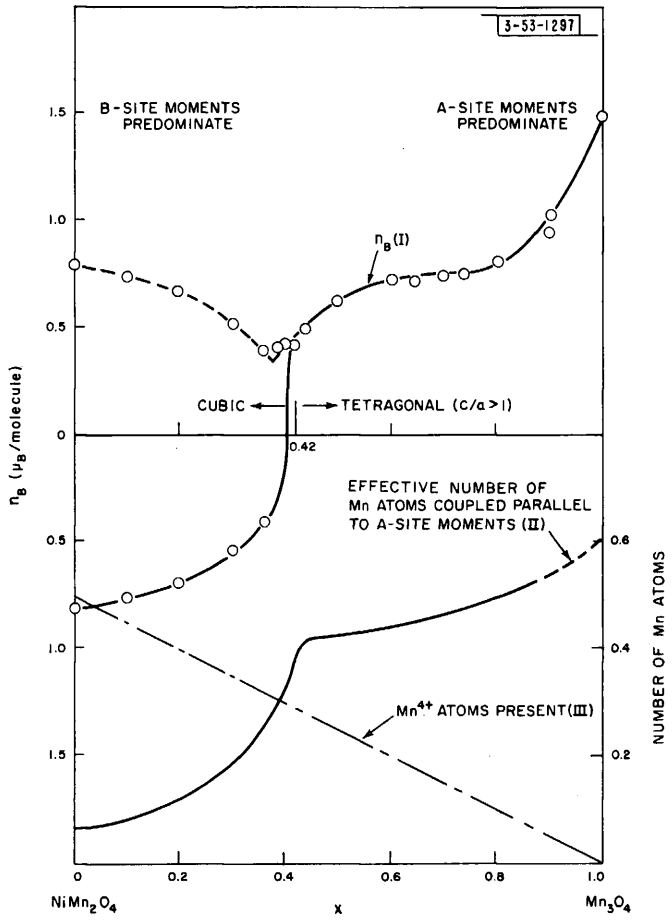

Fig. 53-2. Magnetization (4.2°K, 10,000 oe) for the system

$$Mn^{2+}_{\frac{1+x}{2}}Mn^{3+}_{\frac{1-x}{2}}\left[Ni^{2+}_{1-x}Mn^{3+}_{\frac{1+3x}{2}}Mn^{4+}_{\frac{1-x}{2}}\right]O_4 \quad .$$

We have also assumed Yafet-Kittel angles in our analysis. However, in view of the large anisotropy constants measured for this material,[8] the Lotgering formulation was extended to include anisotropy effects. Thus, using the notation of Lotgering, we find the necessary molecular-field condition for stability of Yafet-Kittel angles to be

$$\alpha\beta = 1 - \frac{\alpha K}{2nb^2} \quad , \tag{2}$$

where α and β are the ratios, respectively, of the A-A and B-B interactions to the A-B interaction, n is the A-B interaction parameter, K is the anisotropy constant in units of ergs/mole, and b is the magnetic moment per mole of the B-site cations. Since all of the above terms are positive, the necessary condition can be rewritten as

$$\alpha\beta < 1 \quad . \tag{2a}$$

The experimental results showed only a small decrease in the anisotropy constant from 4.2°K to nine-tenths of the ferrimagnetic Curie temperature. Such behavior strongly suggests that this temperature represents a transition from a ferrimagnetic state to one in which the B-site cations become antiferromagnetic. Such a transition can occur only for a certain region of the Lotgering α-β diagram.

We carried out the analysis for this region of the diagram and obtained three equations:

$$N = -\frac{T_a[(1/3)\,C_A + (2/3)\,C_B]}{(1/6)\,C_A^2\,\alpha + C_B^2\,\beta + (4/3)\,C_A C_B} \quad , \tag{3}$$

$$T_\Delta = \frac{nC_A}{2\beta}(2 - \alpha\beta) \quad , \tag{4}$$

$$\sin\psi = \frac{2nab}{2n\beta b^2 + K} \quad . \tag{5}$$

In the equations above, C_A and C_B are the Curie constants for cations on the A and B sites, respectively, T_a is the asymptotic Curie temperature obtained from paramagnetic susceptibility measurements (as performed by Bongers[13]), T_Δ is the ferrimagnetic-antiferromagnetic transition temperature, and ψ is the Yafet-Kittel angle made by the B-site cations. All the terms in these equations were determined experimentally except for α, β and n. The system of three equations in three unknowns was then solved explicitly and yielded the unique values: $\alpha = 0.9$, $\beta = 1.55$, $n = 53.3$.

Evidently $\alpha\beta > 1$, which contradicts the necessary condition for Yafet-Kittel angles, as given in Eq. (2a). Neither variation of our data to a far greater extent than the possible experimental error, nor use of the value for T_a obtained by Borovik-Romanov and Orlova,[14] nor reversal of our assumption that the A-site moment dominates can even weaken the contradiction significantly, let alone remove it. Thus the classical Yafet-Kittel model fails to account for the magnetic properties of hausmannite.

In searching for flaws in the theoretical structure, we note that the above analysis is based on a molecular field calculation. It is well known that this approximation, though good at very low temperatures, becomes less accurate at higher temperatures because of the effects of short-range order. Even so, the errors in molecular-field Curie point values are usually not large, and it is almost inconceivable that one be off by a factor of two. Yet Eq. (4) would require $T_\Delta > 75$°K in order to satisfy the condition that $\alpha\beta < 1$, as compared with the experimental value $T_\Delta = 42.3$°K.

We therefore conclude that the flaw must arise in the application of the Yafet-Kittel model to hausmannite. Kasper's neutron diffraction data at 4.2°K show orthorhombic magnetic symmetry with a b/a ratio of 2/1, which he explains on the basis of an ordered spin arrangement within the Yafet-Kittel model. However, we have been unable to find any mechanism whereby energy considerations would favor doubling the unit cell with Kasper's ordered structure. The suggestion of an alternative explanation for this doubling is one of the encouraging qualitative results obtained by T. A. Kaplan[15] in his preliminary work on stable spin configuration in spinels – the Néel arrangements are special cases for extreme values of the parameters.

N. Menyuk
K. Dwight, Jr.

C. Theory

1. Band Structure of the Transition Metals and Their Alloys

The ideas developed a year ago for the band structure of the transition metals and their alloys have continued to evolve, and a write-up will soon be available as Lincoln Laboratory Technical Report No. 208.

The argument departs from the conventional approach to this problem in two ways: first, it assumes that, for elements of the first long period, cubic crystalline fields separate the atomic d states sufficiently that there are several d subbands formed from linear combinations of primarily one or the other of the two subsets e_g and t_{2g} of atomic d orbitals; second, the relative energies of the various subbands are first obtained from qualitative physical arguments about the multielectron problem which introduce intuitively the spin correlations and hence the characterization of the subbands, the one-electron description being used separately for each subband only after their characterization and relative energy have been specified. The characterizations and relative energies are uniquely, though qualitatively, defined in terms of easily visualized atomic orbitals and lattice symmetry. These are expressed in three basic postulates with which it is possible to construct qualitative energy spectra of the density of crystalline states for the transition elements given different crystalline symmetries. The conditions for Pauli paramagnetism, antiferromagnetism and ferromagnetism are also uniquely specified. Simplified density-of-states curves for the b.c.c and f.c.c transition elements are constructed with the aid of available experimental and theoretical information. It is shown that these simplified constructions provide a consistent interpretation of a wide variety of physical properties that hitherto have not been accounted for within a unified framework. The model has been extended to substitutional ordered and disordered alloys. It is hoped to extend this work to the interstitial alloys during the next quarter. One of the most startling predictions from the model is a superstructure in the form factor of ordered alloys of the Fe_3Al type. Recent neutron diffraction work at Brookhaven National Laboratory appears to confirm this prediction.

J. B. Goodenough

2. On Direct Cation-Cation Interactions in Transition-Element Oxides

Some oxides containing transition-element cations have physical characteristics that suggest direct cation-cation interactions via cation d electrons. Such interactions have been independently proposed to account, on the one hand, for certain magnetic interactions,[7] on the other, for some interesting electrical properties.[16] The most favorable crystallographic configuration for such interactions is one where cation-occupied octahedra share a common octahedral face, as in the corundum and NiAs-type structures: in this case cations with outer-electron configuration nd^m, where $0 < m \leqslant 5$, may have direct interactions that profoundly influence the physical properties of the materials. If cation-occupied octahedra share a common edge, direct interactions may be stronger than indirect interactions provided $0 < m \leqslant 3$. These interactions may be sufficiently strong that band formation, and therefore metallic-type conduction, can occur. It has been pointed out that the semiconducting $\rightleftarrows$ metallic transitions frequently observed in such cases can be interpreted to be the result of the formation at low temperatures of covalent-type bonds or of bonding bands, the bonding configuration introducing a lattice distortion that at least partially removes the degeneracy of the atomic orbitals contributing to the original metallic-type band. This model makes definite predictions about the paramagnetic

susceptibility, cation magnetic moments, antiferromagnetic order and crystallographic changes to be associated with the electrical transitions in these materials. Some of these are at variance with those that follow from Morin's[16] model for the semiconducting $\rightleftarrows$ metallic transition. Existing data support the proposed model. The proposed mechanism has been contrasted with the Jahn-Teller distortions that may occur as a result of cation-anion interactions. Metallic-type conductivity arising from direct cation-cation interactions has also been distinguished from possible metallic-type conductivity due to indirect cation-anion-cation interactions.

J. B. Goodenough

3. Spin Configurations in Cubic Spinels

It has previously been pointed out[17] that the Néel configuration (C_N) in the cubic spinel is unstable when a parameter y has a value greater than $y_o = \frac{2}{3}$ (y is essentially the ratio of B-B to A-B interactions, A-A exchange forces being neglected). The corresponding critical value of y found by Yafet and Kittel[10] (under more restrictive assumptions) is $\frac{3}{4}$. It was also found[17] that the Yafet-Kittel triangular configurations (which, by their theory, are improvements over C_N for $y > \frac{3}{4}$) are unstable. Hence knowledge of what spin configurations exist in cubic spinels with large y is nonexistent, and it is of considerable interest to obtain at least some idea of the spin configurations to be expected under these conditions. For example, the neutron diffraction data of Corliss and Hastings[18] on $MnCr_2O_4$ remain unexplained, and the work of Menyuk and Dwight[19] shows an inconsistency in the Yafet-Kittel theory as applied to their experimental results on Mn_3O_4.

As a first step in this direction, a perturbation theory has been constructed that will give the minimum energy configuration for small, positive values of $y - y_o$, given the classical Heisenberg Hamiltonian. Although the ground configuration has not been obtained explicitly, the following conclusions can be drawn:

(a) Equilibrium configurations exist in which, simultaneously, there are nonzero angles between A-spins and B-spins.

(b) The ground state will exhibit a long-range-ordered array of canted spins.

These facts are of interest theoretically because they nullify: (a) the rigorous conclusion, drawn[11] from the Yafet-Kittel assumptions, that angles can exist only between either A's or B's and (b) Anderson's[20] suggestion that long-range-ordering of antiferromagnetic spin-components will not exist on the octahedral sublattice (from exchange energy considerations) in cubic spinels. (We feel that this suggestion is correct when there is no A-B interaction, but a nonzero value of the latter apparently removes the degeneracy that led to Anderson's suggestion.) Experimentally our conclusions seem to correspond more closely to the true state of affairs. In $MnCr_2O_4$ (which is cubic to within the accuracy of present measurements), the diffraction data indicate the presence of angles on both the A- and the B-sites, in a long-range-ordered arrangement. In connection with Mn_3O_4 (which is tetragonal), our first conclusion is apparently necessary[21] in order to make possible any energy reduction due to the cell doubling observed by Kasper.[12] In addition, we find the important symmetry element entering into the first term of our perturbation series to be an approximate doubling in [110] (which corresponds to Kasper's result); this is quite encouraging, of course, but its significance must remain unclear until we explicitly take into account the tetragonal distortion (which we plan to do in the near future).

T. A. Kaplan

4. Spirals in Chromium

Role of Anisotropy:– It has been pointed out[17] that a spiral configuration of spins can exist in a body-centered cubic if first, second and third nearest-neighbor interactions (J_1, J_2 and J_3) are antiferromagnetic with relative values $J_2/J_1 \sim 0.6$, $J_3/J_1 \sim 0.1$, and that a pseudodipolar energy could favor the [100] direction for the k-vector defining the spiral, in agreement with the experiment on chromium of Corliss, Hastings and Weiss.[22] The experimental spiral wavelength is large (about 28 unit cells). This implies that the difference in exchange energy $E_o - E_k$, for the up-down configuration and the spiral, is very small ($\approx 10^{-5}\ E_o$). Since the pseudodipolar energy is generally $\approx 10^{-2}\ E_o$, we must conclude that the latter is very important in determining the spiral properties.

Neutron Diffraction:– Corliss, Hastings and Weiss[22] have been able to interpret their results on chromium in terms of antiphase domains (although there seems to be general agreement that spirals are more reasonable physically). It is thus of interest to show that an interpretation in terms of spirals is equally valid and, further, to investigate the possibility of distinguishing between the two possibilities.

The diffraction cross section has been calculated for both configurations. Comparison[23] of these results with the experimental data led to the conclusions: (a) the present experimental results cannot distinguish between spirals and antiphase domains and (b) a small, theoretically predicted difference between the two diffraction patterns should be detectable in a refined experiment. (The latter effect is that there should occur "sideband" diffraction peaks due to the abrupt changes from the "up-down" configuration in the antiphase domains, whereas no such extra peaks should occur in the smoothly varying spiral configuration.)

T. A. Kaplan

III. MAGNETIC FILMS

A. The Physical Origin of H_k and H_w

1. Angle-of-Incidence Films

Very large magnetic anisotropy has been found in evaporated Permalloy films that are made by allowing the Permalloy beam to strike the substrate at a high angle of incidence.[24] The same effect has been observed in iron by Knorr and Hoffman.[25] They suggest that the magnetic anisotropy is due to an inclined crystallographic texture axis in the film acting in conjunction with either isotropic or anisotropic stresses (such as observed by Finegan and Hoffman[26]).

Results from several different experiments performed in this laboratory are not consistent with their interpretation.

(a) Stress was measured by depositing the metal on thin glass and measuring the deformation of the glass by observing Newton's rings. The stress anisotropies thus obtained for both iron and Permalloy were not reproducible in magnitude or in direction relative to the magnetic axis.

(b) The films were stripped from their glass substrates. Past experience has shown that films with compositions such that their magnetic properties are highly stress-dependent change their magnetic character drastically when subjected to this treatment (e.g., "mottled" films[27]). The magnetic anisotropy of either iron or Permalloy angle-of-incidence films was unaffected by the stripping process.

(c) By changing the composition of the Permalloy, films of either positive or negative magnetostriction constant can be made. When such films were deposited by evaporation at high angle of incidence, no change in direction of the magnetic easy axis at the zero-magnetostriction composition was observed, as would have occurred if stress were responsible for the effect.

(d) Calculations show that crystallographic texture alone, without stress, is insufficient to explain the observed anisotropy.[24]

Angle-of-incidence films of Permalloy on soft-glass substrates were examined by reflection electron diffraction; similar experiments are planned for iron. It was found that films of less than about 1000 Å thickness showed ring patterns, i.e., no preferred crystallographic axis (Fig. 53-3), whereas films having a thickness in the range from about 1000 Å to 3000 Å often had a (110) texture axis (Fig. 53-4). These results are consistent with those of Sachtler[28] for nickel. The texture axis, when it did appear, did not deviate in inclination from the normal to the plane of the film by more than a few degrees for such films, even for high-incidence angles.

Since large magnetic anisotropy is observed for high-incidence-angle Permalloy films that have either no texture or a texture axis perpendicular to the substrate, it is clear that a mechanism based on texture cannot be the primary origin of the phenomenon in question.

A study of the microstructure of Permalloy films by electron microscopy and diffraction showed that such gross structural properties as crystallite size, shape and position also apparently do not play a decisive role in the determination of magnetic anisotropy.

M. S. Cohen
E. E. Huber, Jr.
D. O. Smith

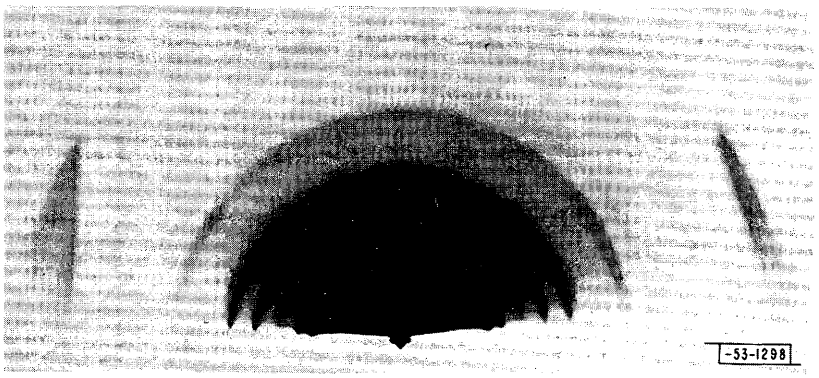

Fig. 53-3. Reflection electron diffraction pattern of Permalloy film. Substrate temperature 400°C, 45° incidence angle, about 700 Å thick.

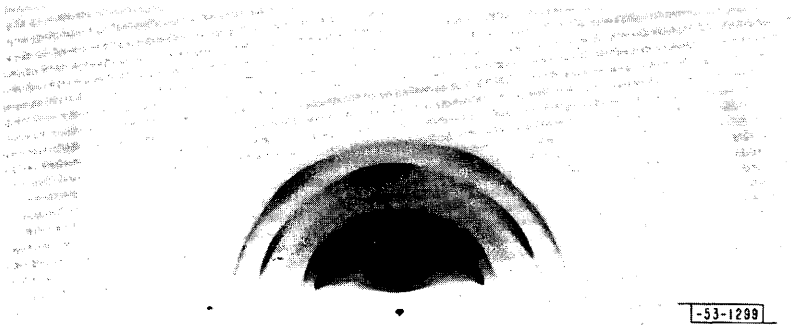

Fig. 53-4. Reflection electron diffraction pattern of Permalloy film. Substrate temperature 200°C, 70° incidence angle, about 1200 Å thick.

2. Inverted Films

The density of some inverted films ($H_w/H_k > 1$) has been measured. The conclusion is that any difference in density between normal and inverted films must be less than 5 per cent. A model for inversion has been suggested in terms of demagnetizing centers.[29] The density measurements do not rule out the possibility that these centers are voids, but clearly such voids must be less than 5 per cent of the total volume.

Electron microscope and diffraction studies have so far failed to reveal the structural origin of locking. No holes or porosity have been observed, nor has the presence of a second phase been detected.

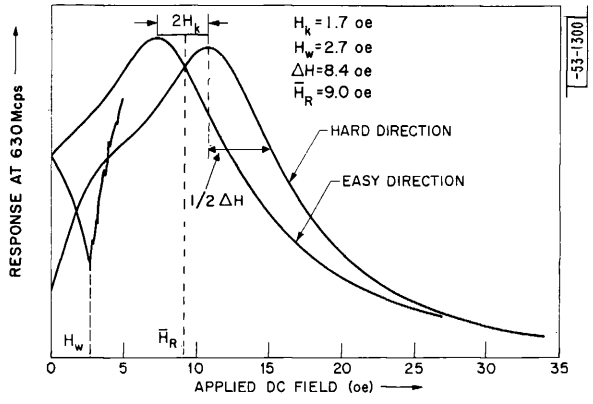

Fig. 53-5. Measurement of H_k, H_w, ΔH and $\bar{H}_R$ by resonance.

It was first thought that inversion was associated with a drastic decrease (~ 30 per cent) in the magnetization M. Further measurements, however, have shown that low M can also occur for what are otherwise "normal" films. The rather wide variation in M that is sometimes observed among films made at the same time is currently interpreted as being due to differing conditions of the substrates just before evaporation.

Additional information on inversion has been obtained from resonance experiments. Figure 53-5 shows the type of data that can be taken. The resonance condition for the DC and RF fields in the film plane is $\omega_o = \gamma\sqrt{4\pi M(H_A \pm H_k)}$, where the ± sign is for the applied field H_A in the easy and hard directions, respectively. Thus the separation between resonance peaks is $2H_k$. Wall coercive force H_w is measured by reversing the DC field in the easy direction and noting the break in the resonance curve. Additional parameters are the line width ΔH and the average resonance field (i.e., resonance field if there were no anisotropy). Measured at 630 Mcps, ΔH and $\bar{H}_R$ are found to increase with the inversion ratio H_w/H_k [Figs. 53-6(a) and (b)]. This is in qualitative agreement with the demagnetizing-center model: an inhomogeneous M will certainly broaden the resonance; the shift to higher resonance fields is in general accord with the work of Frait[30] who studied the effect of demagnetizing fields in ferrite samples.

E. E. Huber, Jr. M. S. Cohen
G. P. Weiss D. O. Smith

3. Resonance Annealing

Apparatus has been built that can take data of the type shown in Fig. 53-5 up to 500°C. Study of the various parameters with respect to intrinsic temperature dependence and structural changes due to annealing are in progress.

G. P. Weiss
D. O. Smith

4. Film Uniformity

It is thought that the main problem in producing uniform films lies in substrate cleaning just prior to deposition. Encouraging initial results by C. Ryan, T. Crowther and J. Raffel[31] using ion bombardment have led to further exploitation of this technique. Care must be taken during bombardment not to sputter cathode material onto the substrate. Best results to date

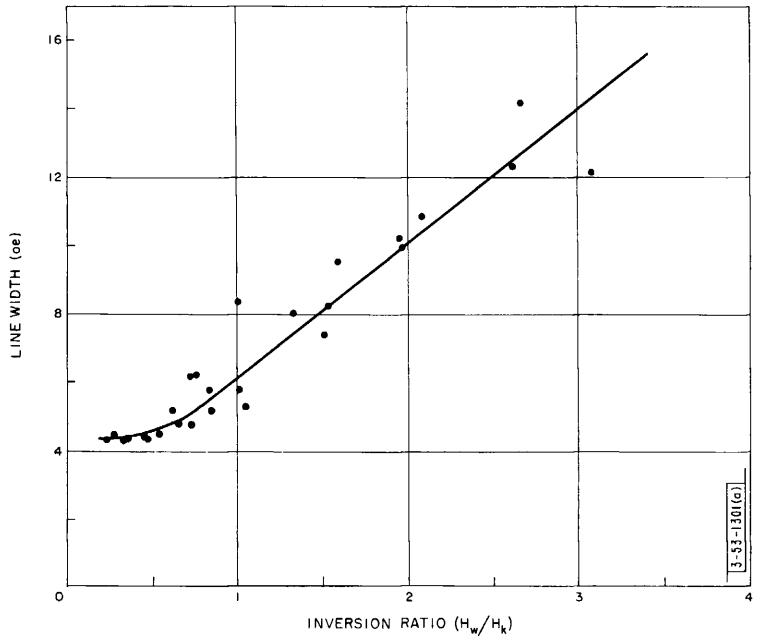

Fig. 53-6(a). Line width at 630 Mcps vs inversion ratio.

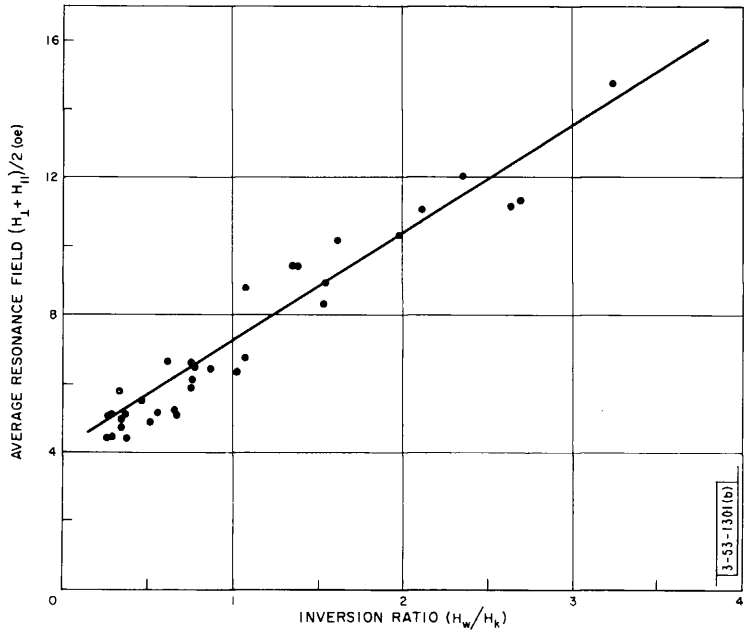

Fig. 53-6(b). Average resonance field vs inversion ratio.

have been obtained using a tantalum* grid as the cathode placed just in front of the glass substrate, which is supported in an all-glass holder. The glow discharge takes place in an argon atmosphere at a pressure of 100 to 150 microns.

G. P. Weiss
D. O. Smith

B. Growth of the Magnetic Moment of Films During Deposition

A torque magnetometer has been constructed for a study of the growth of the total magnetic moment of Permalloy films during deposition. The film is deposited by evaporation from a tungsten filament onto a glass substrate suspended vertically by a gold fiber in a horizontal magnetic field. This field produces a small angular deflection of the substrate proportional to the total moment of the film. A mirror is formed by depositing an aluminum film on the opposite side of the substrate so that deflection can be observed with a telescope and scale. The system is allowed to deflect continuously during the course of an evaporation. Eddy current damping in suitably oriented aluminum disks attached to the suspension results in a noise vibration level that is below the level of detection. Preliminary experiments indicate that the performance of the magnetometer is satisfactory. The instrument will be used to detect any discontinuities that may be present in the growth of the total magnetic moment as a function of film thickness.

R. M. Moon, Jr.

C. Flux Reversal by Noncoherent Rotation

Recent investigations by Olson and Pohm,[32] Humphrey[33] and Hagedorn,[34] indicate that magnetic film flux reversal, for switching time τ less than about 0.3 μsec, takes place by rotation of the magnetization roughly in the plane of the film. However, for τ in the 0.1- to 0.3-μsec range, they have found that switching takes place noncoherently (i.e., the entire film cannot be represented by a single magnetization vector), with a resulting increase in τ over the value expected for coherent switching, and an anomalous behavior of the transverse and longitudinal switching signals.

A model of noncoherent rotation has been proposed, based on a variation along the y-axis (perpendicular to the film) of φ, the angle the magnetization has rotated in the plane of the film. This variation, initially induced by a small angular dispersion of the magnetic easy axis through the film,[35] sets up transient y-directed spin waves. Spin-wave modes are amplified at the expense of the uniform mode through coupling to the uniform rotation, and the time required for the entire film to switch is markedly decreased.

The detailed predictions of the model are being investigated for the case of the switching field, assumed to be a step function, applied antiparallel to the initial magnetization, and a DC bias field perpendicular to this direction in the plane of the film. Anisotropy, demagnetizing and exchange fields are all considered; and the damping is permitted to be anisotropic. The components of the damping tensor are assumed to be constant, and are being found from an exact machine computation of the uniform mode using the Gilbert dynamical equation.

K. Harte

* The sputtering rate of tantalum in gram-atoms/amp is less by a factor of ten than the more commonly used aluminum.

D. Evaporated Wiring for High-Density Magnetic Film Memories

If a high-density (say 10^4 bits/inch^2) magnetic film memory is to be achieved, the spacing between the wiring and the films must be reduced over the present techniques. If this is not done, two kinds of noise will result: (1) a disturbing of the adjacent spots by the drive currents and (2) a poor signal-to-noise ratio in the sense loop. The wire-to-film spacing is limited in the present technique by the glass-substrate thickness. It is necessary to place conductors between the film and the substrate. A sandwich construction is indicated consisting of alternate layers of wiring and insulators, then the film, then the other half of the wiring and insulators.

At first it was hoped that the thicknesses normally achieved in evaporating metals would be sufficient. Calculation of the parameters of a strip line with 3 mil width, 0.28-μ spacing and 1-μ conductor thickness indicated a resistance of 708 ohms/m and a capacitance of 0.0185 μf/m. This gives a time constant of 5 μsec/m^2, which is much too slow.

An exact analysis of the transient response of an RLC transmission line was done[36] which indicated conductor thicknesses the order of a mil were necessary for good response time. Thicknesses of this order have been achieved with special bonding techniques by Petersen.[37] Another technique is plating copper on glass and etching to form the desired pattern.

The evaporation of films on metal substrates indicated that the surfaces must be mirror finished. Any scratches will raise H_k and determine the easy axis. Mechanical polishing of copper and aluminum was tried, but is laborious and probably not suitable for arrays of lines. Electropolishing was tried without success.

The problems to be solved are:

(1) Development of a suitable plating and electropolishing technique or evaporation of thick layers (1 mil) with smooth surfaces,

(2) Investigation of the effect of metal surface on film properties,

(3) Evaporation of an insulator without pinhole shorts.

R. C. Johnston

IV. SEMICONDUCTING COMPONENTS

A. High-Temperature Storage Tests on Microalloy Transistors

Two groups of 20 microalloy transistors have been placed on elevated storage tests, one at 85°C and the second at 100°C. The last set of measurements was made at 166 hours. Initial and 166-hour punch-through voltage measurements are tabulated in Table 53-II. There is essentially no change. One unit was lost as a "short" at 85°C and No. 15 shows a one-volt drop. This unit measured 11.2 volts at 133 hours, however, so quite possibly the reading is in error. The results on earlier units quoted in the Solid State Research Quarterly Progress Report for 1 August 1958 show an average change in punch-through voltage from 15.9 volts to 13.1 volts in 169.5 hours at 104°C. Results so far indicate that the transistor design changes have greatly reduced, if not solved, the punch-through voltage problem at high temperatures.

D. J. Eckl

B. TX-0 Transistor Retest Program

During the past quarter arrangements were made to retest a certain number of transistors from the TX-0 computer. At the time these transistors were removed (July 1959) the computer had accumulated some 10,674 hours operating time, an additional 4474 hours since the last re-evaluation of the transistors.

TABLE 53-II
ELEVATED TEMPERATURE STORAGE, 2N393 TRANSISTORS
PUNCH-THROUGH VOLTAGE MEASUREMENTS

100°C Storage No.	0 hours (volts)	166 hours (volts)	85°C Storage No.	0 hours (volts)	166 hours (volts)
1	13.5	13.4	21	13.9	shorted
2	10.3	10.3	22	11.9	11.9
3	15.0	14.9	23	10.7	10.7
4	10.1	10.2	24	17.1	17.1
5	12.9	12.9	25	14.0	14.1
6	9.2	9.2	26	10.6	10.7
7	12.2	12.2	27	8.7	8.7
8	16.0	15.9	28	12.9	12.9
9	12.2	12.2	29	16.4	16.4
10	9.7	9.6	30	29.6	29.4
11	10.6	10.6	31	11.1	11.1
12	11.6	11.6	32	16.5	16.5
13	10.4	10.4	33	18.0	18.0
14	11.4	11.5	34	20.9	20.8
15	11.2	10.2	35	12.9	12.9
16	14.3	14.3	36	13.4	13.4
17	7.7	7.8	37	12.7	12.7
18	12.1	12.2	38	15.2	15.2
19	14.4	14.4	39	10.8	10.8
20	9.3	9.2	40	13.4	13.4

This is the first retest program since the computer was moved from Lincoln to the Compton Laboratory on the M. I. T. campus. Coincident with the change in location of the computer was the removal of the large 256 × 256 core memory and the substitution of a 64 × 64 transistor-driven core memory (TDCM). This affected two groups of the transistors that had been used in previous life studies. With the installation of the TDCM and its associated TX-2 plug-in units, a group of cascade cable drivers and level input inverters was removed from service. Additional transistors were selected to make up the deficiency in the test data, and the unused transistors were used as a shelf-life check.

The initial processing of the data in the Laboratory IBM card room has been completed. Further manipulation of the data will be continued to obtain the necessary distributions for a complete report.

R. L. Burke

C. Transistor Switching Theory

A class of base impurity distribution functions N(x) for which the minority carrier diffusion equation is capable of exact solution has been found to be of the form

$$N(x) = N_o \left[\frac{1 + a}{1 + ae^{-kx}}\right]^2 e^{-kx} \quad , \tag{6}$$

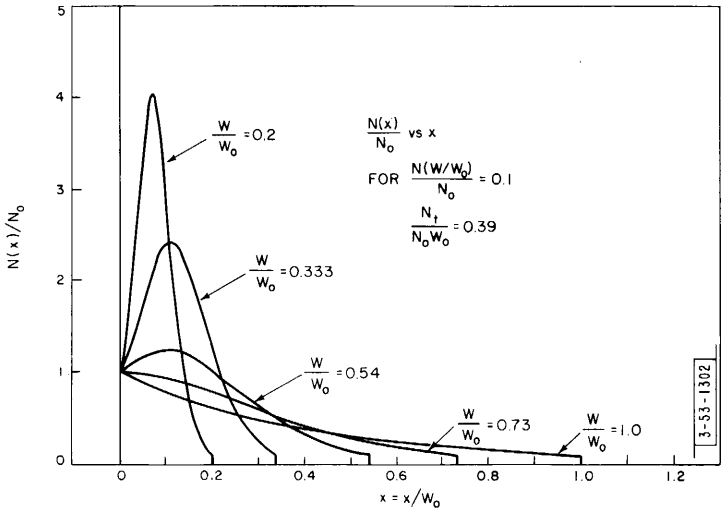

Fig. 53-7. Base impurity density distributions.

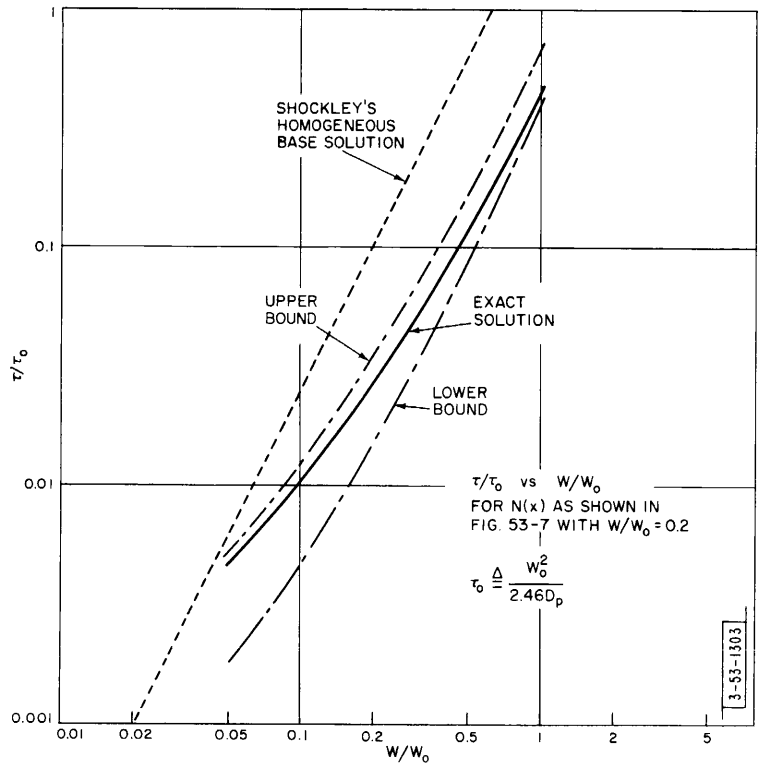

Fig. 53-8. Relative switching time as a function of base width.

where a and k are arbitrary parameters. It is of interest to note that the exponential distribution treated by Johnston[38] among others, is a member of this class as can be seen by setting a = 0. Figure 53-7 shows the behavior of this distribution with relative base width W/W_o as a parameter given a pure exponential distribution (a = 0) at $W = W_o$ and both a constant impurity density at the collector N(W) and a constant total number of impurities N_t. The exact solutions of the diffusion equation for such distributions are of considerable interest since they not only provide a means of checking the approximate techniques described in the previous quarterly progress report on Solid State Research,[39] but also yield a set of eigenfunction solutions that are useful in obtaining approximate solutions to the diffusion equation for other classes of base-impurity-density distribution functions by perturbation or iteration techniques.

The first-order base-layer switching-time constants (where this has been defined to be equal to the inverse of the lowest order eigenvalue of the system) have been calculated for the various impurity distributions of Fig. 53-7. These are shown plotted as a function of the relative base width parameter W/W_o in Fig. 53-8, together with the upper and lower bounds computed for this time constant by the techniques referred to above. The dashed curve is Shockley's solution for the case of the homogeneous base as a function of relative base width. By comparing the two cases, we see that the increase in switching speed is entirely due to the reduction in base width. For W/W_o near unity, the switching-time constants in both cases decrease directly as the square of W/W_o. However, as W/W_o becomes less than unity, the switching-time constant in the case of the inhomogeneously doped base decreases less rapidly than before due to the build-up of an uncompensated retarding field near the emitter. This disadvantage, however, is probably outweighed by the fact that the impurity density in the base at the collector junctions and the total number of impurities in the base may be independently controlled relative to the impurity density at the emitter, thereby allowing the designer to control, within limits, emitter injection efficiency, punch-through voltage and collector breakdown voltage independent of the reduction in base width.

It is well known that at sufficiently high collector current densities, the minority carrier density may be so large that the majority carrier distribution necessary for charge neutrality may partially, or even completely, swamp the effects of the inhomogeneous impurity distribution. Rittner[40] has pointed out in his treatment of junction transistor theory that this effect can occur at the normal current levels ($\sim$ 10 ma or less) in present-day transistors. Accordingly some calculations of the small-signal grounded-base switching-time constants have been made as a function of collector current density J_c in which we assumed the steady-state minority carrier density $P_{ss}(x)$ was not negligible compared with the base impurity density (nx). Figure 53-9 shows a normalized plot of the total majority carrier distribution $P_{ss}(x) + N(x)$ with a normalized collector current density $J_c/qD_p(N_o/W)$ as a parameter and the fixed inhomogeneous impurity distribution shown in Fig. 53-7 for the relative base width $W/W_o = 0.2$. It can be seen that the effect of increasing the collector current density tends to straighten out the minority carrier distribution. The effect of increasing J_c on the switching-time constant is shown in Fig. 53-10. In this figure we have plotted the upper bound of the relative, grounded-base switching-time constant τ/τ_o as computed from the total majority carrier density distributions shown in Fig. 53-9 as a function of the normalized collector current density for the relative base width case $W_b/W_{bo} = 0.2$. In this case we see that, for increasing collector current density, the relative switching time decreases monotonically to a value $\tau/\tau_o = 0.0246$, which is

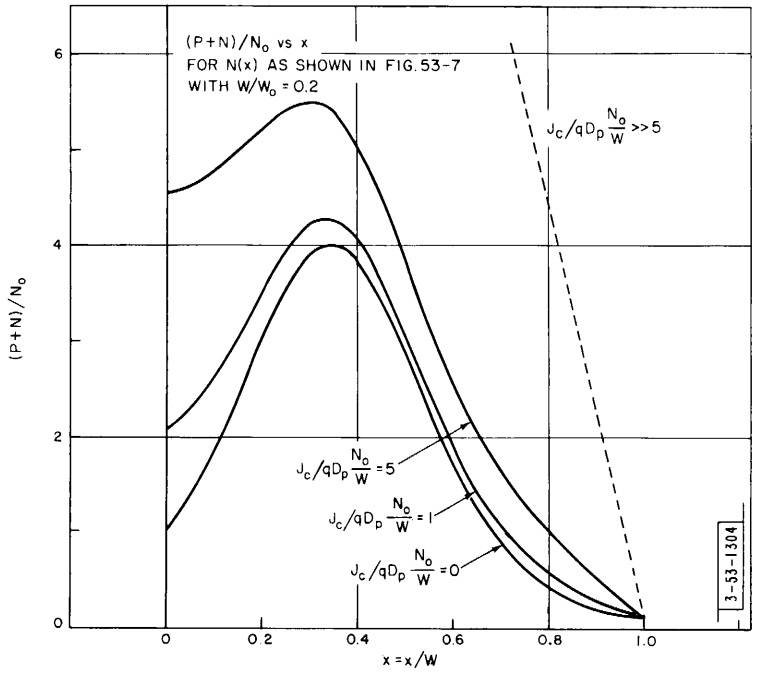

Fig. 53-9. Total base electron density distributions as a function of collector current density.

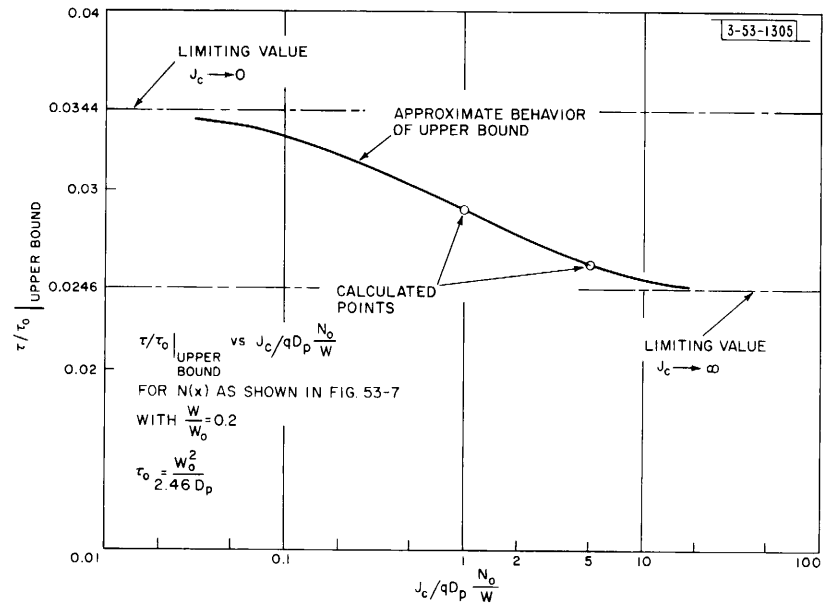

Fig. 53-10. Relative switching time as a function of collector current density.

just the switching time given by Shockley's homogeneous base expression

$$\tau = \frac{W_b^2}{2D_{p\ \text{effective}}} \quad , \tag{7}$$

where the effective diffusion constant is equal to twice the normal value of this constant. Thus we can conclude that, at sufficiently high collector current levels, the base-layer switching-time constant depends, in accordance with Eq. (7), only upon the base width regardless of the base impurity density distribution.

C. T. Kirk

D. Diode Characteristics at Microwave Frequencies

Interest in measuring diode parameters at microwave frequencies arises from possible applications as parametron computer elements. Two methods of measurement will be considered.

1. Waveguide Method

Consider a diode placed inside a waveguide as shown in Fig. 53-11. In order to determine the equivalent network parameters of the diode alone, we must make two complete sets of measurements, one with and one without the diode inserted. Since a discontinuity in a waveguide may be represented by a two-terminal pair with three parameters as shown in Fig. 53-12, three independent measurements with different load impedances as seen at reference plane T must be made for each complete set. The different load impedances can be most easily furnished by a movable short terminating the waveguide. In this case, the load impedance as seen at reference plane T is simply equal to $jZ_o \tan\beta\ell$, where Z_o and β are, respectively, the characteristic impedance and phase constant of the waveguide. The input impedance Z_{in} for the three different load impedances (different positions of the short) could be determined by measuring the VSWR and the position of the first minimum from the junction T. The formulas that relate the network parameters Z_{11}, Z_{12}, Z_{22} to the three Z_{in}'s and the three Z_L's are given elsewhere.[41]

Next the three measurements are repeated with the diode inserted. The new Z_{11}, Z_{12} and Z_{22} so obtained will be different from their previous values, and the difference is obviously attributed to the diode properties.

2. Cavity Method

Since diodes are usually cylindrical in shape, it is expedient to place them in a cylindrical cavity as shown in Fig. 53-13. In this case, an exact boundary value problem could be solved with only the ceramic cylinder of the diode inserted. Then the presence of the wire and p-n junction is treated as a perturbation. For simplicity, the cylinder can be assumed solid as the p-n junction diameter is typically much smaller than the outside diameter of the ceramic cylinder. If the boundary value problem of such a centrally located dielectric cylinder is solved with the TM_{01p} mode assumed, one finds that the resonance frequency of the cavity is determined by the transcendental equation

$$\epsilon k_{ca} J_o(k_{ca} r_c)\, N_o(k_{ca} r_d)\, J_o'(k_{cd} r_d) - k_{cd} J_o(k_{ca} r_c)\, J_o(k_{cd} r_d)\, N_o'(k_{ca} r_d)$$

$$+ k_{cd} N_o(k_{ca} r_c)\, J_o(k_{cd} r_d)\, J_o'(k_{ca} r_d) - \epsilon k_{ca} N_o(k_{ca} r_c)\, J_o(k_{ca} r_d)\, J_o'(k_{cd} r_d) = 0 \quad , \tag{8}$$

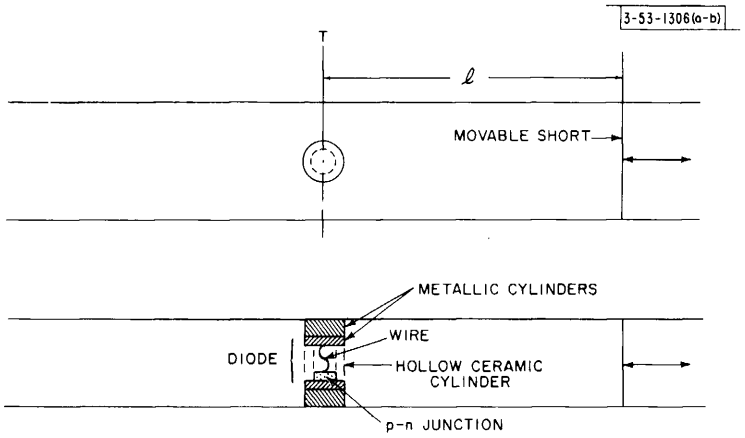

(a) Top view.

(b) Side view.

Fig. 53-11. Diode mounted in a waveguide.

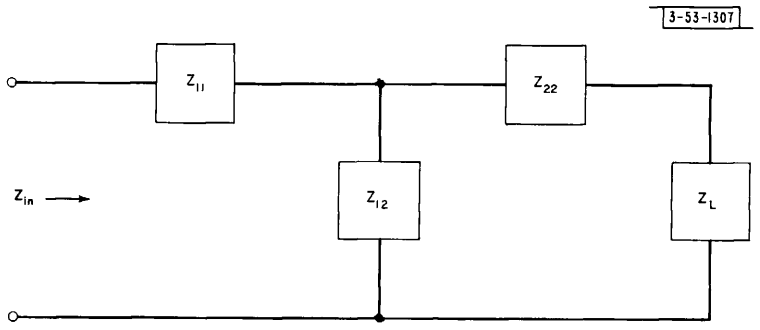

Fig. 53-12. Equivalent circuit of diode junction.

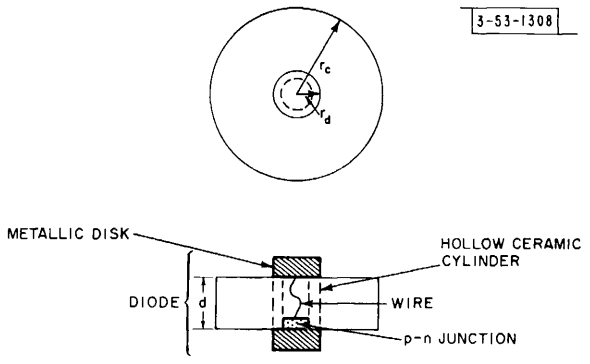

Fig. 53-13. Diode mounted in a TM_{01p} cavity.

where

$$k_{ca} = \sqrt{\left(\frac{\omega}{c}\right)^2 + \left(\frac{p\pi}{d}\right)^2}$$

$$k_{cd} = \sqrt{\left(\frac{\omega}{c}\right)^2 + \left(\frac{p\pi}{d}\right)^2} \qquad (9)$$

and ϵ is the relative dielectric constant of the cylinder. Thus, by measuring the resonance frequency of the cavity, one can determine the dielectric constant ϵ.

Next the wire is inserted. Since the wire is so small, its effect could be treated by perturbation theory. Because of the finite conductivity of the wire, there will be a change in Q as well as in resonance frequency of the cavity. If a complete diode is inserted instead and biased in the forward direction, we can measure the properties of the p-n junction minus the transition region; the transition region nearly disappears when the diode is in forward conduction. Finally, the characteristics of the transition region itself can be obtained by measuring the added shift in frequency of the cavity at various values of reverse-biased voltages.*

In principle, at least, the characteristics of the various portions of the diode could also be evaluated in the same way by using the waveguide method. However, since some of these effects may be very small, the extreme sensitivity of the cavity method may offer some advantages.

R. F. Soohoo

REFERENCES

1. A.E. Paladino, "Research Studies and Investigations of the Solid State Chemistry of Ferrites," Raytheon Manufacturing Company, Final Report, 15 January 1958 to 15 January 1959, Signal Corps Contract DA-36-039-SC-74987, DA Project Task No. 0095-pH-58-91.
2. J. Smiltens, J. Am. Chem. Soc. 79, 4881 (1957).
3. G.H. Jonker, J. Phys. Chem. Solids 9, 165 (1959).
4. A.E. Paladino, J. Amer. Ceram. Soc. 42, 168 (1959).
5. L.G. Van Uitert, J. Chem. Phys. 23, 1883 (1955).
6. D.G. Wickham and W.J. Croft, J. Phys. Chem. Solids 7, 351 (1958); Quarterly Progress Report on Solid State Research, Lincoln Laboratory, M.I.T. (1 May 1958), pp. 79-81.
7. D.G. Wickham and J.B. Goodenough, Phys. Rev. (to be published).
8. Quarterly Progress Report on Solid State Research, Lincoln Laboratory, M.I.T. (15 July 1959), pp. 91-92.
9. I.S. Jacobs, Bull. Am. Phys. Soc. II, 4, 178 (1959).
10. Y. Yafet and C. Kittel, Phys. Rev. 87, 290 (1952).
11. F.K. Lotgering, Philips Res. Repts. 11, 190 (1956); 337 (1956).
12. J.S. Kasper, Bull. Am. Phys. Soc. II, 4, 178 (1959).
13. P.F. Bongers, Ph. D. Thesis, University of Leiden (1957).
14. A.S. Borovik-Romanov and M.P. Orlova, Sov. Phys. JETP (USSR) 5, 1023 (1957).
15. T.A. Kaplan, private communication.

* The author is indebted to C.T. Kirk for suggesting this biasing procedure.

REFERENCES (Continued)

16. F.J. Morin, Phys. Rev. Letters 3, 34 (1959); Bell Sys. Tech. J. 37, 1047 (1958).
17. T.A. Kaplan, Phys. Rev. (to be published).
18. L. Corliss and J. Hastings, unpublished results.
19. N. Menyuk and K. Dwight, private communication.
20. P.W. Anderson, Phys. Rev. 102, 1008 (1956).
21. N. Menyuk and K. Dwight, private communication.
22. L. Corliss, J. Hastings and R.J. Weiss, Phys. Rev. Letters (to be published).
23. Private discussions with J. Hastings.
24. D.O. Smith, J. Appl. Phys. 30, 264S (1959).
25. T.G. Knorr and R.W. Hoffman, Phys. Rev. 113, 1039 (1959).
26. J.D. Finegan and R.W. Hoffman, J. Appl. Phys. 30, 597 (1959).
27. E.E. Huber, Jr. and D.O. Smith, J. Appl. Phys. 30S, 267S (1959).
28. W.M. H. Sachtler, G. Dorgelo and W. van der Knaap, J. Chem. Phys. 51, 491 (1954).
29. Division 5 Quarterly Progress Report, Lincoln Laboratory, M.I.T. (15 March 1959), p. 58.
30. Z. Frait, Czech. J. Phys. 8, 113 (1958).
31. C. Ryan, T. Crowther and J. Raffel, Group 51 Biweekly Report, Issue No. 71, Lincoln Laboratory, M.I.T. (7 August 1959) (not generally available).
32. C.D. Olson and A.V. Pohm, J. Appl. Phys. 29, 274 (1958).
33. F.B. Humphrey, J. Appl. Phys. 29, 284 (1958).
34. F.B. Hagedorn, J. Appl. Phys. 30S, 254S (1959).
35. T.S. Crowther, unpublished data.
36. R.C. Johnston, Group Report 53-18, Lincoln Laboratory, M.I.T. (16 July 1959) (not generally available).
37. M.E. Petersen, "Evaporated Microstrip Transmission Line," SM Thesis, M.I.T. (June 1957).
38. R.C. Johnston, I.R.E.
39. Quarterly Progress Report on Solid State Research, Lincoln Laboratory, M.I.T. (15 July 1959).
40. E.S. Rittner, Phys. Rev. 94, 1161 (1954).
41. S. Ramo and J.R. Whinery, Fields and Waves in Modern Radio, 2nd ed. (Wiley, New York, 1956), p. 459.

PATTERN RECOGNITION
GROUP 54

SELFRIDGE, O. G., *Leader*
GOLD, B., *Assistant Leader*

BERG, R. S.
DOYLE, W. L., Jr.
EVENS, M. W.*
FEISTEL, H.
FREIMER, M.
HODES, L.*
HOWLAND, B.
LAEMMEL, A. E.*
McELWAIN, C. K.
McLAUGHLIN, W. C.
MINSKY, M.
NEISSER, U.*
PITCHER, T. S.
SILVER, R. L.
SLAGLE, J. R.†
WILSON, L. D.*

---

* Temporary.
† Staff Associate.

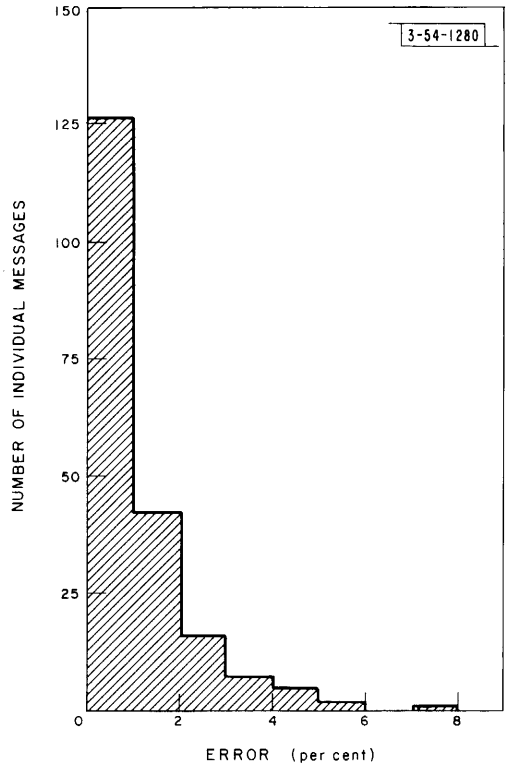

Fig. 54-1. MAUDE: Austin test, total errors.

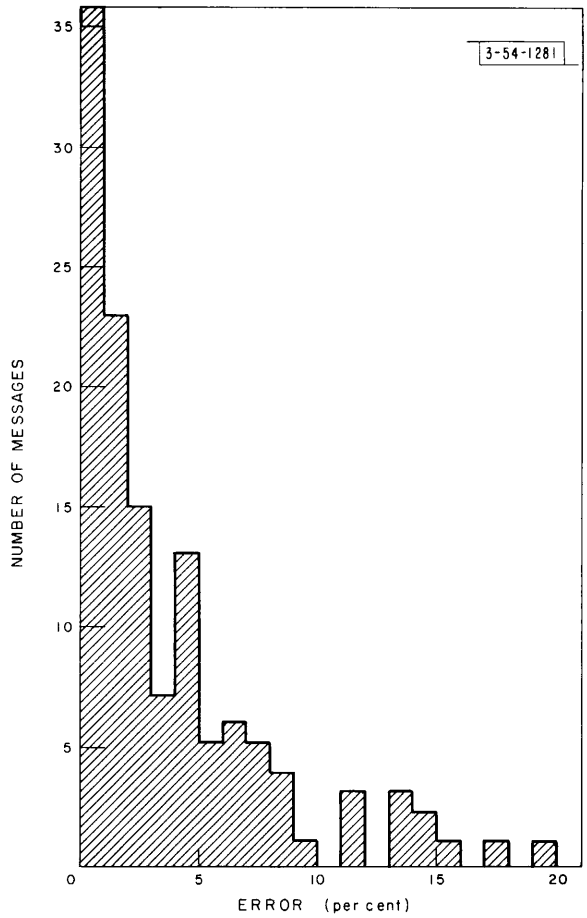

Fig. 54-2. MAUDE: Blow test, total errors.

PATTERN RECOGNITION
GROUP 54

I. INTRODUCTION

At present we are trying to gain experience in applying adaptive and learning techniques to real problems with realistic constraints.

A pandemonium model for character recognition works encouragingly well; its working structure shows signs of extending to other recognition problems. The hill-climber units have been extensively examined in the laboratory and on the computer.

The basic MAUDE Morse code decoder is now undergoing operational testing, and ancillary studies are proceeding.

O. G. Selfridge

II. MAUDE

A. MAUDE Tests

The new laboratory model of MAUDE has been completed and tested. Several hundred messages sent by various operators were run through this new model and the results tabulated. The input data were divided into two tests: the Blow test and the Austin test. In the Blow test, operators sent the same English text message, beginning with "The quick brown fox..." sent 3 times and followed by "Those of us who have responsibilities...". In the Austin test, 12 operators each sent 18 messages, consisting of letter cipher, number cipher, mixed cipher and English text.

For the Austin test, according to criteria previously developed,* essentially all of the MAUDE translations would be readable (Fig. 54-1). For the Blow test, however, by setting 7 per cent error as a criterion of readability, 21 out of 125 translations would be unreadable (Fig. 54-2). Apparently the tests were produced under very different conditions, since the two curves are markedly different.

The combined results of the two tests are similar to the data obtained from the IBM 704 simulation program.

B. Gold Martha W. Evens
R. S. Berg W. C. McLaughlin

B. Degarble

Degarble is a 709 program to reconstruct mutilated text from the first grade primer New Fun with Dick and Jane.† The text is mutilated with random Morse-type garbles in 500-character sections, spelling out all numbers and punctuation except for apostrophes and quotation marks. The total vocabulary count is 190 words.

The present approach uses only the vocabulary in its Morse context and omits grammatical and semantic considerations. A set of rules performs the corrections shown in the example below.

---

*Division 3 Quarterly Progress Report, Lincoln Laboratory, M.I.T. (15 July 1958), pp. 39-40.

†The New Fun with Dick and Jane (Scott, Foresman and Company, Chicago, 1956).

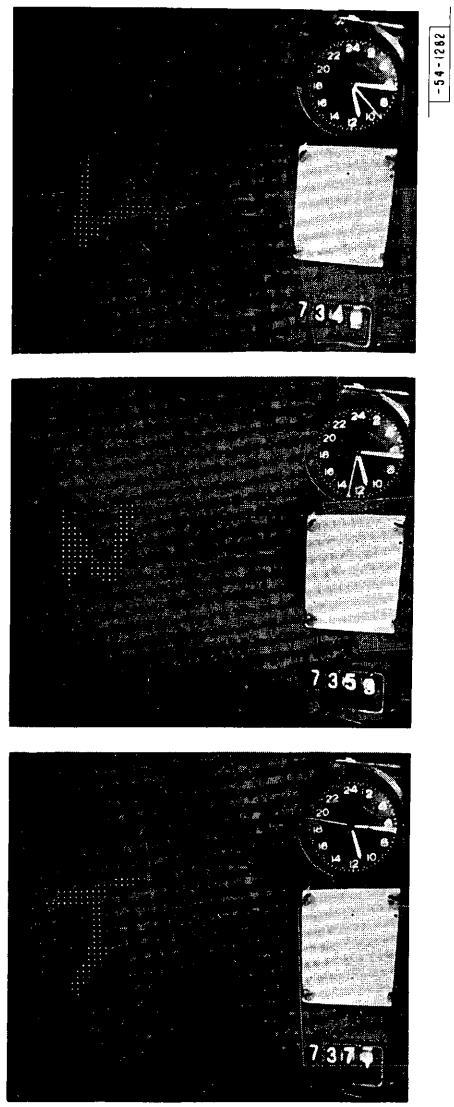

Fig. 54-3. Samples of the characters used.

The space rules isolate the garbled words after reconstructing the correct spacing for the remaining text. The character changing program corrected the underlined words and failed to correct the words still left in parentheses.

Original Message

DIC KSAID COM MA G OODBY COMQ MOTHER PE R IODGOOD KY
COMM AS ALLY PERIOD WEMWST GOTO SCSO O L PERIO D GOODBY
EX CL AM AT I ON POINT GOOD BYECAE AMATION POI NTSAID AMANE
PE RIOD WE MS STGO TO S KHOOL NOM PERIODWE WILL GO WI 6T
OM AND SSSANPERI OD

Message After Applying Space Rules

DICK SAID COMMA GOODBY (COMQMOTHER) PERIOD (GOODKY)
COMMA SALLY PERIOD (WEMWST GOTO SCSOOL) PWEIOD GOODBY
EXCLAMATION POINT GOODBY (EXCAEMATION) POINT SAID (AMANE)
PERIOD (WEMSSTGOTOSKHOOLNOM) PERIOD WE WILL GO WITH TOME
AND (SSSAN) PERIOD

Degarbled Message

DICK SAID COMMA GOODBY COMMA MOTHER PERIOD GOODBY COMMA
SALLY PERIOD WE MUST GO TO SCHOOL PERIOD GOODBY EXCLAMATION
POINT GOODBY (EXCAEAMATION) POINT SAID JANE PERIOD WE MUST
GO TO SCHOOL (NOM) PERIOD WE WILL GO WITH TOM AND SUSAN
PERIOD

We plan to experiment with more sophisticated routines, correction of multiple garbles and a substantial vocabulary increase.

Martha W. Evens
Constance K. McElwain
F. VanHoosen

III. LEARNING

A. Pandemonium Studies

1. Results

The hand-written character recognition work described in the last quarterly progress report has been continued to a point of some success with the available data. At the moment, 28 tests are in use. Application to the data on hand (a total of 243 samples of the ten characters A E I L M N O R S T) gave the following confusion matrix. Samples of the characters are shown in Fig. 54-3 (96 per cent of the samples were correctly identified).*

* All data used were very kindly provided by H. Sherman and E. Howell, Group 25, from samples collected for their work.

Confusion Matrix for Ten Characters

Input	Identified as: A	E	I	L	M	N	O	R	S	T
A	0.91		0.03			0.03		0.03		
E		0.94		0.03						0.03
I			1.00							
L			0.09	0.87		0.04				
M					0.94	0.06				
N					0.04	0.96				
O							1.00			
R								1.00		
S									1.00	
T										1.00

2. Process

The process is as follows: a census, which lists the number of times a given test gave a particular result for each of the characters under consideration, is prepared from a set of samples. These observed frequencies are then replaced (in the census table) by the corresponding inverse probabilities, i.e., the probabilities that we are examining each of the characters given that the test in question produced the result observed. The decision is then made by summing these inverse probabilities and electing the character whose sum is greatest.

Because of the interrelations of the tests, it is not clear how their outputs should best be combined. The equal weighting used will be compared later with some other rules.

3. Test Evaluation

Eventually we must have some way to vary the weighting of the test results to achieve optimum performance under some restriction on the decision scheme. To get some idea of each test's usefulness, we calculated (from the census data mentioned above) the average information gain for each test. The results of the calculation agree with our a priori knowledge about the characters and the nature of the tests.

W. L. Doyle, Jr.

B. Dynamic Programming and Adaptive Processes

In a discrete-time dynamic programming process, we must look all the way to the end of the process ($n = N$) in order to make an optimal first decision x. Since this may involve considerable calculation, we proposed to look ahead just m stages, where $m \ll N$, doing the best we can within this limitation. For the linear-control quadratic-loss problem this policy has been completely analyzed, including a proof that it, and its cost function, converge to the optimal as $m \to \infty$. The question is now being considered with regard to other cost and control functions.

M. Freimer

C. Hill-Climbing

We have constructed a laboratory six-dimensional hill-climber, whose behavior is sufficiently illustrated by Figs. 54-4 and 54-5, which plot the total error of the setting of six potentiometers in series as in Fig. 54-6. Figure 54-4 shows the course of the error for a maximum deviation of one variable, Fig. 54-5 for all six variables. The six identical hill-climber units followed the scheme illustrated in the last quarterly progress report. Other schemes have been tested extensively. The behavior of another scheme is illustrated in Fig. 54-7, showing the error of a twenty-dimensional hill-climber computed on the IBM 709.

B. Howland
M. Minsky
O.G. Selfridge

IV. MISCELLANEOUS

There has recently been considerable interest in the use of nonlinear capacitors, also known as varactors or hole storage diodes, for low noise amplification, harmonic and subharmonic generation, pulse generation, etc.; further applications of this new and useful circuit element are to be expected. An analogue equivalent circuit, which may prove useful for the study of the effects of residual parameters of a varactor, is shown in Fig. 54-8.

This equivalent circuit is composed of Philbrick operational amplifiers, which may optionally be cathode followers boosted for greater current capability. It is the analogue of an ideal nonlinear capacitor with one terminal at ground. The operation is very simple: a conventional feedback integrating circuit keeps track of the apparent supply of stored current carriers in the varactor. This integrator circuit is followed by an electronic switch that connects or disconnects the feedback condenser accordingly as the indicated supply of stored holes is positive or zero. As such, this analogue will simulate an ideal nonlinear capacitor, and its operation will therefore be essentially independent of the size of all circuit elements. With the inclusion of a finite resistance R in parallel with the feedback condenser, the analogue becomes a one-parameter circuit; the RC time constant of the feedback pair represents the hole storage time of the varactor diode.

Mention should be made of the additional feedback loop connecting to the second input of the integrator; the purpose of this is to keep the amplifiers from saturating when the apparent supply of holes reaches zero. With the present circuit, when the supply of holes reaches zero, the outputs of both amplifiers follow, with unity gain and opposite polarity, the input signal. Without this provision, saturation would occur, and the recovery would take many microseconds – the effect would be to produce an apparent delay of onset of conduction in the simulated diode.

B. Howland

V. RECOGNITION AND LEARNING IN MAN

A. Hierarchies in Human Pattern Recognition

Theoretical considerations suggest that the human ability to recognize complex patterns (such as those of language and spatial vision) may be based on a hierarchical system resembling pandemonium. To explore this possibility, a hierarchically organized artificial language has been devised and used as learning material for experimental subjects. Results suggest that the formation of "demons" on a lower level facilitates recognition of patterns. Further work on deeper hierarchies and various sense modalities is planned.

U. Neisser

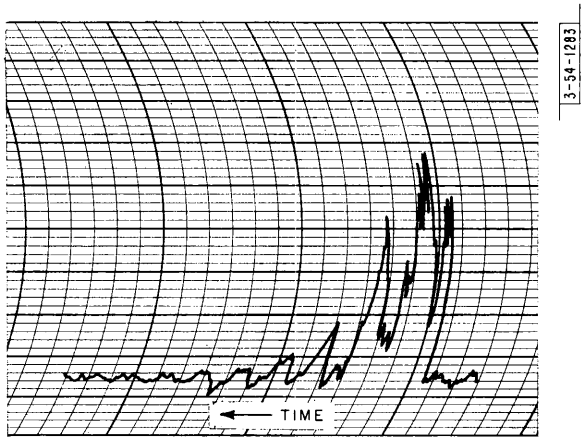

Fig. 54-4. Course of the error for a maximum deviation of one variable.

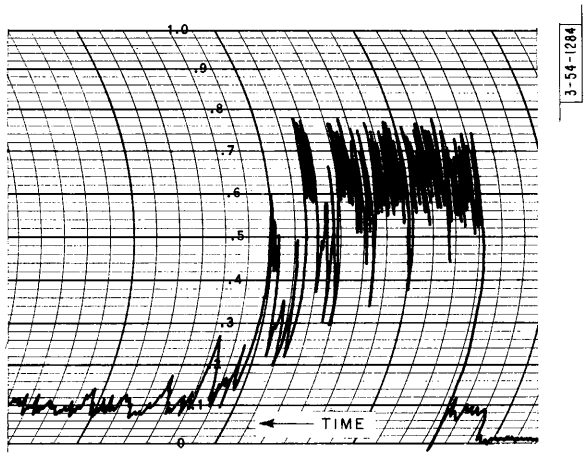

Fig. 54-5. Course of the error for a maximum deviation for all variables.

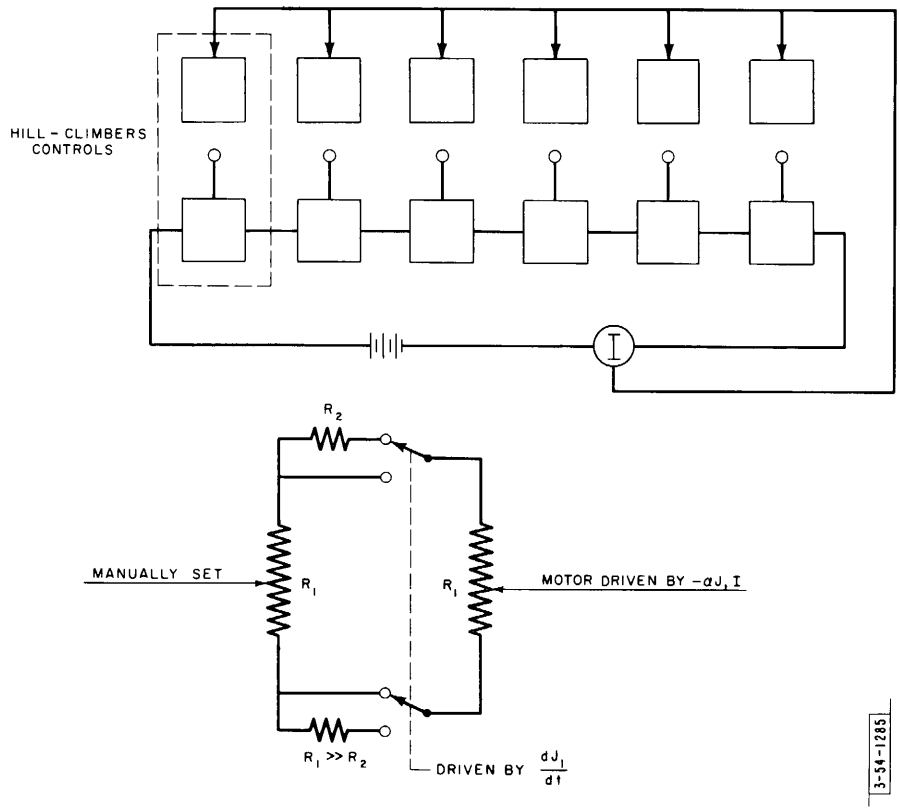

Fig. 54-6. Six-unit hill-climber: to minimize current I.

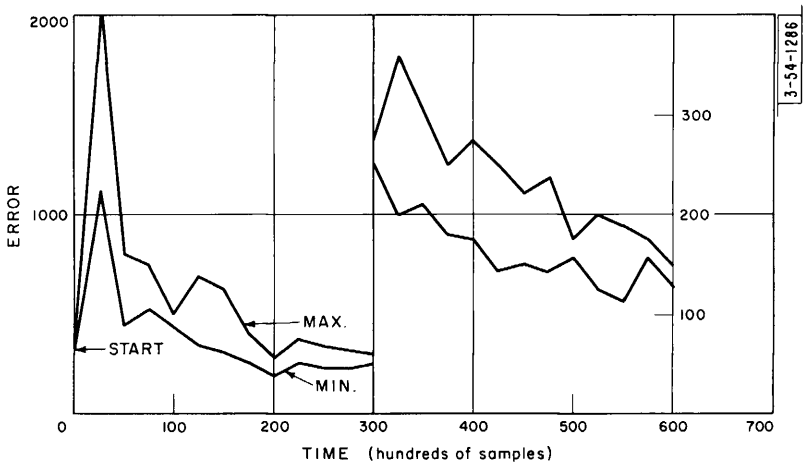

Fig. 54-7. Error history of 20-unit hill-climber.

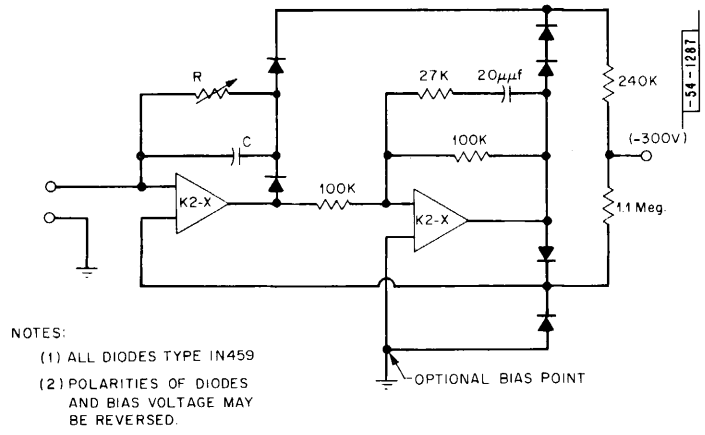

Fig. 54-8. Analogue equivalent for nonlinear capacitor.

B. Process and Procedure in Induction

It may be hoped that some characteristics of human pattern recognition may be inferred from: (1) the difference in the difficulty with which various patterns are recognized and (2) the effect of different procedures of presenting the material. Therefore, subjects have been asked to induce binary functions, which describe a set of stimuli, from examples of the set, with both the function itself and the manner of presentation as experimental variables. All the nontrivial binary functions (A and B, A or not-B, etc.) have been studied with two modes of presentation, termed "discrimination" and "comprehension." In discrimination, the subject's task is to decide whether each stimulus belongs to the set or not, and he is given regular feedback. In the comprehension procedure, the subjects see many examples without making any response, and then attempt to describe the function itself. Analysis of the data from these experiments is in progress.

U. Neisser
P. L. Weene (Group 58)

C. Human Recognition of Hand-Printed Characters

Randomly sampled exemplars of hand-printed letters and numerals were shown, out of context, to experimental subjects for identification. Their error rate, exclusive of the confusions I-one and 0-zero, was about 4 per cent. This is seen as providing a target, and perhaps an upper bound, for the accuracy of mechanical recognition devices. Work is continuing.

U. Neisser

ANALYSIS
GROUP 55

ROOT, W. L., *Leader*

BEYER, W. A.
CONNER, H. E.
KINNEY, J. R.
LEVIN, J. J.
LORDAN, J. D.
WEISS, E.
ZIERLER, N.

ANALYSIS
GROUP 55

I. INTRODUCTION

Unclassified work by Group 55 members for the preceding quarter has been in the following areas: multiple-station queuing theory, decoding of error-correcting codes and general coding theory, decision theory in radio communications, asymptotic behavior of solutions of certain integrodifferential systems, and properties of infinite series with random coefficients.

W. L. Root

II. HAUSDORFF DIMENSION AND INDEPENDENT FUNCTIONS

Let a source $\{X, \mu\}$ be the sequence of independent random variables $x = 0$ (Prob $\frac{1}{2}$), $x = 1$ (Prob $\frac{1}{2}$). We consider a mapping of source messages into real numbers defined by $\alpha = \sum_{i=1}^{\infty} x_i r^i$ where $\frac{1}{2} < r < 1$. J.R. Kinney (Group Report M24-52, 1955, not generally available) has previously discussed a physical model of this mapping. For $1 > r > \frac{1}{2}$ this mapping is many to one. We study the redundancy of the mapping. We define the quantity $\beta(\alpha, r) = \{x : \sum_{i=1}^{\infty} x_i(x)\, r^i = \alpha, 0 < x \leqslant 1\}$ where $x_i(x)$ is the i^{th} digit of the nonterminating binary expansion of x. The mapping redundancy is studied by calculating either the Hausdorff-Besicovitch dimension of $\beta(\alpha, r)$ [written dim $\beta(\alpha, r)$] or the cardinality of $\beta(\alpha, r)$ [written card $\beta(\alpha, r)$]. We assume always that $0 < \alpha < r/(1 - r)$ and that n is a fixed integer > 1. We take c and d to be the cardinality of the continuum and the integers, respectively.

We have proved the following statements. First, $\dim \beta(\alpha, 2^{-1/n}) = 1 - 1/n$. For fixed $r \in (\frac{1}{2}, 1)$ and for almost every α, $\dim \beta(\alpha, r) \leqslant \log_2 2r$. If

$$2^{-1/n} \geqslant r \geqslant 2^{-1/n-1} \quad , \quad 1 - \frac{1}{n} \geqslant \dim \beta(\alpha, r) \geqslant 1 - \frac{1}{n-1} \quad .$$

For $1 > r > (\sqrt{5 - 4/n} - 1)/2(1 - 1/n)$, $\dim \beta(\alpha, r) \geqslant 1/n$. For $1 > r > (\sqrt{5} - 1)/2$, card $\beta(\alpha, r) = c$. For $r = (\sqrt{5} - 1)/2$, card $\beta(\alpha, r) = d$ or c according as α is or is not an algebraic integer in the quadratic field $\mathfrak{R}(\sqrt{5})$. For $(\sqrt{5} - 1)/2 > r > \frac{1}{2}$, there are some sets $\beta(\alpha, r)$ of finite cardinality and some of cardinality c. We have identified the above problem with that of calculating the "size" of the intersection of a certain $(n - 1)$-dimensional hyperplane with an n-dimensional Cantor-type perfect set.

We have also investigated the sets

$$\beta(\alpha, \{a_i\}) = \left\{ x \mid \sum_{i=1}^{\infty} x_i(x)\, a_i = \alpha \right\}$$

where $\sum_{i=1}^{\infty} |a_i| = +\infty$. We find that if $\{a_i\}$ is on ℓ_2 sequence, then $\dim \beta(\alpha, \{a_i\}) = 1$ for every real number α.

Details of the above work are reported in Group Reports 55-9, 55-11 and 55-13 (not generally available). We are continuing the investigation with $\{x_i a_i\}$ replaced by other random variables.

One of the members of the group* has established a connection between Hausdorff-Besicovitch dimension and entropy in the sense of Shannon. Shannon† has given the reason for his own belief that there should be such a connection. He observes that if independent sources $\{X_1, \mu_1\}$, $\{X_2, \mu_2\}$ are combined to form a third source $\{X_1 \otimes X_2, \mu_1 \otimes \mu_2\}$, then $H\{X_1 \otimes X_2, \mu_1 \otimes \mu_2\} = H\{X_1, \mu_1\} + H\{X_2, \mu_2\}$. Likewise, if A and B are linear sets and A $\otimes$ B is their Cartesian product, then dim A $\otimes$ B = dim A + dim B. Work is being done on developing the implications of this observation.

W. A. Beyer

III. A TRANSIENT DISCRETE TIME QUEUE

Queues are examined for the case in which service occurs at integral times whenever customers are present. Any number of customers up to m may be served per unit time. We obtain generating functions for the distribution of the number of customers in the queue for any integral time. A functional relation is found between the generating function of the input-output distribution and that of the busy period. The expressions describing the transients are derived from this relation. This work arises from investigations of buffer storage by I. S. Reed of Group 47.

J. R. Kinney

IV. ON A SYSTEM OF INTEGRODIFFERENTIAL EQUATIONS OCCURRING IN REACTOR DYNAMICS

In the preceding quarterly progress report (Division 5, 15 June 1959) we reported on an investigation of the real system of integrodifferential equations

$$\frac{du}{dt} = -\int_{-\infty}^{\infty} \alpha(x)\, T(x,t)\, dx \quad , \quad a\,\frac{\partial T}{\partial t} = b\,\frac{\partial^2 T}{\partial x^2} + \eta(x)\, u \qquad (0 \leqslant t < \infty) \quad , \tag{1}$$

satisfying the initial condition

$$u(0) = u_0 \quad , \quad T(x, 0) = f(x) \qquad (-\infty < x < \infty) \quad . \tag{2}$$

The system (1) describes the linearized dynamic model of a continuous medium nuclear reactor. The related degenerate system

$$\frac{du}{dt} = -\int_{-\infty}^{\infty} \alpha(x)\, T(x,t)\, dx \quad , \quad a\,\frac{\partial T}{\partial t} = \eta(x)\, u \qquad (0 \leqslant t < \infty) \quad , \tag{3}$$

subject to the initial condition (2), was also discussed.

Since the initial work, we have succeeded in relaxing the hypotheses of the various theorems. The conclusions of the theorems are the same as before (Division 5 Quarterly Progress Report, 15 June 1959), hence we state only the new hypotheses here.

Hypothesis for Theorem 1.

$$\alpha(x), \eta(x), f(x) \in L_2(-\infty, \infty)$$

$$f(x) \in C(-\infty, \infty)$$

$$|\eta(x)| \leqslant K_1 \qquad (-\infty < x < \infty)$$

$$|\eta(x_1) - \eta(x_2)| \leqslant K_2 |x_1 - x_2| \qquad (-\infty < x_1, x_2 < \infty) \quad .$$

* J. R. Kinney, Proc. Am. Math. Soc. 9, 603 (1958).

† C. E. Shannon, Trans. I.R.E., PGIT-2, 174 (1953).

Hypothesis for Theorem 2.

Same as for Theorem 1, as well as $\mathrm{Re}\{\hat{\eta}(x)\,\hat{\alpha}(-x)\} \geqslant 0$, $\mathrm{Re}\{\hat{\eta}(x)\,\hat{\alpha}(-x)\} > 0$ on a set of positive measure $(0 \leqslant x < \infty)$

$$\alpha(x), \eta(x), f(x) = 0(\exp[-\lambda x]) \qquad (\lambda > 0;\ |x| \to \infty)$$

$$\left(\int_{-\infty}^{\infty} \alpha(x)\,dx\right)\left(\int_{-\infty}^{\infty} f(x)\,dx\right) \neq 0 \quad .$$

Hypothesis for Theorem 3.

Same as for Theorem 1, as well as

$$|f(x)| \leqslant K_1 \qquad (-\infty < x < \infty) \quad .$$

Hypothesis for Theorem 4.

$$\alpha(x), \eta(x), f(x) \in L_2(-\infty, \infty)$$

$$(\alpha, \eta) = \int_{-\infty}^{\infty} \alpha(x)\,\eta(x)\,dx > 0 \quad .$$

Hypothesis for Theorem 5.

Same as Theorem 1, as well as

$$(\alpha, \eta) = \int_{-\infty}^{\infty} \alpha(x)\,\eta(x)\,dx > 0 \quad .$$

J.J. Levin
J.A. Nohel*

V. COMMUNICATIONS THROUGH UNSPECIFIED ADDITIVE NOISE

The problem has been considered of specifying a decision rule that will guarantee a maximum reliability of reception in a radio data link operating in the presence of unspecified additive noise. Two examples have been worked out, and for each, the information rate that the resulting channels (including the decision making) will permit has been calculated.

In both examples, it is assumed that the signal is corrupted only by additive noise, but the additive noise need have no statistical regularity or predictability that can be taken advantage of. Thus the "noise" may be natural or man-made and subject to influences unknown to the communicators. Essentially, the only restriction on the noise is that its power be bounded. The idea of using a decision criterion at the receiver which guarantees the greatest possible average reliability of reception, no matter what the noise may be, leads to a maximin decision criterion at the receiver and to the use of concepts from the theory of zero-sum two-person games.

The first example is a keyed-carrier system using a binary alphabet in which the MARK symbol is transmitted as unmodulated carrier for an interval of duration T, and the SPACE symbol is "transmitted" as an interval of silence of duration T. The system is synchronous only with respect to the modulation; RF phase is not necessarily known. The only constraints

* Mathematics Research Center, U.S. Army, Madison, Wisconsin and Georgia Institute of Technology. Supported by U.S. Army under Contract No. DA-11-022-ORD-2059, and, in part, by the National Science Foundation NSF G-7343.

on the noise are that the total noise energy arriving at the receiver during one symbol interval T is bounded, and that the noise is incoherent with the signal as far as RF phase is concerned (the noise and signal powers add). Under these conditions a randomized decision rule is exhibited which guarantees a probability of making a correct choice for each received symbol of

$$p = \frac{1}{2} + \frac{1}{2[a+1]}^{*}$$

where a is the ratio of possible noise energy per symbol-to-signal energy. It is further shown that no decision rule can guarantee a probability of making a correct choice greater than 1/2 + 1/2a. If the maximum possible noise power density is constant over the whole frequency spectrum at N watts/cycle/second and the signal power is S watts, and if the receiver bandwidth B is given by $B = \rho/T$, ρ = constant, then for NB/S large the information rate through the channel is

$$R = \frac{\log_2 e}{4\rho} \cdot \frac{1}{B} \left(\frac{S}{N}\right)^2 + 0\left(\frac{1}{B^2}\right) \quad .$$

The second example is a phase-reversal-modulation system in which the SPACE symbol is the negative of the MARK symbol. In this example RF phase is known at the receiver, and the noise may be coherent with the signal (cancellation of transmitted signal is possible). Otherwise, everything is as in the previous example. Under these conditions a randomized decision rule is exhibited which guarantees a probability of making a correct choice for each received symbol of

$$p = \frac{1}{2} + \frac{1}{2[\sqrt{a}+1]}$$

and it is shown no decision rule can guarantee a probability p of greater than $1/2 + 1/2\sqrt{a}$. The asymptotic information rate, under the same conditions as above, is

$$R = \frac{\log_2 e}{4\rho} \cdot \frac{S}{N} + 0\left(\frac{1}{B^{\frac{1}{2}}}\right) \quad .$$

W. L. Root

VI. REED-MULLER CODES

We have been studying linear codes of the error-correcting type, and can give a rather natural description of the Reed-Muller codes within the framework of Grassman algebras. Our procedure is comparatively transparent — especially since the "error correction theorem" (Reed's Theorem A) and the "decoding theorem" (Reed's Theorem B) both appear as simple consequences of some very general considerations.

E. Weiss

VII. DECODING LINEAR ERROR-CORRECTING CODES

A class of decoding schemes for linear codes has been found which depends on the existence of a group of symmetries of the received message space V with respect to a "decoding function." Such a group induces a group of automorphisms of the character group of the space, and the functions on V obtained by adding all the characters in an orbit provide a natural method of computing the decoding function.

* [x] = the largest integer less than or equal to x.

A natural candidate for the role of decoding function is the function W which assigns to each element of V the norm of its coset leader. It is easy to see that the group Π of coordinate permutations of V which map the alphabet (= transmitted message) subspace A on itself preserve W. Now, any automorphism of V mapping A on itself clearly induces a permutation of the coset space V/A, and it is only this latter permutation which is of practical interest. A consequence of the following theorem is that with W as the decoding function, and under a very slight restriction on A, we need not look outside of Π for suitable symmetries of V.

Theorem.

Suppose $||v|| > 2$ for every v in A except 0, and let α be any automorphism of V which maps A on itself and fixes W (i.e., $W(\alpha(u)) = W(u)$ for all u in V). Then the permutation of V/A induced by α coincides with that induced by some member of Π.

The ideas and techniques involved in this class of decoding procedures have been illustrated by the construction of two decoding procedures for the (12, 23) 3-error-correcting code of Golay.

N. Zierler

PSYCHOLOGY
GROUP 58

GREEN, B. F., Jr., *Leader*
TORGERSON, W. S., *Associate Leader*

BOWDEN, D. M.*
FORGIE, C. D.
GROVES, M. L.
HARRIS, W. P.
KLEM, L.
MITCHELL, R. T.
MUESER, G. E.
RESNICK, R.
SMITH, J. E. K.
STOWE, A. N.
WAUGH, N. C.
WEENE, P. L.*
WHITE, B. W.
WOLF, A. K.
YNTEMA, D. B.

*Summer.

PSYCHOLOGY
GROUP 58

I. INTRODUCTION

The development of more effective means for men to communicate with machines continues to be a major goal of Group 58. Most of the effort on the speech recognition project during the present reporting period was spent in transferring the program and the equipment to the TX-2 computer. This is the project's third computer; it enjoyed early successes on TX-0 and was later transferred to Whirlwind which has now been shut down. Still another computer, the IBM 709, is being used in work on speech segmentation. This work has been accelerated by equipment recently completed by Group 33 for converting analogue magnetic tapes to digital tapes for the 709. Results from the speech segmentation study have been used in a pilot study of the inverse problem: synthesizing speech from isolated syllables. The results showed limited promise, but the need for rapid access to a large inventory of stored syllables makes the system seem unreasonable at present for most applications. Finally, a project in computer interpretation of English language inputs has been started; the goal is to program a computer to answer questions stated in normal English about a set of data contained in its storage.

Studies of human information processing are being conducted in the fields of visual and auditory perception, judgment, learning and memory. A precise psychophysical study of visual dark adaptation has been conducted this summer, with the help of two summer staff members. Experiments on human memory for changing events, human decision making in complex situations, and human rote learning are continuing, and an experiment on the auditory encoding of English text has begun. These experiments, and others now being planned, will be greatly facilitated by a new contract with Tufts University, under which student subjects will participate in psychological experiments.

Staff members of Group 58 continue to participate in Laboratory projects outside the group. W. P. Harris is a member of the AICBM summer study group. W. S. Torgerson has been working with members of Group 22 on the automatic data processing study being carried out for CONARC. R. T. Mitchell is helping the MITRE Corporation to evaluate new systems for lighting the SAGE direction centers.

II. MAN-MACHINE COMMUNICATION

A. Automatic Speech Recognition

The speech input equipment for the speech recognition program has been transferred from Whirlwind to TX-2. Necessary new circuitry has been constructed, installed and checked out. The input system as a whole is now operating satisfactorily. An electronic commutator has been ordered which should eliminate maintenance and synchronization problems associated with the present mechanical commutator. The new commutator should be in operation by the end of the next quarterly period.

A number of utility programs have been completed and checked out. These include programs for:

(1) Getting data into the computer,
(2) Printing a brief summary of over-all amplitude levels and durations,
(3) Printing a complete numerical spectrum of selected speech segments,
(4) Printing a bar graph spectrum of the data.

The analysis program currently consists of the first steps toward:

(1) An improved version of the Whirlwind I vowel recognition program,

(2) A segmentation scheme based on amplitude and formant-motion information,

(3) A classification scheme for fricatives, nasals and semivowels.

Carma D. Forgie
J. W. Forgie (Group 51)

B. Syllable Segmentation

As described in the last quarterly progress report (Division 5 Quarterly Progress Report for 15 June 1959), a series of IBM 709 computer programs has been written which simulates the operation of a speech segmenting device. Speech is segmented by the analysis of configurations of the amplitude envelope of the speech wave form. The data used are therefore samples of the envelope at regular intervals of time.

The programs have been checked out with data obtained by using a diode and an RC filter as an envelope detector. However, the RC filter introduced ripple into the envelope signal, so that slope measurement, which is part of the envelope analysis, could not be made accurately. Two methods of solving this problem have been tried. First, a filter with a sharper cutoff, the Krohn-Hite 330a, has been modified by M. L. Groves, and is now being used. Second, the computer programs have been modified. For negative-to-positive and positive-to-negative slope change detection, the new slope direction must now be detected for at least two sample times, before the occurrence of the negative-to-positive or positive-to-negative features is recorded. For a more accurate measure of slope, which is needed in order to detect a slope change, the slope is averaged over a longer time. The effect of these modifications will be tested shortly.

A. N. Stowe

C. Speech Synthesis

An experiment was performed to investigate the possibility of speech synthesis from prerecorded syllables, using some of the principles that are being used in the work on the segmentation problem.

Twenty Egan sentences were used as text for the experiment.[1] Syllables spoken in an artificial context were recorded on magnetic tape and spliced together to construct the text. Length of syllables and phrasing in the sentences were not controlled. Amplitude was normalized so that the average amplitude of all the syllables was roughly the same. Key words were spoken at about 105 cps for the fundamental, and others at about 100 cps. The rate was about 200 words per minute. The constructed text was used for an intelligibility test. Seven listeners from Group 58 recognized an average of 83 per cent of key words. This score corresponds to about a 55 per cent phonetically balanced (PB) word score.[2] Unexploded final stops and complex nuclei accounted for half of the errors. Since a PB word score of 55 per cent is just on the border of "intelligible" speech, a standard error of about 6 per cent, which we obtained, is considerable. Also the errors were unevenly distributed in the test sentences.

About 1370 syllables are needed to include 93.4 per cent of English speech.[3] There are probably at least 8000 syllables needed if over 99 per cent of speech is to be covered. If inventories of this size are considered, together with the results of the present experiment, a

stored-syllable speech synthesis system may be practical in only limited applications, such as a situation that would combine the acceptability of a limited vocabulary and an extremely pressing demand for economy in channel use.

A. N. Stowe

D. Information Processing Language (IPL-V)

A program has been written for the IBM 709 computer to enable the computer to interpret and execute programs written in a special information processing language devised for non-numeric symbol manipulation problems by Newell, Shaw and their collaborators. The 709 program is completely coded, and nearly checked out. Arrangements are now being made to distribute it as a SHARE program. The program is completely compatible with similar programs being prepared elsewhere for the IBM 704 and 650 computers. A complete set of coding notes has been prepared, and a manual has been prepared giving instructions for the operation of the 709 version of IPL-V. The 709 version differs from the other versions only in some details of the input and output processes, and in the monitoring system, which is quite extensive in the 709 version.

IPL-V is expected to be very useful in programming for pattern recognition, data retrieval and other artificial intelligence problems.

B. F. Green, Jr.
Alice K. Wolf

E. Information Retrieval and Analysis – "Baseball"

A project has been planned to program the IBM 709 computer to answer questions posed in normal English about a table of data in its memory. The data will all pertain to a particular topic, but almost any question that can be answered by referring to the data will be allowed. The goal is for the computer to print out an acceptable – and correct – answer to the question. The computer program must analyze the input question, locate the data pertinent to its answer, process the data if necessary, and construct an English sentence presenting the answer.

The initial context in which the program will operate is baseball scores. The computer's table of data will be the score of every game played in the American League this season; an entry will consist of the two team names, the number of runs each team scored, the place and the data of the game. Typical questions are: "Who did the Yankees play on July 4?" "How often did the Red Sox beat the Yankees in Boston?" "Which team scored most runs in a single game?" The baseball context is sufficiently simple to permit use of a restricted vocabulary but sufficiently complex to pose a challenge. Many of the features of the baseball data are representative of the characteristics of a large class of data.

The program will be coded in IPL-V (see above) and will eventually have several self-adapting features. It will be able to enlarge its vocabulary, to reorganize its data table for maximum efficiency and to enlarge the table by the addition of ancillary information.

B. F. Green, Jr.
Alice K. Wolf

III. HUMAN INFORMATION PROCESSING

A. Auditory Encoding of Text

Work has begun on an investigation of the ways in which English text can be transmitted to human readers most efficiently with displays other than the conventional printed page, and

through channels other than the visual. At present the auditory channel is being explored. A Flexowriter has been modified so that when an operator types a letter he hears either a single tone of unique pitch, or a chord made up of some unique subset of five tones. Either of these two auditory outputs can be generated by driving the Flexowriter from punched paper tape. Initial experiments will seek to determine with which of these auditory outputs the greatest reading speeds can be attained. Preliminary work indicates that readers can more easily discriminate differences between words when the single tone output is used. However, there was fairly rapid improvement in accuracy of discrimination with the chords, so that with continued practice the difference between the two methods might well diminish or even reverse. In addition to augmenting our knowledge of information transmission to human operators, this work may have implications for the design of a reading machine for the blind.

B. W. White

B. Visual Psychophysics

As mentioned in previous reports, a redetermination of the relationship between the intensity of preadapting luminance and the time required for the eyes to dark adapt is being carried out. Earlier determinations[4] described the data with a simple smooth curve. This would seem to contradict expectations based on accepted views of the photochemistry of the retinal rod receptors which predicate two modes of regeneration of rhodopsin with differing velocities.

This reporting period has been devoted exclusively to data collection. The present plan is to measure the course of dark adaptation five times following each of eleven different preadapting light intensities (ranging from 1.5 to 4.5 log Trolands) for each of four subjects. Data gathering was about 80 per cent complete on 1 September. Preliminary analysis of the data now available indicates that the relationship should be described by a curve having two distinct limbs, with the transition region occurring at a preadapting intensity of about 1000 Trolands.

R. T. Mitchell
Rhoda Resnick

C. Prediction of Complex Judgments

A possible technique for enabling a man to summarize a temporary set of decision rules so that a computer can make decisions for him was discussed in the last quarterly reporting period. During this quarter a preliminary experiment was done to investigate the method further: by combining in an additive manner a man's evaluation of the separate attributes of a situation, an attempt was made to predict his judgment of the complex situation.

Eight Laboratory staff members were used as subjects. Each subject was asked to make a series of choices between pairs of hypothetical jobs which were described by three attributes. Then he was asked to give an evaluation of each attribute, both its relative importance to him and his scale for the specific values the attribute assumed. The subjects were run through the experiment twice. The difference between the two sessions was a description, included in the instructions, of imaginary outside conditions affecting the jobs. These outside factors caused changes in the job choices which were reflected in changes in the over-all evaluation of attributes. Since a method of summarizing temporary sets of rules should be sensitive to changes in the rules this result was encouraging.

In the case of an extremely close decision a man does not always make the same choice on a second trial: the solid line in Fig. 58-1, which represents the results of the 16 runs, shows

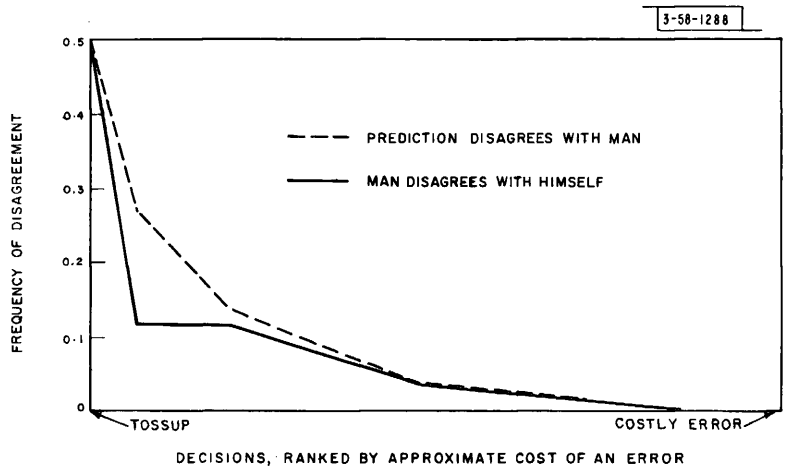

Fig. 58-1. Success of simple linear prediction of a complex judgment from the weights the subject assigns to the various factors.

the frequency with which a man disagreed with himself in this experiment. (Any scheme for predicting his choices could not do better than this.) The dotted line shows the frequency with which it was not possible to predict his choice on the basis of his summarized judgment. Although for the most difficult decisions the prediction was not always correct, as the error became costly the frequency of correct prediction came close to the limit set by the subjects' own inconsistency. Thus the pilot experiment suggests that the simple additive prediction of a man's judgment would be accurate enough to use in many practical man-computer systems, especially in applications where making many judgments rapidly is more important than making all of them perfectly, and where the operators must be kept free for more important tasks.

Laura Klem
D. B. Yntema
W. S. Torgerson

D. Remembering the Present States of a Number of Variables

The second and third in a series of experiments on a kind of memory that seems to be needed by control-center operators have been completed. In order that the subject would not see an old message when posting a new one, the procedure was changed slightly from that described in earlier reports. The subject was seated before a number of boxes that held stacks of 3 × 5 file cards. He was read a series of messages, each of which referred to one of the boxes. As each message was read, he recorded it on the top card in the appropriate box and then put that card on the back of the stack, where it would be out of sight. From time to time he was asked what the last message he had written in one of the boxes was. Thus each box represented a variable whose current state he had to try to remember.

These experiments were concerned with the effects of: (1) the number of states that each variable might assume and (2) the probability that a given message would change the state of the variable to which it referred. One experiment investigated these two questions in the case of six "attributes" of one "object" – that is, in the case of six variables that all had different, mutually exclusive sets of possible states. The other experiment investigated the same two questions in the case of six "objects" with one "attribute" – six variables that all had the same set of possible states.

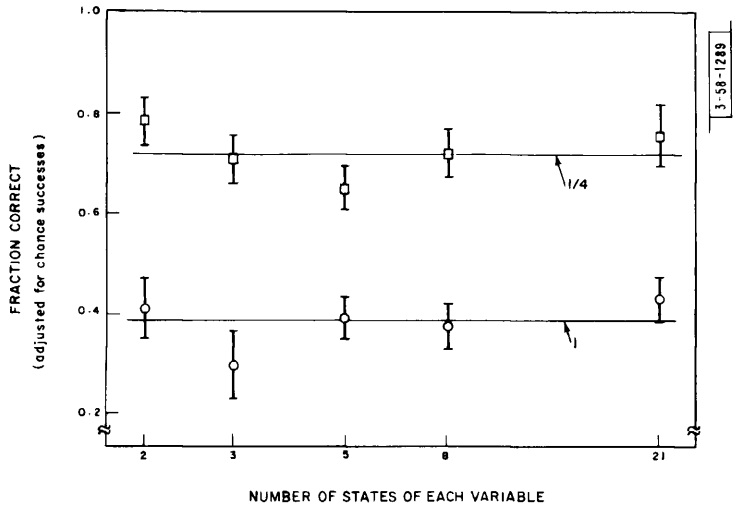

Fig. 58-2. Effect of number of states in the case of six variables that represent the same "attribute" of six different "objects." The parameter is the probability that a given message will change the state of the variable to which it refers. The vertical bars extend one standard error of estimate to either side of the points.

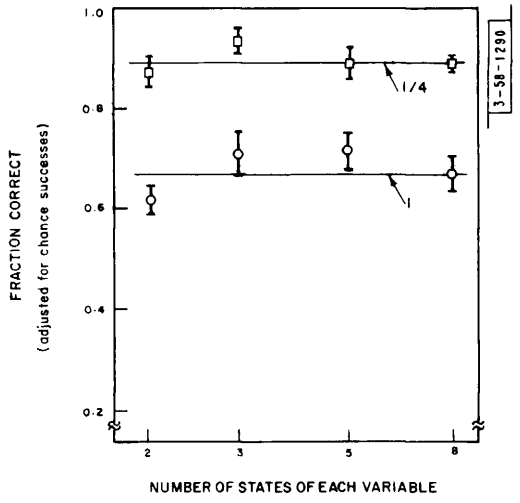

Fig. 58-3. Effect of number of states in the case of six variables that represent six different "attributes" of one "object." The parameter is the probability that a given message will change the state of the variable to which it refers. The vertical bars extend one standard error of estimate to either side of the points.

The results are shown in Figs. 58-2 and 58-3. Two conclusions may be drawn. First, the probability of change has a considerable effect: as might be expected, people keep better track of a relatively static situation than of a rapidly changing one. And second, when the scores have been corrected to allow for chance successes, the number of states that the variables may assume has little or no effect.

The second conclusion has implications for the proper design of control centers. It suggests that when a man must keep abreast of a complex, fluid situation, the situation should be reported and displayed to him in terms of a few large variables that have many possible states, not in terms of a host of small variables that have only a few states.

The second conclusion is also of theoretical interest. It supports Miller's conjecture that, in general, human memory is used most efficiently when the material to be remembered is coded into a few items, each of which conveys a large number of bits of information.[5]

D. B. Yntema
Gayle E. Mueser

E. Rote Verbal Learning

Three experiments on the recall of series of English monosyllables have been carried out, and a fourth is under way. The words were in each case flashed onto a screen at a constant rate by means of a slide projector.

In one of these experiments, subjects recalled lists of 48 words after each of six exposures. Three conditions of recall were compared. Under the first, recall was serial and the order in which the words were presented was kept constant from trial to trial. (Serial recall means that the subject must write the words down in order from first to last, each in its appropriate numbered blank.) Under the second condition, recall was free, and the order of presentation was again the same on each trial. (Free recall means that the subject may write the words down in any order that he chooses.) Under the third condition, recall was also free, but the order of the words was scrambled before each trial.

The results were as follows. First, the trial-by-trial recall scores were identical under both conditions of free recall. When recall is free, therefore, presenting the words in a different order on each trial does not appreciably affect the rate at which they are memorized. Second, when recall is serial, the learning curve – which shows the total number of words recalled as a function of the number of trials – can be fitted by a straight line through the origin. (An essentially similar result had been found previously when subjects recalled series of octal digits. Cf. Division 5 Quarterly Progress Report for 15 March 1959, p. 105.) When recall is free, on the other hand, the learning curve is exponential. An analysis of the trial-by-trial recall scores for individual words may shed some light on this difference in the learning curves, which is an interesting one from the point of view of learning theory. The analysis is now under way.

Two other experiments were concerned with the effects of list-length on recall scores. In one of them, lists of 16, 24, 32, 40 and 48 words were recalled serially after one exposure. The number of words recalled in the correct serial position was constant for different lengths of list (as had been the case with serial digits), whereas the total number of words recalled increased with list-length. In the other experiment, lists of 24, 36 and 48 words were shown and recalled after 2, 4 and 6 trials. Preliminary analysis of the data indicates that the serial recall scores on trials beyond the first, as well as on the first trial, are likewise independent of list-length.

In a fourth experiment, now in progress, the subject controls the length of time that each word in a 24-word list is exposed. The purpose of this study is to determine whether the time that a person needs to memorize a word in a given serial position is different when recall is serial than when it is free, and whether such a difference could help account for the difference in the learning curves obtained under these two conditions.

Nancy C. Waugh

IV. METHODOLOGY

A. Queuing Studies

In this quarter Group Report 58-6 (Ref. 6) was completed and work is in progress to extend the results of that study. The essential result was that the variability of observed waiting-time distributions increases greatly as system load increases. This was demonstrated for a random input, constant service-time queue, and an empirical description of this relation was constructed. Currently the study is being repeated using an exponential service-time distribution rather than a constant service-time distribution. These two distributions should bracket those commonly met in practice.

J. E. K. Smith
Laura Klem

B. The Stochastic Design of Psychophysical Experiments

A common problem in psychophysics is to estimate the stimulus intensity yielding a certain probability of response. How bright should a symbol be painted so that a subject correctly identifies it 75 per cent of the times it is shown to him? is a typical question. This has traditionally been studied by presenting the stimulus a number of times at each of a number of intensities and fitting a response curve to the data relating percentage correct to stimulus intensity. What intensities should be used to yield efficient estimates?

It can be shown mathematically that the most efficient estimate of any percentile is obtained if all the data are concentrated at the intensity yielding that per cent correct. This is, of course, a useless result since knowing which intensity to use makes the experiment superfluous. More important, the experimenter usually wants to know the shape of the function, and not just one but several percentiles, and consequently a number of intensities must be used. These may either be chosen before the experiment, as has commonly been done, or if the experimental materials allow, the next stimulus used can be made to depend on the results of previous trials. The use of a predetermined stimulus pattern will be called constant programming, and the latter will be called stochastic programming.

An example of constant programming would be for the experimenter to choose five stimulus intensities at equal intervals along the scale, attempting to have the middle one at the 50^{th} percentile, and present an equal number of trials at each level. An example of stochastic programming would be for the experimenter to choose an intensity interval and to present the stimuli one at a time, increasing the intensity each time a stimulus is missed and decreasing it each time one is detected. These methods have both been used, and it can be shown that stochastic programming can lead to equal precision with as few as half as many observations in estimating the 50^{th} percentile.

The stochastic programming technique described above is the only one yet to be described in the literature. However, it is only one of a large class of potentially useful designs taking advantage of the sequential nature of many psychophysical experiments. A project has been started to catalogue these designs, and to determine where they could prove useful and what their inherent efficiencies are.

J. E. K. Smith

REFERENCES

1. J.P. Egan, et al., "Articulation Testing Methods II," Psycho-Acoustic Laboratory, Harvard University, OSRD Report No. 3802 (1944).

2. J.P. Egan, et al., op. cit.

3. G.A. Miller, Language and Communication (McGraw-Hill, New York, 1951), p. 88.

4. S. Hecht, C. Haig and A.M. Chase, J. Gen. Physiol. 20, 831 (1937); C. Haig, J. Gen. Physiol. 24, 735 (1941).

5. G.A. Miller, Psychol. Rev. 63, 81 (1956).

6. J.E.K. Smith and Laura Klem, Group Report 58-6, Lincoln Laboratory, M.I.T. (19 August 1959) (not generally available).